พอลิเอทิลีนเคลย์นาโนคอมโพสิทที่ผลิตจากอินซิทูพอลิเมอร์ไรเซชันด้วยตัวเร่งปฏิกิริยาเซอร์โคโนซีน

นางสาวพิมพ์ปฏิมา ปาณุปกรณ์

วิทยานิพนธ์นี้เป็นส่วนหนึ่งของการศึกษาตามหลักสูตรปริญญาวิศวกรรมศาสตรมหาบัณฑิต
สาขาวิชาวิศวกรรมเคมี ภาควิชาวิศวกรรมเคมี
คณะวิศวกรรมศาสตร์ จุฬาลงกรณ์มหาวิทยาลัย
ปีการศึกษา 2554

PE/CLAY NANOCOMPOSITES PRODUCED BY *IN SITU* POLYMERIZATION WITH ZIRCONOCENE CATALYST

Miss Pimpatima Panupakorn

A Thesis Submitted in Partial Fulfillment of the Requirements
for the Degree of Master of Engineering Program in Chemical Engineering
Department of Chemical Engineering
Faculty of Engineering
Chulalongkorn University
Academic Year 2011

Thesis Title	PE/CLAY NANOCOMPOSITES PRODUCED BY *IN SITU* POLYMERIZATION WITH ZIRCONOCENE CATALYST
By	Miss Pimpatima Panupakorn
Field of Study	Chemical Engineering
Thesis Advisor	Associate Professor Bunjerd Jongsomjit, Ph.D.

Accepted by the Faculty of Engineering, Chulalongkorn University in Partial Fulfillment of the Requirements for the Master's Degree

……. Dean of the Faculty of Engineering
(Associate Professor Boonsom Lerdhirunwong, Dr.Ing.)

THESIS COMMITTEE

…….. Chairman

(Associate Professor Muenduen Phisalaphong, Ph.D)

…….……. Thesis Advisor

(Associate Professor Bunjerd Jongsomjit, Ph.D.)

…….. Examiner

(Associate Professor Supakanok Thongyai, Ph.D.)

…….. External Examiner

(Ekrachan Chaichana, Dr.Eng.)

พิมพ์ปฏิมา ปาณูปกรณ์ : พอลิเอทิลีนเคลย์นาโนคอมโพสิทที่ผลิตจากอินซิทูพอลิเมอร์ไรเซชันด้วยตัวเร่งปฏิกิริยาเซอร์โคโนซีน. (PE/CLAY NANOCOMPOSITES PRODUCED BY *IN SITU* POLYMERIZATION WITH ZIRCONOCENE CATALYST) อ. ที่ปรึกษาวิทยานิพนธ์หลัก : รศ.ดร.บรรเจิด จงสมจิตร, 97 หน้า.

พอลิเอทิลีนเป็นพอลิเมอร์สังเคราะห์ชนิดหนึ่งซึ่งนิยมนำมาใช้ประโยชน์อย่างกว้างขวาง เนื่องจากมีน้ำหนักเบา ราคาถูก รวมถึงมีกระบวนการผลิตที่ค่อนข้างง่าย แต่อย่างไรก็ตามพอลิเอทิลีนยังมีคุณสมบัติบางประการที่เป็นข้อจำกัดต่อการใช้งาน เช่น สมบัติเชิงกล สมบัติเชิงความร้อน เป็นต้น ดังนั้นจึงจำเป็นต้องปรับปรุงสมบัติของพอลิเมอร์ วิธีหนึ่งที่นิยมคือ การเติมสารปรุงแต่งลงในพอลิเมอร์เพื่อใช้เป็นตัวรองรับของตัวเร่งปฏิกิริยา โดยเฉพาะการเติมสารปรุงแต่งที่มีขนาดนาโนเมตรลงในพอลิเมอร์ จะเรียกพอลิเมอร์นั้นว่าพอลิเมอร์นาโนคอมโพสิท ซึ่งการเตรียมพอลิเมอร์นาโนคอมโพสิทด้วยวิธีอินซิทูพอลิเมอร์ไรเซชัน สารปรุงแต่งเกิดพันธะโดยตรงกับตัวเร่งปฏิกิริยา ส่งผลให้สารปรุงแต่งกระจายตัวในพอลิเมอร์ได้ดี ในงานวิจัยนี้ศึกษาผลของการเติมสารปรุงแต่งนาโนเคลย์ต่อความว่องไวของตัวเร่งปฏิกิริยาเซอร์โคโนซีนในปฏิกิริยาพอลิเมอร์ไรเซชันของเอทิลีน รวมถึงศึกษาสมบัติของพอลิเอทิลีนเคลย์นาโนคอมโพสิทที่ได้จากการสังเคราะห์ด้วยวิธีอินซิทูพอลิเมอร์ไรเซชัน ซึ่งในงานวิจัยนี้ศึกษาผลของนาโนเคลย์ 2 ชนิด (TOB_2 และ TOB_3) ปริมาณนาโนเคลย์ (5, 10, 20 และ 40 เปอร์เซ็นต์โดยน้ำหนัก) และระยะเวลาที่ใช้ในการปั่นกวนนาโนเคลย์กับตัวเร่งปฏิกิริยาร่วมเมทิลอะลูมินอกเซน (30, 60, 90, และ 120 นาที) พบว่าเคลย์ TOB_2 ให้ความว่องไวของตัวเร่งปฏิกิริยาสูงกว่า TOB_3 ปริมาณนาโนเคลย์ที่เพิ่มขึ้นส่งผลให้ความว่องไวของตัวเร่งปฏิกิริยาลดลง โดยปริมาณเคลย์ 5 เปอร์เซ็นต์โดยน้ำหนัก สามารถปรับปรุงสมบัติทางความร้อนและความเป็นผลึกได้สูงสุด และระยะเวลาที่ใช้ในการปั่นกวนที่มากขึ้นส่งผลให้ความว่องไวของตัวเร่งปฏิกิริยาลดลงเล็กน้อย

ภาควิชา วิศวกรรมเคมี ลายมือชื่อนิสิต .....

สาขาวิชา วิศวกรรมเคมี ลายมือชื่อ อ.ที่ปรึกษาวิทยานิพนธ์หลัก .....

ปีการศึกษา 2554

5370469921 : MAJOR CHEMICAL ENGINEERING
KEYWORDS : POLYETHYLENE / NANOCOMPOSITE / METALLOCENE / NANOCLAY / IN SITU

PIMPATIMA PANUPAKORN : PE/CLAY NANOCOMPOSITES PRODUCED BY *IN SITU* POLYMERIZATION WITH ZIRCONOCENE CATAYST. ADVISOR : ASSOC. PROF. BUNJERD JONGSOMJIT, Ph.D, 97 pp.

Polyethylene is the synthetic polymer that has been the most useful and widely used because of their light weight, low cost, and good processability. However, polyethylene properties have some restriction on its use such as mechanical and thermal properties. Therefore, improving the polyethylene properties is important. The addition of additive into polymer is commonly used to improve polymer properties, especially, nano-sized additives. The polymer with the addition of nano-sized additive is called polymer nanocomposite. Preparation of polymer nanocomposite via *in situ* polymerization results in well dispersion of additive in the polymer due to direct interaction between catalyst and nanoclay. In this research, the effect of nanoclay on catalytic activity and polyethylene properties which produced via *in situ* polymerization was investigated. Three variables in this research are types of nanoclay (TOB_2 and TOB_3), amount of nanoclay (5, 10, 20, and 40 % wt), and aging time between nanoclay and methylaluminoxane cocatalyst (30, 60, 90, and 120 min). It found that TOB_2 gives higher catalytic activity than TOB_3. Catalytic activities can be decreased with increasing amount of nanoclay. The addition of 5 % by weight of clay resulted in maximal thermal properties and crystallization. Increasing the aging time result in catalytic activity slightly decreased.

Department : Chemical Engineering Student's Signature .....
Field of Study : Chemical Engineering Advisor's Signature .....
Academic Year : 2011

ACKNOWLEDGEMENTS

The author would like to express my greatest gratitude and appreciation to Associate Professor Bunjerd Jongsomjit, my thesis advisor, for his invaluable suggestions, guidance, useful discussions, and devotion to revise this thesis throughout encouragement during my study. His advice is always worthwhile and without him this work could not be possible. In addition, the author would also be grateful to Associate Professor Dr. Muenduen Phisalaphong, as a chairman, and Associate Professor Supakanok Thongyai, Dr. Ekrachan Chaichana, as the members of the thesis committee.

I appreciate to the Thai Nippon Chemical Industry Co., Ltd. for the nanoclay support of this work.

I would like to thank Ms.Mingkwan Wannaborworn, Ms.Sasiradee Jantasee, Mr.Jirawat Pinyocheep, and Mr. Therdthai Therdjittoam for their helpful suggestions and patience to correct my thesis and paper manuscript writings.

I wish to thank the member of the Center of Excellence on Catalysis and Catalytic Reaction Engineering, Department of Chemical Engineering, Faculty of Engineering, Chulalongkorn University for their assistance and encouragement.

Finally, I would like to express my highest gratitude to my parents who always pay attention for all times and have provided their support and encouragement. The most success of graduation is devoted to my parents.

CONTENTS

LIST OF TABLES

LIST OF FIGURES

Figure **Page**

CHAPTER I

INTRODUCTION

During the growth of polyolefin production, polyethylene (PE) is the synthetic polymer that has been the most useful and widely used. It has become a part of our daily life with a global demand 50 million metric tons. There are many things around us ranging from our basic necessities such as tooth brushes, clothing, storage bottles and carry bags to special applications like gas pipelines, bullet proof jackets, aerospace application and biomedical implants that are made of polyethylene [1]. The extensive and still increase using of polyethylene due to their unique properties such as light weight, high chemical resistance, low dielectric constant and low dielectric losses, good processability and economical advantages. In many applications their performance are better than conventional materials such as metals, wood and natural fibers.

Polyethylene can be produced via homogeneous system with several advantages, such as high catalytic activity, high performance of comonomer insertion, and narrow molecular weight distribution. However, there are three main problems of homogeneous system. Soluble homogeneous catalyst is difficult to control polymer morphology and inability to use in gas or slurry phase processes. The other main problem is requiring very large amount of methylaluminoxane (MAO) as cocatalyst operated with metallocene catalyst to obtain maximum catalytic activity. Therefore, it is necessary to develop the catalyst for usable application. Possibility route to solve these is immobilization of catalyst on support. Moreover, it also improves some polyethylene properties [2].

The polyethylene properties have some restrictions on its use. Polyethylene has not enough stiffness, low gas permeability and can easily catch fire [3]. Therefore, improving the polyethylene properties are important by changing the method of synthesize, adjusting the conditions of polymerization reactions, using irradiation process, and the addition of additives into the polymer. Addition of additives as support can improve polyethylene properties such as mechanical properties, thermal properties, barrier properties and flame resistant. Especially, nano-sized addivtives or

nanofiller give better properties than micro-size additive. The polymer with the addition of nanofiller is called polymer nanocomposties.

Polymer nanocomposites (PNC) are materials in which nanoscale particles, typically 10-100 Å in at least one dimension, are dispersed in the polymer matrix in order to dramatically improve the performance properties of the polymer, even when a small amount of filler is used [4]. Polymer nanocomposites represent a new alternative to conventionally filled polymers. For using clay as nanofiller, the platelets of clay are dispersed in the polymer matrix making several dispersed layer which force gas difficult to flow through the polymer in a diversion path. The present of more diversion path in a polymer matrix cause higher barrier properties. Productively, higher degree of dispersion of nanofiller in the polymer matrix reduces its permeability. Moreover, the degree of dispersion of nanofiller relates to improvement in barrier and mechanical properties of polymer nanocomposite. Because of their nanometer sizes, filler dispersion nanocomposites exhibit improved properties when compared to the pure polymers or their traditional composites. These include increased modulus and strength, outstanding barrier properties, improved solvent and heat resistance and decreased flammability. There are mainly three methods to prepare polymer nanocomposites: solution method, melt mixing and *in situ* polymerization. Using the solution method, nanofillers are added to a polymer solution using solvents such as toluene, chloroform and acetonitrile to integrate the polymer and filler molecules. Since the use of solvents is not environmentally-friendly and it has the expense of solvent [5]. For the melt mixing process, required high temperature for blending between nanofiller and polymer, this can sometimes cause concern with regards to surface modifications [6,7]. For *in situ* polymerization, the filler is added directly to the liquid monomer during the polymerization stage, nanofiller is well distribution in polymer because of direct interaction between catalyst and surface of nanofiller [5].

Generally, the production of polyolefin use Ziegler-Natta, chromium catalysts or Phillips catalyst, and also the more new metallocene catalysts. The latest catalyst is expected to enter a broad array of polymer markets in order to develop the new class of polyolefin that were not possible with conventional catalyst. The primary reason of using metallocene catalyst, it produces polymer with the preferable properties

compared to conventional catalyst. The metallocenes are single-site catalysts. Therefore, polyethylene produced with metallocene catalysts have narrower molecular weight distribution (MWD) than the polymers produced with the other catalyst systems. The molecular weight of metallocne polymer is less than other polymers. This reduces the smoke and other difficult processes involved with low molecular weight polymers. Metallocenes allow control of stereoregularity and incorporation of comonomer. A comparison of the comonomer performance, the metallocene catalysts have better performance in using comonomer to reduce the density or these require less comonomer to produce the same density. Therefore, these reduce the production cost of linear-low density polyethylene. In addition, catalytic activity of metallocene is 10–100 times higher than Ziegler–Natta systems [8]. The metallocene activity also be extremely increase by using the combination of metallocene and methylaluminoxane (MAO) as cocatalyst.

In this present study, the combination of metallocene catalyst and methylaluminoxane as cocatalyst was used for synthesize PE/clay nanocomposites via *in situ* polymerization. The activity of metallocene catalyst using commercial nanoclay as support was studied. This research aimed to estimate the appropriate types of nanoclay, amount of nanoclay and aging time between clay and MAO on activity. PE/clay nanocomposites were synthesizes as various conditions. The properties of polyethylene/clay nanocomposites were investigated.

1.1 Objective of the Thesis

1. To synthesize PE/clay nanocomposites and LLDPE/clay nanocomposites with MAO/zirconocene catalyst via *in situ* polymerization.
2. To study the metallocene catalytic activity as various condition.
3. To characterize properties of PE/clay nanocomposites and LLDPE/clay nanocomposites prepared via *in situ* polymerization method.

1.2 Scope of the Thesis

1. Synthesize PE/clay nanocomposites and LLDPE/clay nanocomposites via *in situ* polymerization with metallocene catalyst upon the specified condition.

2. Determine the effect of kind of nanoclay on the catalytic activity and polymer properties for the ethylene polymerization.
3. Determine the effect of the amount of nanoclay on the catalytic activity and polymer properties for the ethylene polymerization.
4. Determine the effect of stirred time of clay mixed with MAO on the catalytic activity
5. Characterize the PE/clay nanocomposites and LLDPE/clay nanocomposites with X-ray diffraction (XRD), Scanning electron microscopy (SEM), Transmission electron microscopy (TEM), Differential scanning calorimetry (DSC), Thermo Gravimetric Analysis (TGA) and ^{13}C Nuclear magnetic resonance (^{13}C NMR).
6. Characterize the nanoclay with X-ray diffraction (XRD) and fourier transform infrared spectroscopy (FTIR).

1.3 Benefits

1. Polymer/clay nanocomposites were synthesized by *in situ* polymerization with metallocene catalyst and addition of nanoclay as support was change the catalytic activity.
2. Some properties of polyethylene/clay nanocomposite can be improved due to the dispersion of nanoclay in the polymer matrix.
3. This information will be used as a reference for polymer industries.

1.4 Research methodology

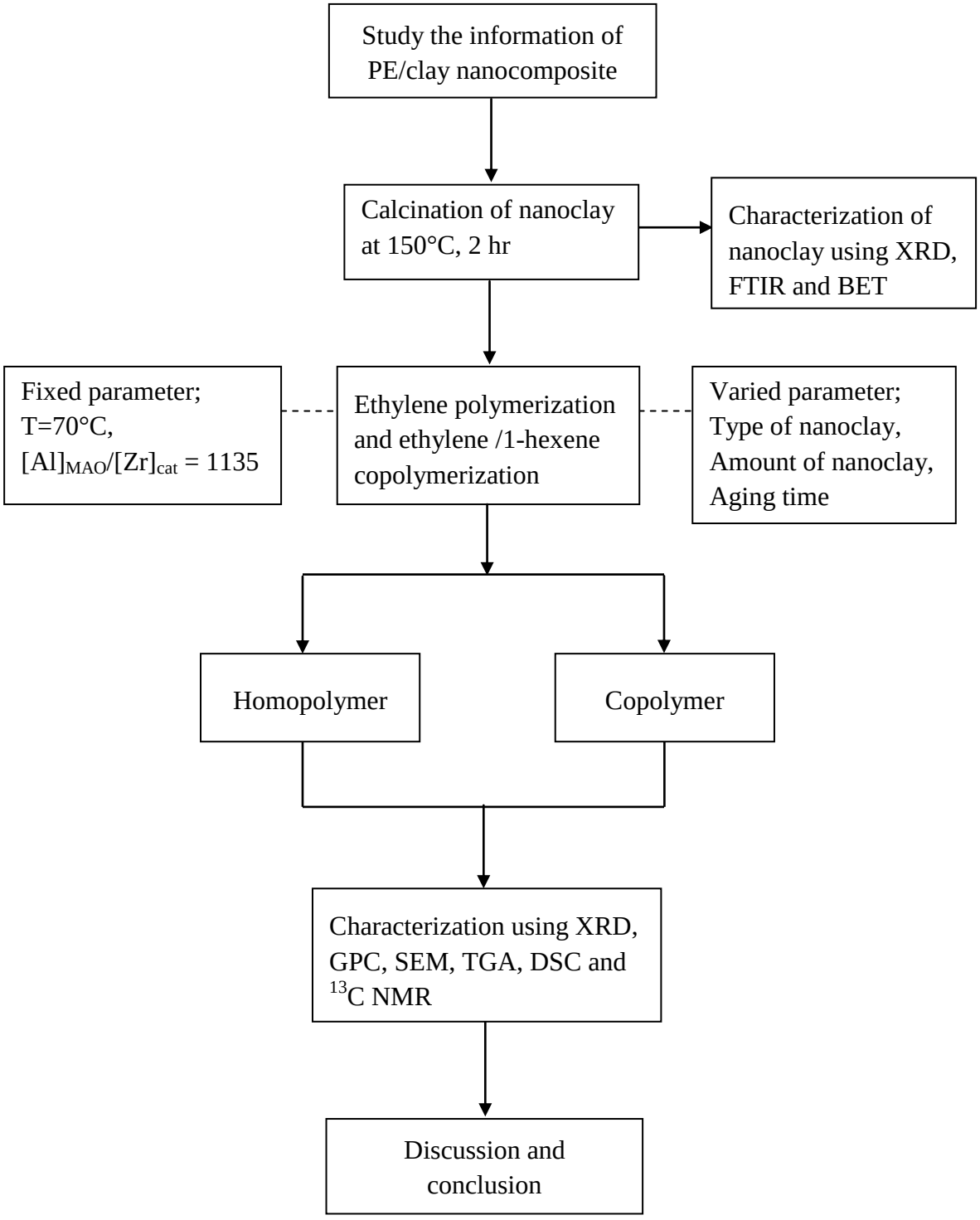

Figure 1.1 Flow diagram of research methodology

CHAPTER II
THEORY AND LITERATURE REVIEWS

2.1 Polyethylene

Polyethylene was first synthesized as a waxy solid by accident in 1989. It was characterized and found that it consisted of long ethane chains. The first industrial also synthesized polyethylene by accident in 1933, when Eric Fawcett and Reginald Gibson from ICI chemicals apply extremely high pressure (1400 bar and 170°C) to ethylene and benzaldehyde, then a waxy solid is occurred [1]. Polyethylene has developed until now it has become a part of our daily life with a global demand 50 million metric tons due to its light weight, high chemical resistance, low dielectric constant and excellent processability. These properties are appropriate for any application, especially packaging. It has the simplest chemical structure of all the commercial polymers as Figure 2.1.

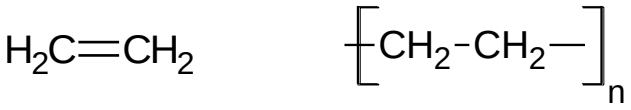

(a) Ethylene (b) Polyethylene

Figure 2.1 The structure of (a) ethylene and (b) polyethylene

2.1.1 Polyethylene structures

Based on the structures of molecule of polyethylene, degree of branching, crystallinity, and their molecular weight, they are classified into three main types. These are high density polyethylene (HDPE; few short or no branches), low density polyethylene (LDPE; various branches on branches) and linear low density polyethylene (LLDPE; many equal short branches) as shown in Figure 2.2. The types of polyethylene depend on temperature, pressure, and catalyst during polymerization reaction.

High Density Polyethylene (HDPE) is more liner molecule with low degree of branching. There are few short or no branches. Thus, its density is the highest and it is

the most rigid compare to other type of polyethylene. HDPE is occurred at low reaction temperature and low reaction pressure and it can be produced different ways such as slurry process, gas phase process and using metallocene catalyst [9]. HDPE is used to make fuel tanks because of its low permeability and excellent chemical resistance. Bottles, Tupperware, and milk jugs are usually made of HDPE because they need to be made with thin walls to reduce material costs, but they also need to be strong in order to hold their shape.

Low Density Polyethylene (LDPE), high degree of short and long chain branching of LDPE due to some of the carbon atoms are attached to three carbon atoms instead of two. This caused a branch which relatively long, interlace and link with other polyethylene molecules. The chains do not pack into the crystal structure as well, thus it has less strong intermolecular forces. This results in a lower tensile strength and increase ductility. It has great flexibility, impact toughness and stress cracking resistance. The high degree of branches with long chains gives molten LDPE unique and desirable flow properties. LPDE is polymerized under high reaction temperature and high reaction pressure. As a result of extremely polymerization conditions of LDPE, the molecular structure is mostly amorphous. Because of the amorphous structure, the branches are very high in quantity and length. Shopping bags are often made with LDPE because it's lightweight, flexible, and transparent.

Linear-Low Density Polyethylene (LLDPE) is essentially a mix of HDPE and LDPE. It has more linear polymer like HDPE and low density polyethylene molecule like LDPE. However, it still has a large number of side branches which these branches are shorter. These branches are long enough to prevent the molecules from being closely packed together. LLPDE is commonly made by copolymerization of ethylene with short chain 1-olefins as comonomer (e.g. 1-butene, 1-hexene, and 1-octene). The comonomer increases chain complication, which results in improved physical properties due to stronger secondary bonding. The disadvantages of LLDPE are higher melt processing temperatures, greater shrinkage and less flexibility [10,11]. LLDPE is used when LDPE and HDPE cannot be used, or when cost becomes a problem, including plastic wrap and stretch wrap.

Other than common three types of polyethylene, a special class of HDPE is ultra high molecular weight polyethylene (UHMWPE) with a molar mass of over $1\times$

10^6 g/mol whereas HDPE commonly has a molar mass between 50,000-300,000 g/mol. UHMWPE is made through metallocene catalysis polymerization. The high molar mass results a very good packing of the chains into the crystal structure. It can produce very tough material.

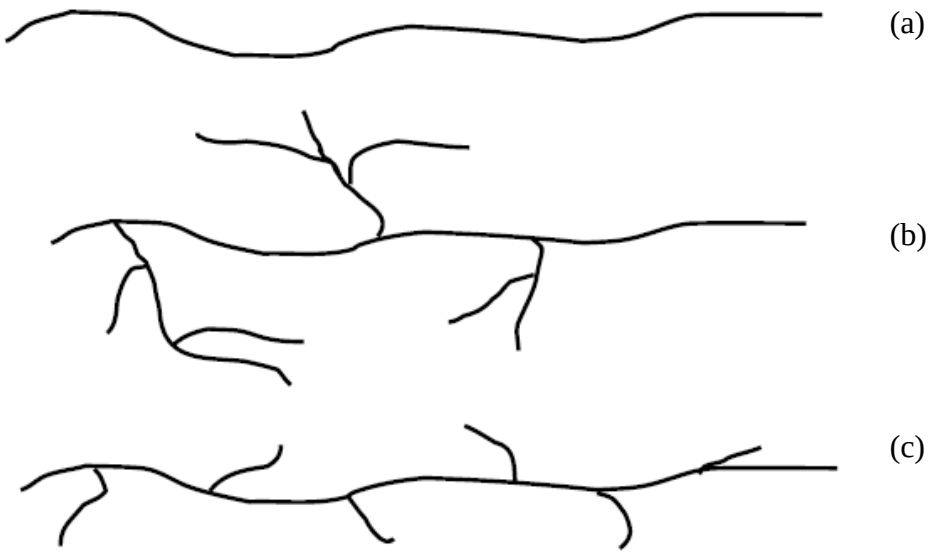

Figure 2.2 Chemical structures of various kinds of polyethylene (a) HDPE (b) LDPE (c) LLDPE [1]

2.1.2 Polymerization process

Polyethylene is prepared by polymerizing ethylene by two fundamentally different methods, the high pressure process and the low pressure process. The high pressure process is carried out at pressures above 1500 bar (150-400 MPa) and proceeds by a free-radical process using oxygen, peroxides or other strong oxidizing chemicals to initiate the reaction to produce low-density polyethylene. Because of safety and expensive cost problems, using high-pressure polymerization method is not extensive as low-pressure polymerization.

For ethylene polymerization process, the low-pressure process is carried out at pressure below 100 bar. This method can produce a low level of branching polymer, relatively high crystallinity and high density polymer (HDPE and LLDPE) compared

to the high-pressure process. The polymer obtained from the low-pressure process are usually of a linear structure with little branching and have a high level of crystallinity (generally 60-90%), a high melting range (typically 120-135° C), and a high density (generally 0.93-0.97 g/cm3). The polymer obtained has high density in a polyethylene with a high glass transition temperature, high hardness, a high melting range, high brittleness, and low tackiness. There are three major types of low pressure technologies, namely solution, slurry and gas phase process [12].

Solution process, both the catalyst and the obtained polymer remain dissolved in a solvent. Recovery of polymer can be obtained by difference methods such as solvent vaporization, which leaves the polymer as non-volatile residue, and cooling of the solution to cause precipitation of the polymer, thereafter being consequently separated by filtration. Vaporization process for solvent removal in particular is characterized by the inherent difficulty in removing the last tract of solvent from the polymer. This difficulty arises from the fact that as the solution becomes more concentrated. Its viscosity increases sharply even if molten. For this reason, a high molecular weight polyethylene cannot be obtained by solution polymerization. Moreover, the one of disadvantage of this process is expensive. However, it gives high catalytic activity.

Slurry process is performed in the hydrocarbon diluents in which the catalyst is impregnated on an inert support. The polymer is obtained in the form of solid which suspense in the solvent. Hence the polymer easily separates out from the diluent as fine particles. Thus, the viscosity of the diluent does not increase as rapidly as in the solution process. Therefore, a higher concentration of polymer can be maintained in the reactors. Moreover, some advantages of slurry include a higher volume yield of product and easily diluent removal. On the other side, residence times in slurry process are usually longer than in the solution processes. Moreover, another advantages are the potential for making powders, suitable for rotomoulding, and directly in the reactor, thus avoid the expensive grinding step. Reactors for slurry processes can control the reactor temperature due to kettles to loop-type designs have high surface/volume ratios. Thus, the molecular weight and molecular weight distribution can be controlled as desired. A disadvantage of the slurry process is more

difficulty of automation. It hardly senses any changes in the product itself. Also, many processes are sensitive to fouling. Most slurry processes give high molecular weight which it is not commercially useful. Thus, this process requires a chain stopper or chain transfer agent.

Gas phase process performs in the fluidized bed, in which at least one of the α-olefins is fed in presence of a catalyst under reaction conditions. The streams of ethylene, hydrogen, and possibly a carrier gas flow upward, while the polymer particles flow downward to the bottom of reactor through a special valve system. Introducing chilled monomer through the bottom porous plate controls reaction temperature. The obtained polymer is low in ash. After it is pelletized, it can be directly used without further purification.

2.2 Polyethylene catalyst system

Over the years, development of polyethylene has increased due to the additions of catalyst. This makes ethylene polymerization possible at a lower temperatures and pressures. Generally, the production of polyolefin use Ziegler-Natta, Chromium catalysts or Phillips catalyst, and also the more new metallocene catalysts. The latest catalyst is expected to enter a broad array of polymer markets in order to develop the new class of polyolefin that were not possible with conventional catalyst. It produces polymer with the preferable properties compared to conventional catalyst.

2.2.1 Metallocene catalyst

Metallocene is one in the class of organometallic complexes [13]. They are activated with cocatalyst to form single-site catalyst system for olefins polymerization. The simplest structure of metallocene is show in Figure 2.3.

M is the center metal, normally Ti, Zr and Hf.

X is halogen, normally Cl or methyl group (Me).

R is substituent, normally H or Me.

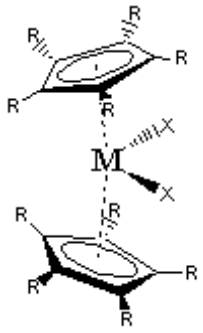

Figure 2.3 The simplest structure of metallocene

The catalyst properties result in difference structures of metallocene. The factors that have the effect on the structures of metallocene are as follows.

1) Type of ligand
2) Type of substitution on ligand
3) The bridging between ligands
4) The metal
5) The cocatalyst

Ligands are normally cyclopentadiene (Cp), indene (Ind) and fluorene (Flu). The simplest metallocene composes of two Cp ligands which form π-bond with the central metal atom.

Substituent on the metallocene ligands is one of the most important for catalyst systems. For example, compare two difference structure of metallocene between the simple metallocene Cp_2ZrCl_2 (R=H) and the pentamethyl-substituted (R=Me) Cp*2ZrCl2 system. The latter catalyst produces higher molecular weight polyethylene than the first catalyst.

Bridge, these are either there or not. The simple metallocenes $(Ind)_2MX_2$ have no bridges. The unbridged $(Ind)_2MX_2$ catalyst can rotate around the metal-Cp bond, thus it can easily changing from the racemic to the meso form. The meso form can produce only atactic polyolefins whereas the racemic form can produce isotactic polyolefins.

The metal atoms are commonly zirconium (Zr), and titanium (Ti). Sometimes use hafnium (Hf) as metal atom to produce high molecular weight polyolefins.

Cocatalyst is commonly use alkylaluminums including methylaluminoxane (MAO), triethylaluminum (TMA), triethylaluminum (TEA), triisobutylaluminum (TIBA), and cation forming agents. These cocatalysts can activate the metallocene catalyst [14].

Representative examples of different metallocene catalysts symmetries relevant to stereoselective for olefin polymerization are shown in Figure 2.4 and examples of ethylene copolymerization with metallocene catalysts are shown in Table 2.1.

Different structures of metallocenes have the effect on catalytic activity. Kaminsky, W., and Laban, A. [8] synthesized polyethylene with difference structures of metallocene catalyst. The polymerization of ethylene with some structures of metallocene catalyst under the same conditions (temperature 30◦C, monomer pressure 2.5 bar, metallocene concentration $6.25 \times 10{-}6$ mol l^{-1}, and molar MAO/metallocene ratio = 250/1) is summarized in Table 2.2.

Table 2.1 Examples of ethylene copolymerization with metallocene Catalysts [15]

Monomer/comonomer	Metallocene catalyst
ethylene/propene	$(C_5H_5)_2ZrCl_2$/MAO
	$C_2H_4(Ind')_2ZrCl_2$, $C_2H_4(Ind'H_4)_2ZrCl_2$/MAO
	compared to unbridged metallocene catalysts
ethylene/isobutene	$Me_2Si(C_5Me_4)$(Ncyclodecyl)$TiMe_2$/MAO or borate
ethylene/1-hexene	$C_2H_4(Ind')_2ZrCl_2$, $C_2H_4(Ind'H_4)_2ZrCl_2$/MAO
	compared to unbridged metallocene catalysts
	$(C_5H_5)_2ZrCl_2$, $Me_2Si(C_5H_4)_2ZrCl_2$,
	$C_2H_4(Ind')_2ZrCl_2$, $(Ind)_2ZrCl_2$/MAO
	$C_2H_4(Ind')_2ZrCl_2$, $(C_5H_5)_2ZrCl_2$/MAO
	$(C_5H_5)_2ZrCl_2$/MAO
	$Me_2C(C_5H_4)(Flu')ZrCl_2$
ethylene/1-octene	$(C_5H_5)_2ZrCl_2$, $Me_2Si(C_5H_4)_2ZrCl_2$,
	$C_2H_4(Ind')_2ZrCl_2$, $(Ind)_2ZrCl_2$/MAO
	$(C_5H_5)_2ZrCl_2$/MAO
	R_2Si(2-Me-benz[e]indenyl)(N-t-Bu)$TiCl_2$
ethylene/1-dodecene	$Me_2C(C_5H_4)(Flu')ZrCl_2$, $Me_2Si(Ind')_2ZrCl_2$/MAO
ethylene/1-tetradecene	$(C_5H_5)_2ZrCl_2$/MAO
ethylene/1-octadecene	$Me_2C(C_5H_4)(Flu')ZrCl_2$, $Me_2Si(Ind')_2ZrCl_2$/MAO
	$(C_5H_5)_2ZrCl_2$, $(C_5H_5)_2HfCl_2$/MAO
ethylene/1,3-butadiene	$(C_5H_5)_2ZrCl_2$/MAO
ethylene/norbornene	$Me_2C(C_5H_4)(Ind')ZrCl_2$,$Me_2C(C_5H_3Me)(Ind')ZrCl_2$,
	$Me_2C(C_5H3$-3-t-Bu$)(Ind')ZrCl_2$/MAO
ethylene/5-vinyl-2-norbornene	$(C_5H_5)_2ZrCl_2$/MAO
ethylene/2-allylnorbornane	$(C_5H_5)_2ZrCl_2$/MAO
ethylene/4-vinylcyclohexene	$Ph_2C(C_5H_4)(Flu')ZrCl_2$/MAO
ethylene/4-methyl-1-pentene	$C_2H_4(Ind')_2ZrCl_2$, $(C_5H_5)_2ZrCl_2$/MAO
ethylene/styrene	$C_2H_4(Ind')_2ZrCl_2$/MAO
	$Me(Ph)C(C_5H_4)$(Flu0)$ZrCl_2$/MAO/TMAy2
	$Me_2Si(C_5H_4)(NR)TiCl_2$

a Ind'= indenyl connected to one other ligand or substituent, C_9H_6. Ind = free indenyl, C_9H_7. Flu = free fluorenyl, $C_{13}H_9$. t-Bu = tert-butyl. Flu' = fluorenyl connected to another ligand or substituent, $C_{13}H_8$. TMA = trimethylaluminum, Me_3Al. Me = methyl, CH_3. Ph = phenyl, C_6H_5.

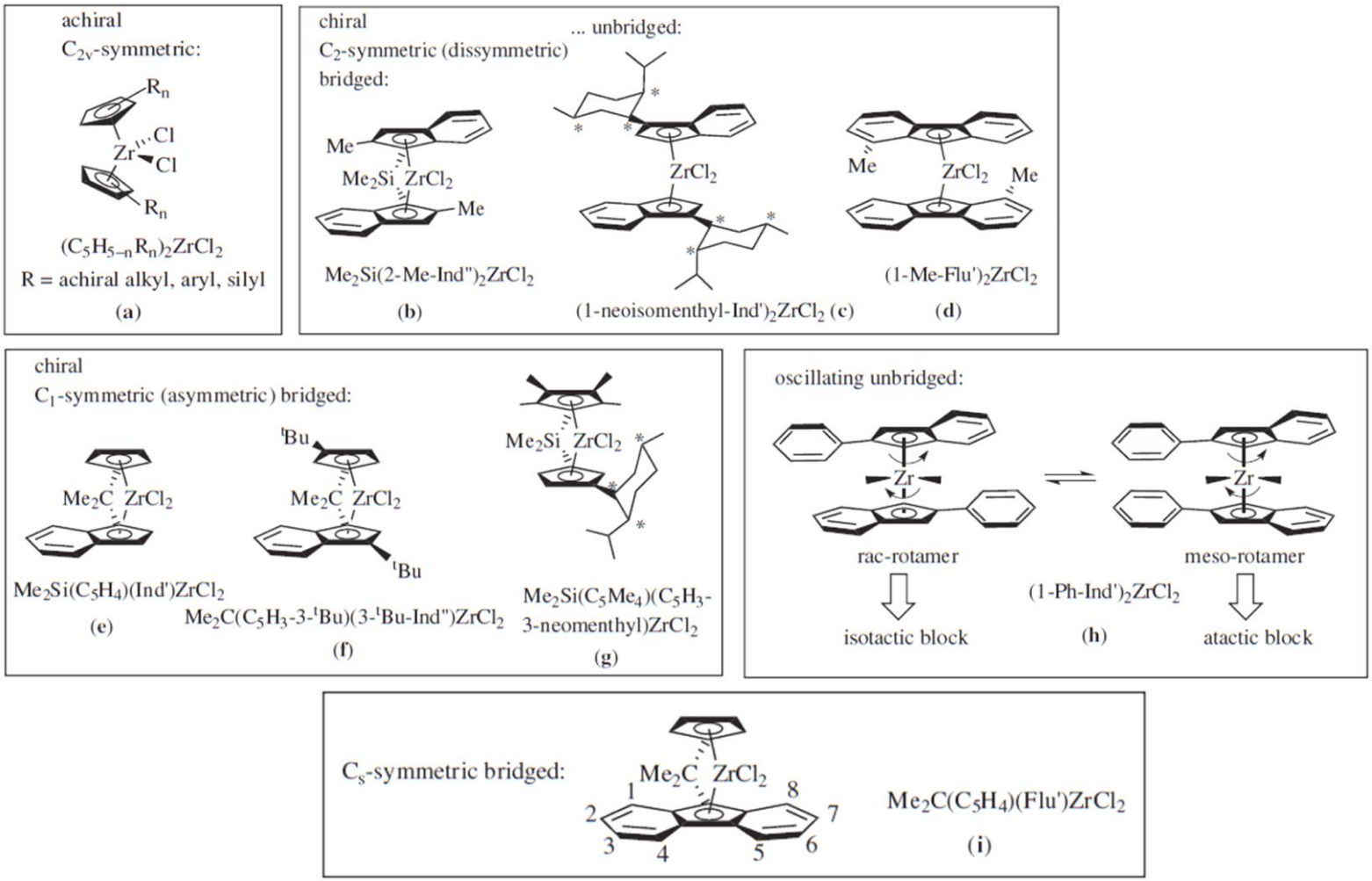

Figure 2.4 Some structures of different metallocene catalysts symmetries relevant to stereoselective for olefin polymerization [15]

Table 2.2 Catalytic activity of ethylene polymerization with different metallocenes [8]

	Catalyst	Activity[a]
1	Cp_2ZrCl_2	60,900
2	$(C_5Me_4Et)_2ZrCl_2$	12,200
3	$(Me_4EtCp)_2ZrCl_2$	18,800
4	$[O(SiMe_2Cp)_2]ZrCl_2$	57,800
5	rac-$[En(Ind)_2]ZrCl_2$	41,100
6	rac-$[En(Ind)_2]HfCl_2$	2,900
7	rac-$[En(IndH_4)_2]ZrCl_2$	22,200
8	rac-$[En(2,4,7\text{-}Me_3Ind)_2]ZrCl_2$	78,000
9	rac-$[Me_2Si(Ind)_2]ZrCl_2$	36,900
10	rac-$[Me_2Si(IndH_4)_2]ZrCl_2$	30,200
11	rac-$[Me_2Si(2,4,7\text{-}Me_3Ind)_2]ZrCl_2$	111,900
12	rac-$[Me_2Si(2\text{-}Me\text{-}4\text{-}Ph\text{-}Ind)_2]ZrCl_2$	16,600
13	rac-$[Me_2Si(2\text{-}Me\text{-}4,5\text{-}BzoInd)_2]ZrCl_2$	7,600
14	$[Me_2C(Ind)(Cp)]ZrCl_2$	15,500
15	$[Me_2C(Flu)(Cp)]ZrCl_2$	2,000
16	$[Me_2C(Flu)(Cp)]HfCl_2$	890
17	$[Ph_2C(Flu)(Cp)]ZrCl_2$	2,890

[a] Measured in kg polyolefin per mol metallocene per h per concentration of metallocene

2.2.2 Advantages and disadvantages of metallocene

Advantages of using metallocene catalyst [15]

1) Metallocene is single-site catalyst. Thus, this gives a uniform type of polyolefins chain such as narrow molecular weight distribution, narrow tacticity distribution and more uniform composition.

2) The utility of metallocene structure can produce better range of polyolefin types.

3) The utility of metallocene structure can control of polyolefins stereoregularity.

4) Metallocenes can control incorporation of comonomer. It has better performance in using comonomer to reduce the density or these require less

comonomer to produce the same density. Therefore, these reduce the production cost of linear-low density polyethylene.

5) Catalytic activity of metallocene is 10–100 times higher than Ziegler–Natta systems [8].

Disadvantages of using metallocene catalyst [16]

1) Require large amounts of cocatalyst such methylaluminoxane (MAO).
2) The lack of morphology control of the polymer particle.
3) Reactor fouling problem when these catalysts are used in homogeneous processes.

2.2.3 Methlylaluminoxane cocatalyst

Metallocene must be activated for the polymerization by cocatalysts such as methylaluminoxane (MAO) or borate compound. A new era in the polyolefins industry was started in 1976 when the discovery of methylaluminoxane (MAO) as cocatalyst by Sinn and Kaminsky [1,2]. The combination of metallocene catalyst and methylaluminoxane (MAO) as cocatalyst can improve the catalytic activity for ethylene polymerization due to the advantages of being able to adapt the ligands of the catalyst. The ratio of MAO/metallocene is served as [Al]/[Zr] molar ratio when zirconocene is used as a catalyst [17].

Methylaluminoxane consist of aluminium and oxygen atoms which they arranged alternately and free valences are saturated by methyl substituents. The simple structure of methlylaluminoxane is shown in Figure 2.5. However, structures detail of methylaluminoxane still not defined. The structure of MAO has been suspected to consist of a mixture of linear and cyclic oligomers as shown in Figure 2.6.

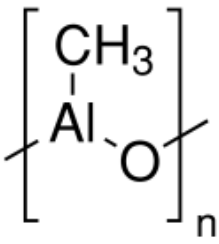

Figure 2.5 The simple structure of methylaluminoxane (MAO)

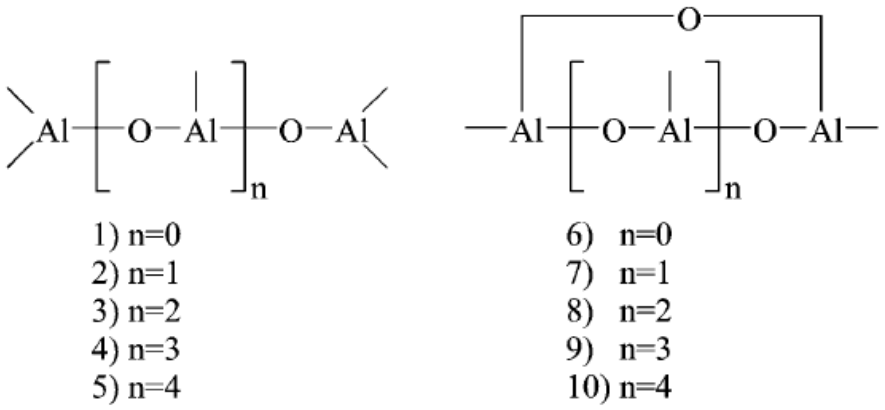

Figure 2.6 Structures of linear and cyclic methylaluminoxane (MAO) [18]

The major role of methylaluminoxane is forming active site of metallocene. In addition, it acts as an impurity scavenger and alkylation agent, it also prevents bimetallic deactivation of metallocene active sites. Methylaluminoxane is high reactively, so rapidly react with oxidizing compound in the reactor, thus preventing them from deactivating with the sensitive metallocene. Moreover, methylaluminoxane and other cocatalysts may also be used in the catalyst supporting process as support pretreatments. This may prevent catalyst deactivation and simplify active site formation [19].

The activated form of bis(cyclopentadienyl) zirconium dichloride (Cp_2ZrCl_2) is shown in Figure 2.7 the function of methylaluminoxane (MAO) rapidly exchanges its methyl substituents with the metallocene dichloride (halogen group). After complexation into the active species produce alkylated metallocene cation and MAO anion. The alkylated metallocene cation acts as active center for polymerization the latter.

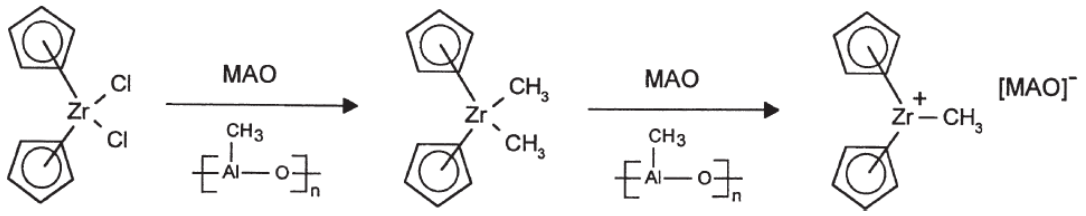

Figure 2.7 Activation of Cp_2ZrCl_2 [20]

2.2.4 Polymerization mechanism

Knowledge of the mechanisms and kinetics of polymerization process able to expect the structure of the polymer formed. Propagation and termination rates can determine molar mass and molar mass distribution. Also in the copolymerization system, they can determine comonomer content and distribution. The catalyst initiation and deactivation processes have an effect on the kinetics, and the cocatalyst may have an effect on the extent of the general mechanisms [20].

The mechanisms of polymerization of olefins by metallocene catalyst are compost of three reactions such as initiation, propagation, and termination reaction. These separate steps are explained below (Figure 2.8-2.9).

Initiation (Step1), cocatalyst methylaluminoxane (MAO) converts the zirconocene after complexation into the active species which has a free co-ordination position.

Propagation (Step 2-4), the monomer is assigned to the complex. In the next step, monomer inserts into the zirconium-alkyl bond and result in a new free co-ordination position. In step 4, repeat previous step, insertion of another monomer can produce polymer chain [21].

Termination

The most common chain transfer mechanisms of ethylene polymerization by metallocene catalyst are shown in Figure 2.9. β-H elimination (chain transfer to the metal) and chain transfer to the monomer are generally believed to be the dominant chain transfer reactions in the olefin homopolymerization. They lead to the formation of vinyl (CH_2=CH−R) or vinylidene (CH_2=C(R')−R) bond in ethylene or α-olefin polymerization, respectively. Chain transfer to the aluminum (cocatalyst) is usually of minor importance in ethylene polymerization. Chain transfer to the aluminum leads to the formation of an Al-CH_2-R compound. The aluminum-alkyl bond is highly reactive and the treatment with hydrochloric acid and ethanol − a standard laboratory washing procedure results in a saturated end-group in the polymer.

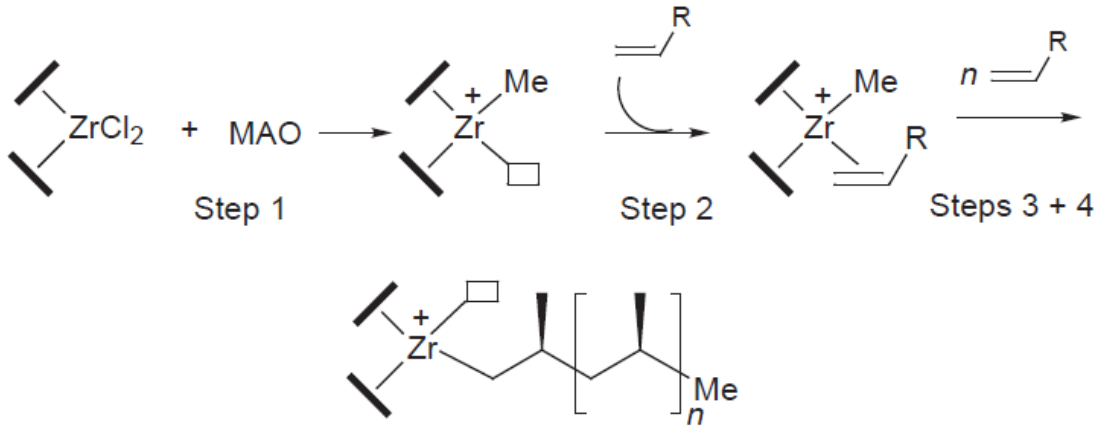

Figure 2.8 Initiation and propagation mechanism of the polymerization of olefins by zirconocenes [21]

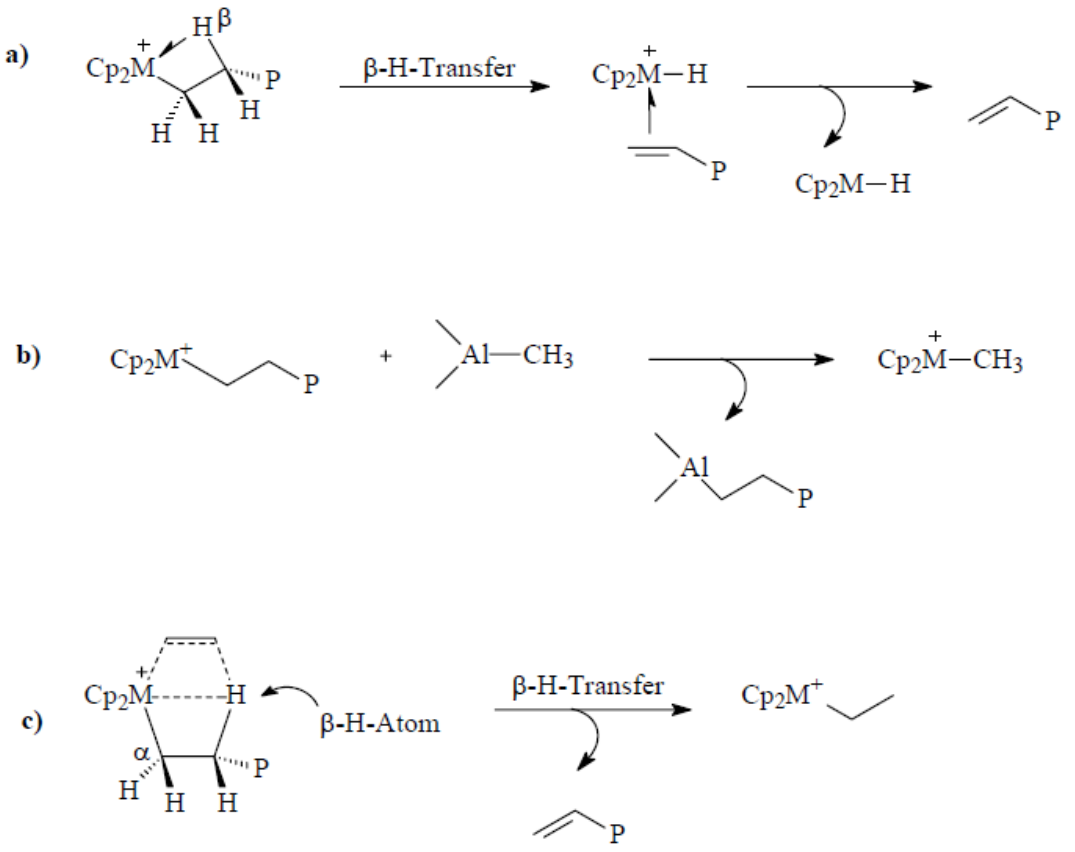

Figure 2.9 Termination mechanism of the polymerization a) β-H elimination, b) chain transfer to the cocatalyst, c) hydrogen transfer to the monomer. [22]

2.3 Heterogeneous system

Single-site catalysts such as metallocene and late transition metal catalysts are soluble in hydrocarbon solvents. They are classified as homogeneous system. The solution process is used for homogeneous system with high temperatures to prevent polymer precipitation [20]. Thermal control of the exothermic polymerization reactions is very difficult due to continuous operation of the polymerization process. As the polymer forms, it precipitates onto reactor surfaces and causes fouling problem. Changing metallocene/methylaluminoxane catalysts from homogeneous to heterogeneous catalyst is actually importance to make metallocene catalysts suitable for commercial use. However, catalytic activity of heterogeneous catalyst is lower than homogeneous system due to the partial deactivation or undesirable reactions among metallocene compound and active site on the support surface. Recently, heterogeneous system has been developed in order to enhance their value for commercial applications. Heterogeneous system such as slurry and gas phase processes are commonly used about 70% of the total industrial polyolefin production.

2.3.1 Supported metallocene

Before supported catalyst can be used in slurry or gas phase, soluble catalysts must be fixed onto insoluble support. The morphology of the obtained polymer depends on the morphology of support. For this reason, the types of the support have the effects on particle size distribution and bulk density of the polymer. The advantages of supported catalyst over their homogeneous system are [16]: (1) The supported catalyst require lower [cocatalyst]/[catalyst] ratio than homogeneous system to reach maximum activity. (2) The types of support can control the average molecular weight of polymer. (3) The molecular weight distribution (MWD) may broaden upon catalyst supporting and facilitating processability; (4) Some supported catalysts can be activated by common alkyl aluminum compounds instead of using more expensive MAO. And (5) different single-site catalysts can impregnate on the same support for producing polymers with tailored MWD and chemical composition distribution (CCD).

There are mainly three methods to prepare supported metallocene as follows [2];

Method 1 The basic principle of this method is impregnation of metallocene on the dry support (modified by previous treatment or not). At first, the support is reacted with the metallocene compound in a solvent such as toluene. Then, it is filtrated to obtain solid part and washed with a hydrocarbon. It is one of the first preparation method used. This method can be occurred at mild impregnation condition (room temperature) or at high temperatures and long contact time. The mixing temperature and the contact time are important parameters.

Method 2 The basic principle of this method is impregnation of MAO on the support followed by reaction with the metallocene compound. At first, the support is pretreated by a small amount of MAO in a solvent such as toluene under mild condition. After filtration and washing with toluene, MAO support is then mixed with metallocene. A modified version of this method involves the replacement of MAO by an aluminum alkyl.

Method 3 The third method deals with the synthesis of catalysts where metallocene ligands are chemically bonded to the support. This method is to first attach ligands such as cyclopentadienyl to the support. Then, add the metal compound, for example zirconium chloride, onto the carrier. Recently, titanium and neodymium halides have also been used to form the attached metallocene.

After each modification step, the support is filtered and washed. Finally, it is evaporated to dry under vacuum. These supported metallocenes can be used with either methylaluminoxane (MAO) or a common trialkylaluminum as the cocatalyst.

2.3.2 Clay supported metallocene

As a result of many disadvantages of homogeneous catalyst system, heterogeneous catalysts are recently performed to reduce these problems by immobilizing the metallocene on various supports such as calcium carbonate ($CaCO_3$), silica (SiO_2), alumina (Al_2O_3), Zinc oxide (ZnO) and clay**.**

Clay mineral is one in the type of support for metallocene catalysts, which is used as metallocene catalyst support after activation by MAO. The supported catalyst

initiated ethylene polymerization, effect as the excellent dispersion of the clay in the polyethylene matrix. The obtained polymer properties are improved [16]. Furthermore, clay also acts as cocatalyst for olefin polymerization by common alkylaluminums (trimethylaluminum, triethylaluminum, and triisobutylaluminum) without methylaluminoxane (MAO) [23,24]. Si-OH groups on the clay surface can produce a cocatalyst for metallocene activation by the reaction with Lewis acids (Figure 2.10). First, an aluminium alkyl, triisobutylaluminium ($Al(iBu_3)$, TIBA) or trimethylaluminium ($AlMe_3$, TMA) is added to a suspension of the dried inorganic carrier. In a second reaction step, metallocene is added to the suspension to produce active heterogeneous catalyst system for olefin polymerization.

Hiroshi Nakano et al [23] synthesized polyethylene using metallocene catalyst and acid treat clay as cocatalyst without methylaluminoxane (MAO). Clay was treat by various amount of 2,6 dimethylpyridine to control acid strength of clay. The resultant acid strength is in the oder of strong, intermediate, and weak. The result shows that strong acid site is able to activate metallocene complex. It makes a tight bonding between metallocene complex and clay to give higher Zr-content (or Ti, Hf-content) of the catalyst and higher activity for ethylene polymerization.

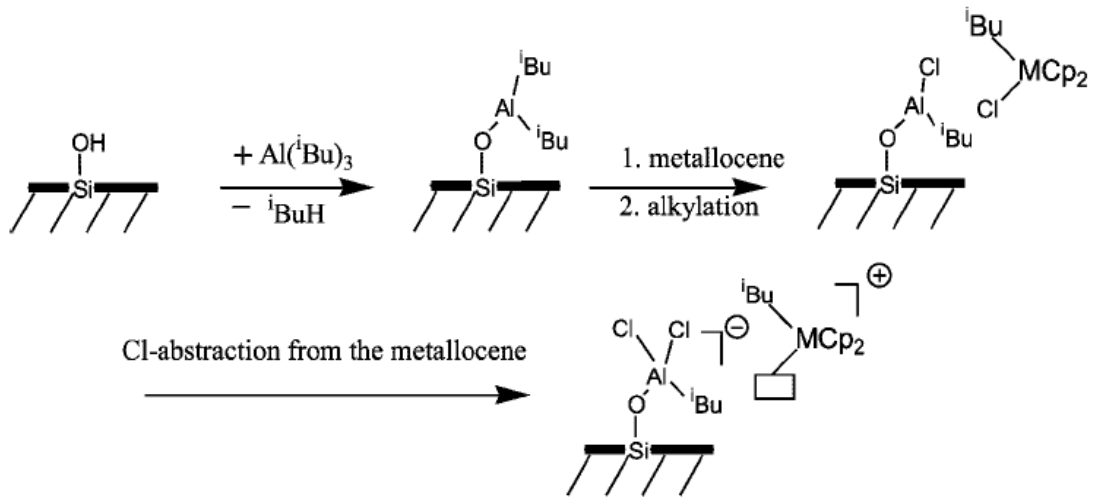

Figure 2.10 Supporting of a metallocene catalyst on clay layer [25]

2.3.3 Effect of supported metallocene

Immobilization of metallocene compounds on a supports have several effect on ethylene polymerization and the polymer properties. The aluminoxane/metallocene ratio of supported metallocene is significantly lower than homogeneous metallocene or it means that require smaller amount of methylaluminoxane (MAO) in the supported metallocene system. This heterogeneous system can be reduced methylaluminoxane/metallocene ratio from several thousands to the range 50 – 400. In the case of homogeneous system, deactivated metallocene by bimolecular processes are occurred, whereas support on the metallocene catalyst can act as spacer centers hindering bimolecular deactivation. Therefore, heterogeneous catalyst system need smaller amount of methylaluminoxane to reach the maximum activity. Generally, polyethylene which produced by single-site catalyst have narrow molecular weight distribution (MWD) about 1-2 range but supported metallocene catalyst can produce polyethylene with broader MWD about 2-5 range. Interactions between the metallocene and the support lead to the formation of different character of active sites. Therefore, supported metallocene can produced broad MWD polyethylene [2]. The obtained polymer also has broad chemical composition distribution (CCD) due to rather irregularity of catalytic active sites. Different single-site catalysts can impregnate on the same support for producing polymers with tailored MWD and chemical composition distribution (CCD). Supported metallocene system can control the polymer morphology. Mostly active sites place on the internal of porous support and small amount locate on external. The obtained polymer replicates the support morphology according to replication phenomenon. Thus, the morphology of the obtained polymer depends on the morphology of support. Furthermore, it able to control size of polymer [23].

However, when metallocene is attached to the support in heterogeneous system, the catalytic activity is significantly decreased compare to homogeneous system due to steric hindrance of support on metallocene or as a consequence of the fixation of the metallocene on less accessible sites in the support structure. Bunjerd Jongsomjit et al [26] compared the catalytic activity of homogeneous and heterogeneous system in ethylene/1-octene copolymerization. It can be found that the

catalytic activities of silica dioxide and titanium dioxide supported metallocenes are reduced 39% and 45 % of homogeneous catalyst respectively.

2.4 Polymer nanocomposite

Immobilization of catalyst on support is possible route to solve several disadvantages of homogeneous catalyst. Moreover, Addition of additives as support can improve polyethylene properties such as mechanical properties, thermal properties, barrier properties and flame resistant. Especially, nano-sized addivtives or nanofiller give better properties than micro-size additive. The polymer with the addition of nanofiller is called polymer nanocomposties.

The polymer nanocomposite is a material composed of polymer matrix and a filler called nanofiller because of its nano dimensions, typically 10-100 Å in at least one dimension. The nanofiller are dispersed in the polymer matrix in order to improve the performance properties of conventional polymer [5].

Polymer nanocomposites will be commonly used in a new era in materials development. The first reason for this development is their high mechanical properties. The complete dispersion of clay in a polymer matrix results in increase the number of reinforcing elements which can be applied load and diverged the developing cracks. Moreover, the linkage between the large surface area of the filler and the polymer matrix simplifies the stress transfer to the reinforcing phase. Thus, it can improve the tensile stress and toughness of the polymer [27].

The second major advantage of the nanocomposites is their improved barrier properties. The clay layers force a tortuous pathway for a permeant transversing the nanocomposites. Gas permeability through polymer films can be reduced by 50–500 times even with small loadings of nanoclays. The relevant research on polymer-clay nanocomposite concerns mostly oxygen, carbon dioxide, nitrogen and moisture barrier films [27].

The third reason for using nanocomposites is their good fire retardant properties. The large surface area of nanoparticles extremely increases their physical or chemical interaction with each other and with the macromolecules restricting the

mobility of the flowing phase in the polymer melt. The rheological effect of nanoparticles reducing the melt flow, result in improve the fire retardant properties of nanocomposites. However, it is not effect on ignitability [28]. During the combustion of the PE/clay nanocomposite, the formation of char is occurred. The heat release rate and mass lose rate reduce dramatically due to char can act as a barrier to mass and heat transfer.

2.4.1 Degree of dispersion

Some type of support such as clay is hydrophilic and does not well disperse in hydrophobic polyolefins such as polyethylene and polypropylene. The modification of support affect on degree of dispersion. There are three levels of the degree of dispersion which are shown in Figure 2.11 [29]. The first level is called phase separated because one can find two phases, polymer and clay (polymer does not enter between clay plates). The second level is intercalated. Polymer enters between clay plates to a lower extent which causes interlayer spacing increasing. The highest level is exfoliated. Plates of the fillers have random orientation in polymeric matrix. This structure is called nanostructure.

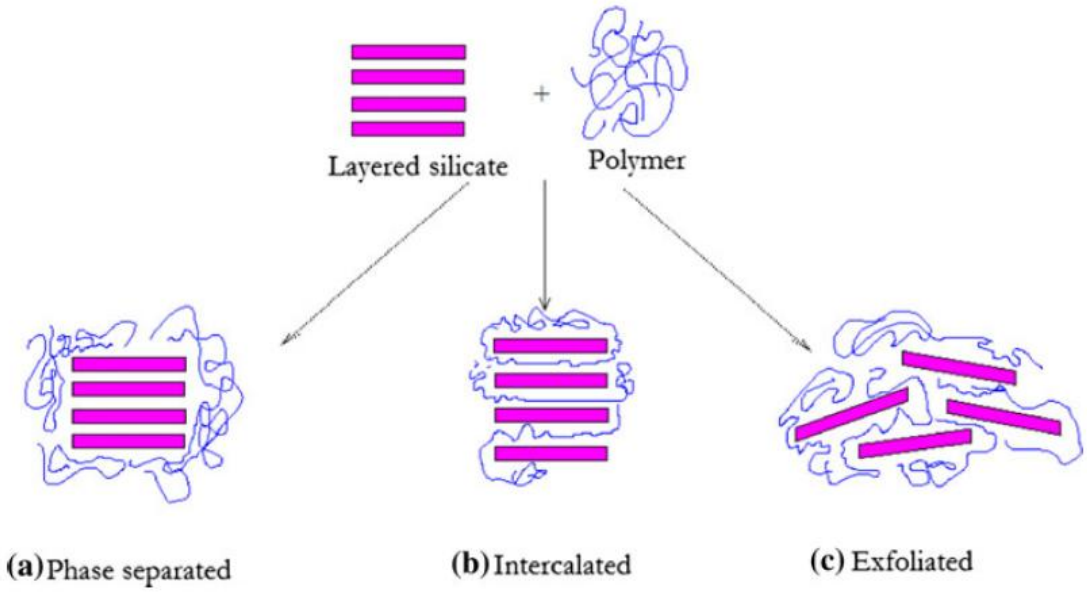

Figure 2.11 Three degree of dispersion of nanofiller in polymeric matrix [29]

The degree of dispersion of nanofiller in polymeric matrix can be characterized using wide angle X-ray diffraction (XRD) and transmission electronic microscopy (TEM). The peak of XRD curve can be determined interlayer spacing between individual platelets after compounding from bragg's equation [30]. That is $2d\sin\theta=n\lambda$, where n is the order of reflection which may be any integer (1, 2, 3, . . .), λ is the wavelength of incident wave, θ is the complement of the angle of incidence, and d is interlayer spacing between individual platelets. On the other hand, TEM is only gives qualitative information on the dispersion of nanoparticles, due to the small investigable area. In addition, structural and morphological data relate to very small samples, must be related to mechanical and rheological properties to obtain a proper scale-up of nanocomposites fabrication.

2.4.2 Preparation of polymer nanocomposites

There are mainly three method to synthesize polymer nanocomposites, such as solvent solution, melt blending and *in situ* polymerization.

Solvent solution can be used as the reaction medium in order to reduce the viscosity of the bulk medium and to distribute the heat more uniformly. Using the solution method, nanofillers are added to a polymer solution using solvents to integrate the polymer and filler molecules. In such cases, a solvent is chosen in which the polymer and monomer are soluble and the solvent also is able to swell the clay. After polymerization, recovery of polymer can be obtained by solvent vaporization, which leaves the polymer as non-volatile residue and cooling of the solution to cause precipitation of the polymer. The precipitate can be collected and dried. However, solvent vaporization process is characterized by the inherent difficulty in removing the last tract of solvent from the polymer. This difficulty arises from the fact that as the solution becomes more concentrated. Its viscosity increases sharply even if molten. Moreover, the use of solvents is not environmentally-friendly and it has the expense of solvent.

For melt blending process, require high temperature to operate. Because of high molecular weight polymers, such as polypropylene, polyethylene, and polystyrene can be melted at high temperature. First, add the modified filler powder

(such as modified clay) to the melt polymer. The modified filler is then mixed and complicated with the melt polymer in order to achieve uniform dispersion with high degree of dispersion of the filler. As a result of using high temperature to melt polymer, this can sometimes cause involve with considers to surface modifications. Clay surface modifications have an onset of degradation close to 200 °C, which is a basic temperature used for melt blending of the polymers [31].

In situ polymerization is one method used to prepare exfoliated and intercalated polymer/clay nanocomposites. Generally, there are two basic stages for *in situ* polymerization. First, the modified clay is added directly to the liquid monomer. Then *in situ* polymerization in the presence of clay is occured. Nanofiller is well distribution in polymer because of direct interaction between catalyst and surface of nanofiller, it possible to be exfoliation and intercalation of clay in the polymer matrix. The viscosity of the polymer/clay dispersions is important for the *in situ* formation of polymer nanocomposites. Processing conditions such as mixing temperature and time, shearing speed, molecular weight of prepolymer and incorporation of nanofillers are all important factors which influence the flow nature of the mixture. A lower viscosity means a better flow ability and more homogeneous mixing. Furthermore, low viscosity is very helpful in removing bubbles before any chemical reactions, which is a key step in polymer preparation.

2.5 Nanoclay

Among the polymer/inorganic nanocomposites, polymer/clay nanocomposite is one of the commonly used because of they can improve physical and mechanical properties including barrier properties, flammability resistance, environmental stability, and solvent resistance have received so much interaction.

2.5.1 Crystal structure of clay

2.5.1.1 Kaolinite

Layered silicates are clay minerals, consist of two structural units. The simplest is the 1:1 structure in kaolinite, which a silica tetrahedral sheet is linked with an aluminium octahedron sheet and share the oxygen atoms (Figure 2.12). The charge

within the layers is nearly balanced, and the chemical formula is $Al_4[Si_4O_{10}](OH)_8$ or $2Al_2O_3.4SiO_2.4H_2O$.

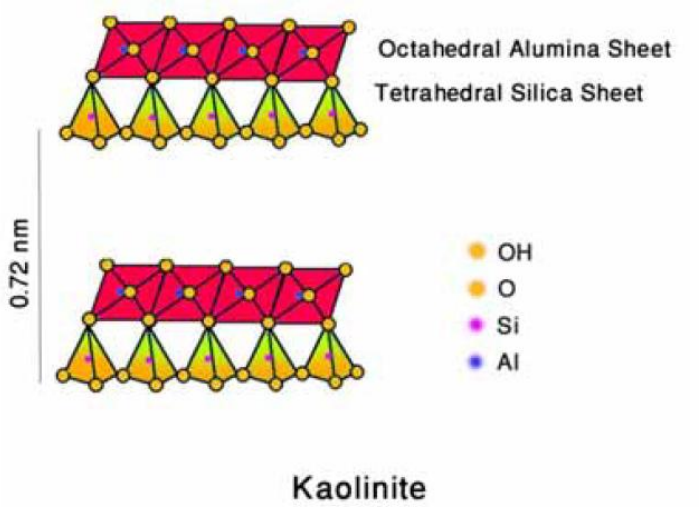

Figure 2.12 Structure of kaolinite [32]

2.5.1.2 Pyrophyllite

Pyrophyllite is called a 2:1 type of layered mineral that is composed of two linked silica tetrahedral sheets sandwiching an edge-shared octahedral sheet of alumina (Figure 2.13). The chemical formula is $Al_4[Si_4O_{10}](OH)_2$.

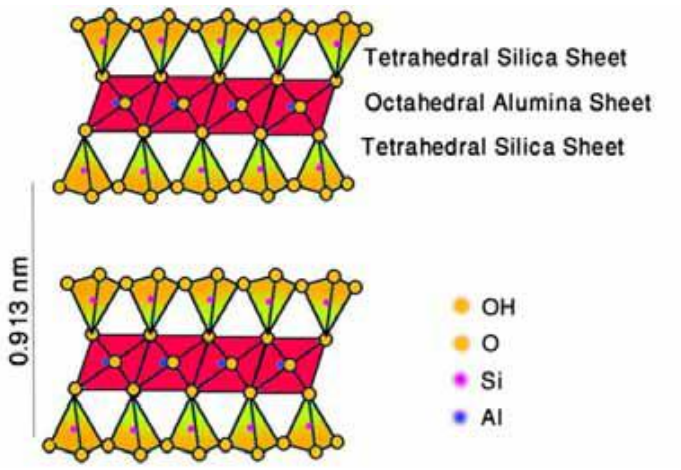

Figure 2.13 Structure of pyrophilite [32]

2.5.1.3 Montmorillonite

The most commonly use of the layered silicates is montmorillonite (MMT), owing to its natural abundance and high aspect ratio. MMT is a derivative of pyrophyllite. The difference between the crystal structure of MMT and pyrophyllite is that the latter is neutral, while the MMT has layer charges due to isomorphic substitution. Substitutions occur in the octahedral sheet with $Mg^{2+}$and $Fe^{2+}$for Al^{3+} (Figure 2.14).

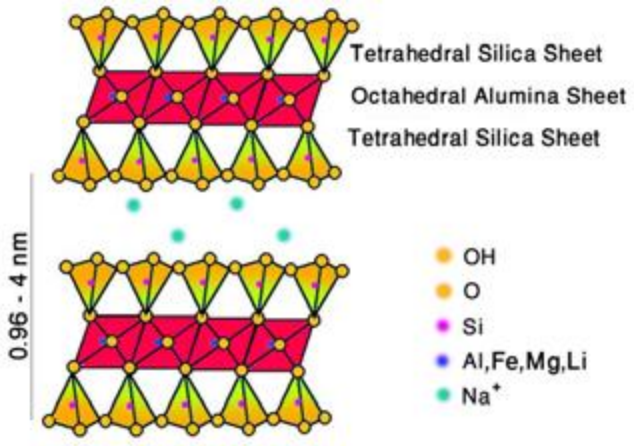

Figure 2.14 Structure of sodium montmorillonite [32]

2.5.2 Organoclay modification

The most commonly use of the layered silicates is montmorillonite. Due to isomorphic substitutions in the octahedral and tetrahedral sheets, the layers have a net negative charge. The montmorillonites (MMTs) also have wide range of layer charges or charge densities, depending on their source. The most common substitutions are Al^{3+} for Si^{4+} in the tetrahedral sheet and Mg^{2+} for Al^{3+} in the octahedral sheet. The negative charges are balanced by the interlayer alkali or alkaline earth metal cations, result in the 2:1 layers are linked together in stacks by electrostatic and van der Waals forces. Most of these inorganic minerals such as clay have forceful hydrophilic surfaces, which make them incompatible with the hydrophobic polymer matrices. Hydrophilic montmorillonites easily swell in water, and accordingly can be delaminated in water to give nano sized platelets, the inorganic surface cations of which can then be exchanged with organic cations. An exchange of inorganic cations

with organic cations reduces the surface energy of the clay layers and gives the clay organophilic and hydrophobic. It then becomes possible for compatible of the organic polymer with the clay layers and delaminate the clay platelets to individual layers. Even after the surface modification with the long-chain alkyl ammonium ions, layered silicate platelets are still partially polar. This technology is called organoclay modification which has been widely developed. Long-chain alkyl ammonium salts have been widely used for modification of the clay because they increase the basic spacing of the clay to broader. Due to lowering the surface energy, which can help to achieve exfoliation of the clay layers in the polymer matrix, result in a larger interlayer spacing. Figure 2.15 shows a surface modification of the clay process. Although, conventionally use the alkyl ammonium ions for the surface modifications, in recent years more advanced surface modifications for the fillers have been developed. These include surface modifications with reactive groups, initiator molecules or monomer molecules. Based on the interlayer spacing, it can also be predicted that either the alkyl chains lied flat on the silicate surface in monolayer, bilayer or pseudo-tri molecular arrangement, or radiate away from the surface. This may also help in predicting their possible interactions with the polymer matrix. It should be noted that the layered silicate platelets are still partially polar and therefore after drying would again form thick stacks of platelets joined together by electrostatic forces. Thus, it is very importance to give the uniform and nanoscale dispersion of these platelets in the polymers matrix by the action of thermodynamic and kinetic forces [31].

Aside from the conventional modifications by long-chain alkyl ammonium, several surface modifications were developed for inorganic fillers. Generally, the aim of these modifications is higher organophilization of the filler surface, in order to make them more easily exfoliation when disperse in the polymers. Extensively study the surface reactions on the clay in order to produce polymer chains with obtain more interlayer spacing of the clay platelets. However, modifications of inorganic fillers are difficult to complete the exchange of preformed long chains, due to their solubility property and steric hindrance problems. Figure 2.16a is showed two forms of polymerization reaction; (1) polymerization “to” the surface, the basic principle of this

method is exchanging a monomer on the filler surface. After that, it polymerize with the another external monomer. (2) polymerization "from" the surface, the basic principle of this method is bounding ionically of an initiator to the filler surface. After that, the initiator act to initiate the polymerization of an externally added monomer.

In addition to two choices above, there are other surface reactions, including surface esterification. The basic principle of this method is exchanging reactive surface modifications on the clay surface. Then, it can be used to carry on simple esterification reactions in oder to achieve higher interlayer spacing of the individual clay platelets. Additionally, the route to accomplish organophilization of the clay surface (Figure 2.16b) is physical adsorption. After surface modification of clay, organic substance is then physical adsorbed into vacant spaces on the clay surface. There are vacant spaces on the clay surface due to the area available per cation is normally larger the cation exchange the clay surface. These vacant spaces can be purposed for possession by organic molecules with hydrogen bonds. The lower interaction of this bond reduced electrostatic forces of interaction among the clay platelets.

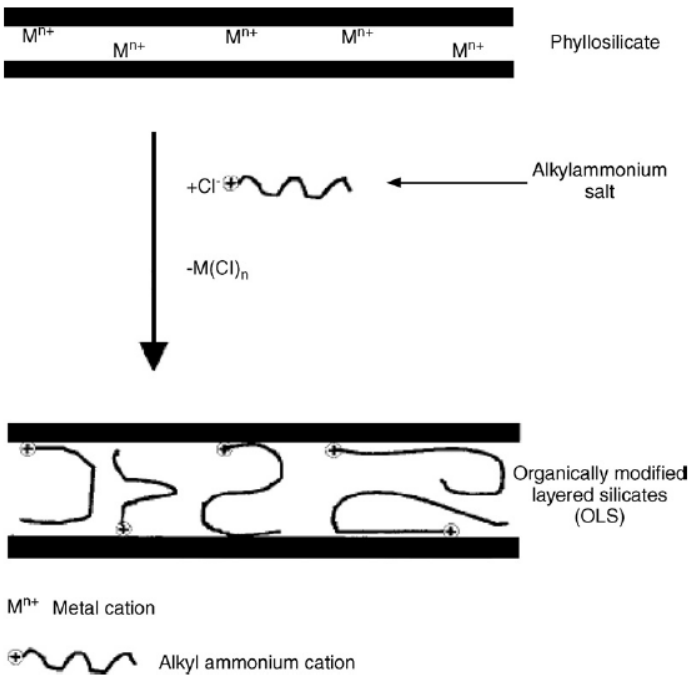

Figure 2.15 Surface modification of the clay process. [33]

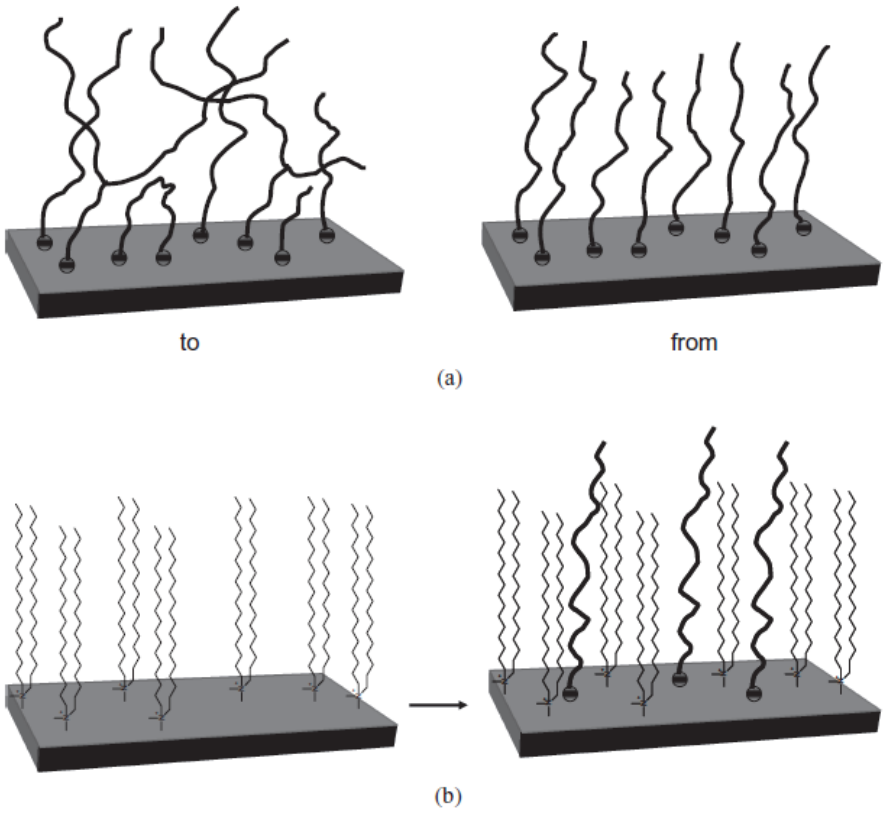

Figure 2.16 (a) The polymerization “to” the surface and polymerization “from” the surface; (b) Physical adsorption onto the clay surface [31].

2.6 Characterization of polymer nanocomposite [32]

2.6.1 Scanning electron microscopy (SEM) and atomic force microscopy (AFM)

Morphology and shape of surface of material in polymer nanocomposite are determined by SEM. Polymer nanocomposite especially when low amount of nanoparticles is added to polymer, polymeric chains cover the nanoparticles, In the case of high amount of nanoparticles is added to polymer, the surface image of SEM can be detected nanoparticle in matrix. However, when low amount of nanoparticles is added to polymer, it cannot be seen nanoparticles. The way for determined of nanoparticles in polymeric matrix is using cross sectional SEM image. For preparation images of cross section of polymeric nanocomposite, immerse a small amount of sample in liquid nitrogen closely a minute to ensure it is completely frozen.

Then, remove from the liquid nitrogen and suddenly broke it. AFM also determined surface of thin film sample, and can be seen nanoparticle in polymeric matrix at high loading nanoparticle.

2.6.2 Transmission electron microscopy (TEM)

TEM is widely used as a tool for direct visualization of the nanocomposite structure of polymer nanocomposites. It is the simplest bright-field mode. It has exists sufficient contrast for the transmitted electrons between the polymer matrix and most filler. In the extreme case, high-resolution TEM can even provide a qualitative picture of the inorganic filler crystal structure. For one TEM information obtained, requires a very little piece of material and cannot be certain that this is representative of the whole. The morphology can only be clearly determined by either sampling enough of the material.

2.6.3 X-Ray Diffraction (XRD)

Interlayer spacing or d-spacing of the clay can be determined by XRD. From the peak of XRD, interlayer spacing is determined by Bragg's equation. If the interlayer spacing in the polymer nanocomposite is unchanged from the pristine clay, this indicates that clay is not good dispersion the in polymer metrix. If the interlayer spacing increases, indicates that its degree of dispersion is intercalation. Since no peak of XRD is detected, it mean degree of dispersion is exfoliated. Unfortunately, this same situation will occur if the clay has extensively disordered, so XRD information alone is not enough to identify the morphology.

2.6.4 Thermo Gravimetric Analysis (TGA)

TGA is an experimental technique in which the weight of a sample is measured as a function of sample temperature or time. The sample is generally heated at a constant heating rate. The informations from TGA measurement are showed as TGA curve in which percent weight is plotted with temperature. The sample might be loss due to different effects as following; (1) Evaporation of volatile constituents; such as desorption of gases and moisture (2) Thermal decomposition in an inert atmosphere with the formation of gaseous products, and (3) Oxidation of constituents.

TGA are often equipped with DTA (differential thermal analysis). In addition to showing the energetic nature of weight loss events, the DTA signal can also show thermal effects that are not accompanied by a change in mass, e.g. melting, crystallization or a glass transition.

2.6.5 Differential scanning calorimetry (DSC)

DSC is the most widely used as a tool for thermal techniques. This provides fast and simple method for obtaining beneficial information about a material. The energy change of the sample is measured while a sample is heated, cooled or held isothermally. The energy changes enable the user to find and measure the transitions that occur in the sample quantitatively such as measurement of glass transitions.

2.6.6 Cone calorimeter

Cone calorimeter is one of the most effective medium-sized polymer fire behavior tests. The cone calorimeter measures the rate at which heat is released in a fire. This instrument calculates the quantity of heat released per unit of time and surface area (heat release rate; HRR) expressed in kW/m^2. The evolution of the HRR over time, especially the value of its peak (pHRR), is used to determine the fire properties. Currently, many fire retardant fillers for the preparation of polymer nanocomposites have been proposed.

2.6.7 Nuclear Megnetic Resonance (NMR)

The NMR phenomenon is based on the fact that nuclei of atoms have magnetic properties that can be determined chemical information. It is the response of the atomic nucleus that is measured in the form of a spectrum. In some atoms (eg 12C, 16O, 32S) these spins are paired and cancel each other out so that the nucleus of the atom has no overall spin. However, in many atoms (^{1}H, ^{13}C, ^{31}P, ^{15}N, ^{19}F etc) the nucleus does possess an overall spin. This movement induces a magnetic moment. Different nuclei spin or resonate at different frequencies. Thus, the nucleus of a particular atom may behave differently in a different surrounding. For example, the nucleus of C may spin differently when attached to H compared with the one that is

attached to O. This response is due to shielding of the particular mucleus by neighboring nucleus.

When the nucleus is exposed to radio waves of a magnetic field, it causes the magnetic field of the nucleus to resonate. This induces a charge that flows through a coiled wire that surrounds the specimen in an NMR spectrometer. This signal is detected and transformed into peaks that correspond to specific nuclei. Before the peaks are identified, the spectrum has to be chemically shifted with the most shielded molecules. The peak corresponding to this is assigned. The units of chemical shifts are usually read as ppm (part per million).

2.6.8 Dynamic mechanical analysis (DMA)

Dynamic mechanical analysis (DMA), also known as dynamic mechanical thermal analysis (DMTA), is technique used to determine the mechanical and thermal behavior of polymer nanocomposite. This technique is widely use for characterizing the viscoelastic nature of polymer. The basic principle of this technique is applying oscillating force to the sample. Result in, the sample is deformation. From this, the stiffness of the sample can be determined and the sample modulus can be calculated. By measuring the time lag in the displacement compared to the applied force it is possible to determine the damping properties of the sample.

2.6.9 Gel Permeation Chromatography (GPC) [34]

Polymer nanocomposite is important to consider the polydispersity index (PDI) and the molecular weight including the number average molecular weight (M_n), the weight average molecular weight (M_w), the size average molecular weight (M_z), or the viscosity molecular weight (M_v). These can be determined by GPC in which separates polymers on the basis of molecular size. The sample is fed at the top of the column and then is purified with a solvent. The polymer molecules diffuse through the gel at rates depending on their molecular size. The smaller polymers spend more time traveling through the pores of the gel and are eluted later than the larger polymers which spend less time in the pores. They are detected by a differential refractometer from which a molecular size distribution curve is plotted.

CHAPTER III

EXPERIMENTAL

In this study, PE/clay nanocomposite was synthesized via the *in situ* polymerization with MAO/zirconocene catalyst as various conditions. The experiments were divides into four parts:

(i) Preparation of nanoclay
(ii) Preparation of catalyst
(iii) Ethylene polymerization
(iv) Characterization of nanoclay and PE/clay nanocomposite

All chemicals and procedure of experiments are described as follows.

3.1 Chemicals

All chemicals which were employed in the experiments are listed in Table 3.1 as follows

Table 3.1 Chemicals were used in experiments

NO.	Chemicals	Supplier	Details
1	Ethylene gas	National Petrochemical Co., Ltd. Thailand.	99.9%
2	Methylaluminoxane	Tosoh Akso, Japan	10% in toluene
3	Rac-ethylenebis(indenyl) zirconium dichloride	Aldrich Chemical company	-
4	Nanoclay (TOB_2, TOB_3)	Thai Nippon Chemical industry Co., Ltd., Thailand.	-
5	Toluene	EXXON Chemical Ltd., Thailand.	-
6	Argon	Thai Industrial Gas Co., Ltd.	99.999%
7	Hydrochloric acid	Sigma.	Fuming 36.7%
8	Methanol	SR Lab	commercial grade
9	1-Hexene	Alrich Chemical Company, Inc.	99+%

3.2 Equipments

All kinds of equipments were used in the experiments are listed below:

3.2.1 Glove Box

Glove Box System 30905C from Vacuum Atmospheres Company of United States of America was used for preparation of catalyst in order to prevent catalyst deactivation.

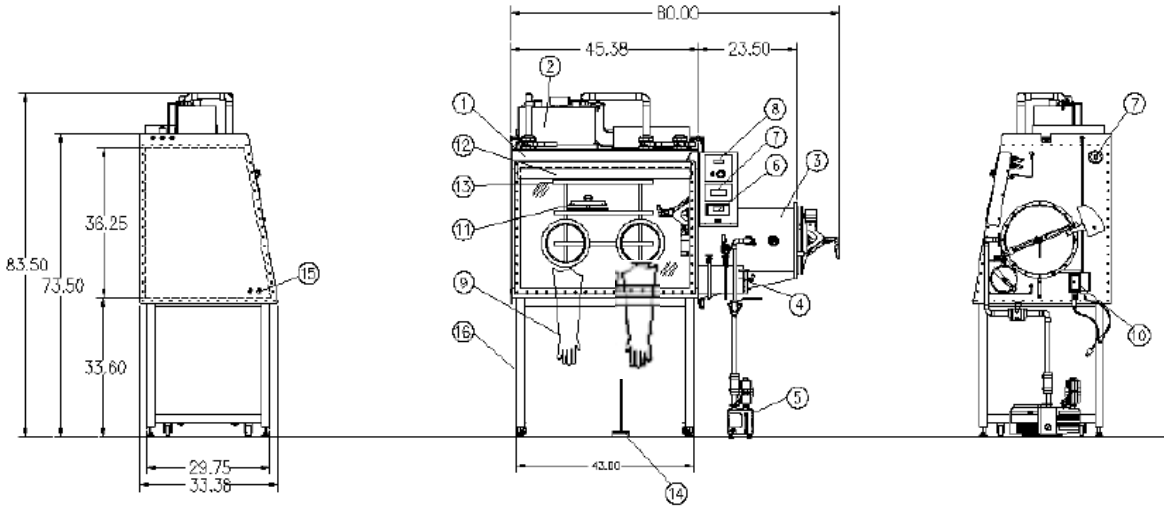

Figure 3.1 Glove box schematic diagram

1. Omni vac chamber
2. Purification unit
3. 15”diax24”lg. antechamber
4. 6”dizx12”lg. mini antechamber
5. Vacuum pump, 4.1cfm
6. Control panel
7. Moisture analysis (Optional)
8. Oxygen analysis (Optional)
9. Butyl rubber glove
10. Electrical J-Box
11. Glove port cover
12. Fluorescent light
13. Shelves
14. Foot switch
15. Feedthru, ¼” NPT, 2 PL
16. Support frame

3.2.2 Schlenk line

Schlenk line composts of two parts, the first part is attached to vacuum system and another part is attached to purified inert gas such as Argon. Vacuum system part is connected with solvent trap in order to trap solvent before pass through vacuum pump. The Argon system is connected with glass tubing contained quartz wool and sodium hydroxide (NaOH), which increase pressure drop before release to atmosphere through oil bubble.

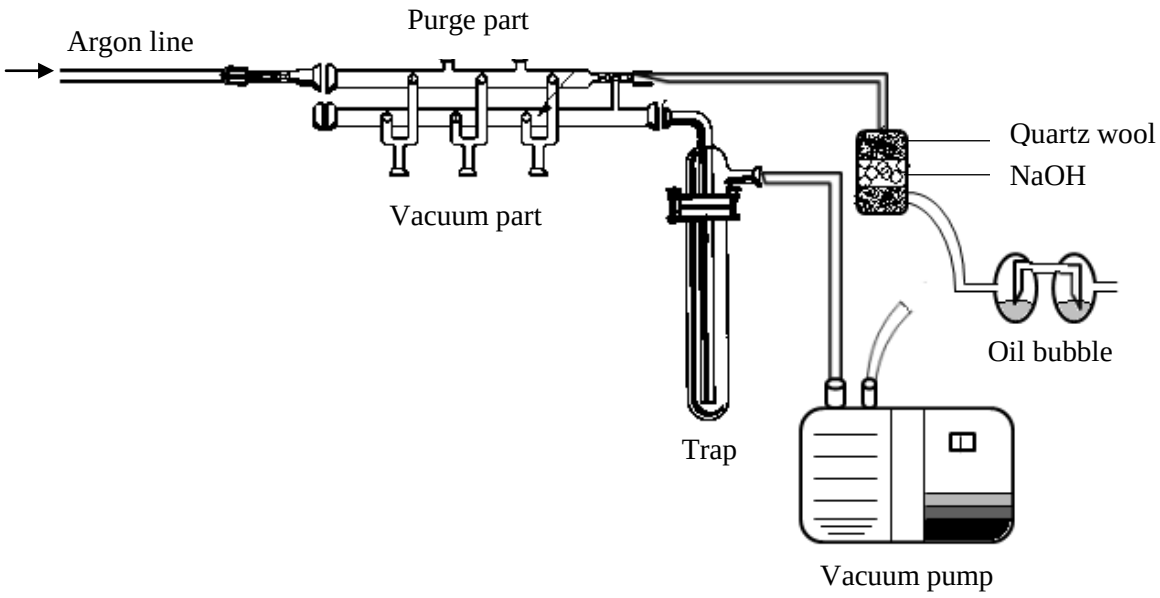

Figure 3.2 Schlenk line

3.3.3 Reactor

Polymerization was carried out in a 100 mL semi-batch stainless steel autoclave reactor equipped with a magnetic stirrer.

3.3.4 Magnetic stirrer and hot plate

Magnetic stirrer and hot plate moded RCT Basic from IKA Labortechnik is used to prepare catalyst solution and mix reactants for polymerization.

3.3.5 Cooling system

Cooling system was used for condense the recently evaporated solvent in distillation system.

3.2.6 Schlenk tube

Schlenk tube consists of ground glass joint connected with side arm. Side arm is three-way glass valve. The sizes of shlenk tube are 50, 100 and 200 ml which used to calcine nanoclay and keep chemicals which are sensitive to oxygen and moisture.

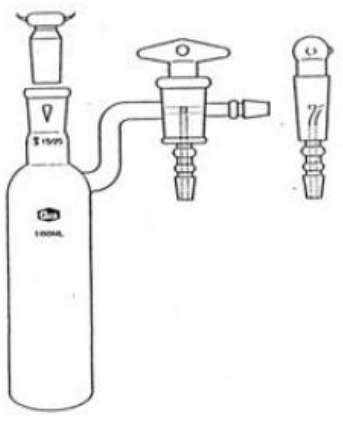

Figure 3.3 Schlenk tube

3.3.7 Vacuum pump

Vacuum pump model 195 from Labconco Coporation was effective 10^{-4} – 10^{-3} mmHg pressure. The range of this pressure was enough for vacuum supply to the vacuum line in the schlenk line. Suction port is connected to the chamber or piping to be vacuum-pumped.

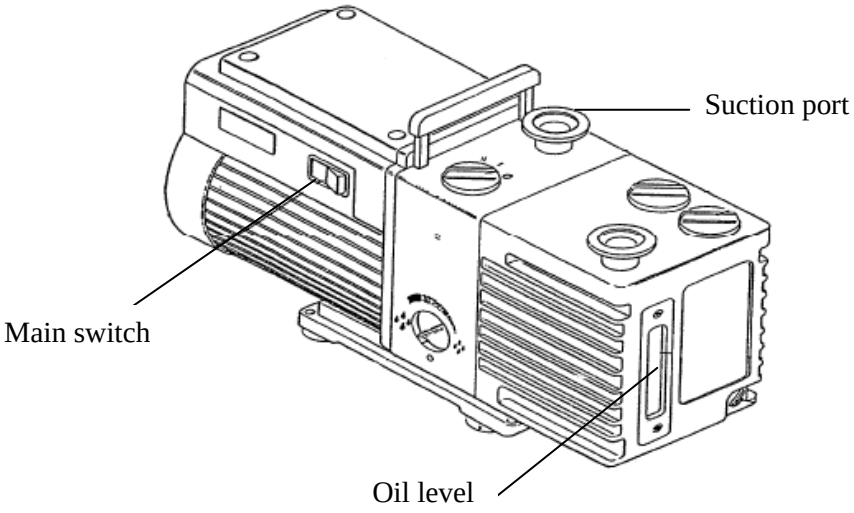

Figure 3.4 Vacuum pump

3.3.8 Inert gas purification system

Argon (Ar) was used in the experiment as inert gas. It was used for preparation of catalyst and polymerization. Argon purification system composts of molecular sieve, columns of BASF catalyst R3-11G, and dehumidify unit. Molecular sieve was used to remove moisture. BASF catalyst acts as scavenger to remove oxygen contamination in the argon before preparation of catalyst and polymerization, due to high reactivity of catalyst and cocatalyst with oxygen. Dehumidify unit composts of two glasswares which are packed with sodium hydroxide (NaOH) compound and phosphorus pentoxide (P_2O_5) compound, respectively. For the purpose of moisture elimination, it can reduce catalyst deactivation.

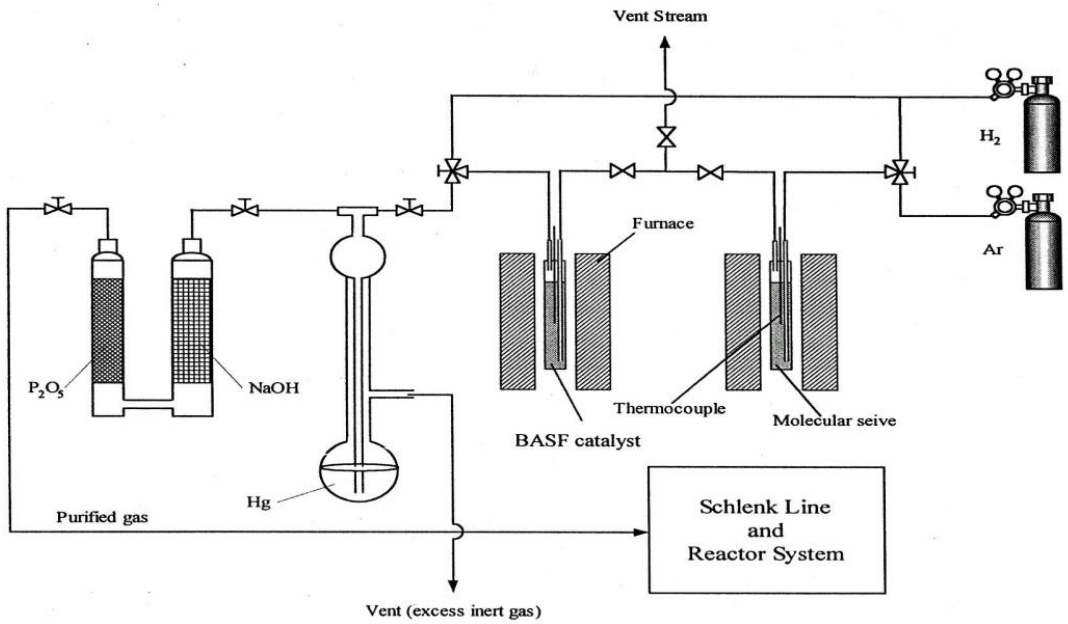

Figure 3.5 Inert gas purification system

3.3.9 Polymerization line

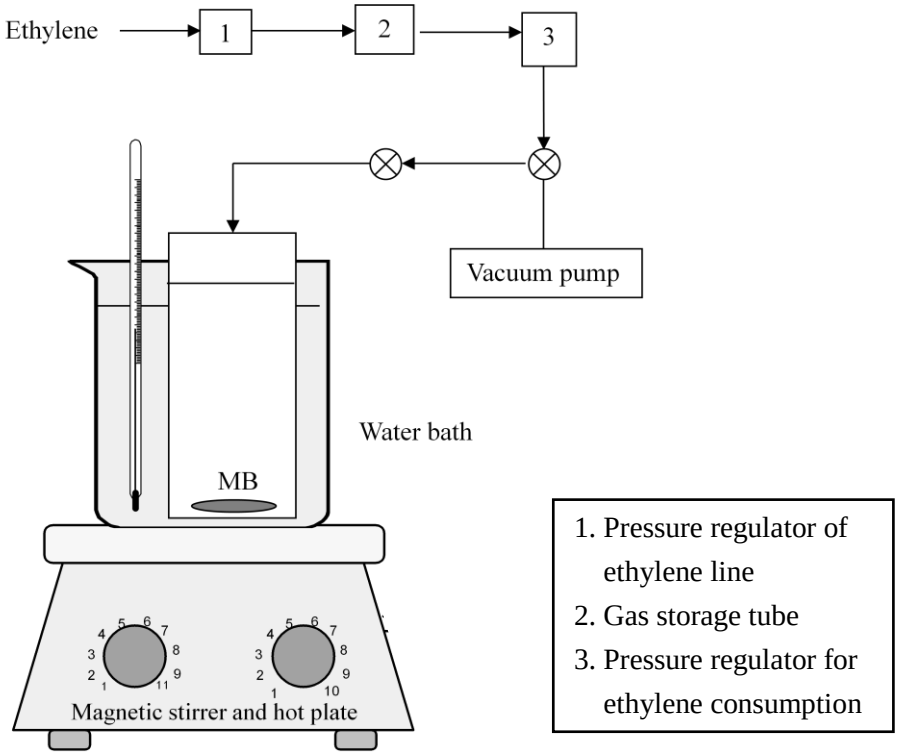

Figure 3.6 Slurry phase polymerization diagram

3.3 Preparation of nanoclay

The nanoclay was heated at 150°C for 2 h under atmosphere, and then heated at 150°C for 2 h under argon atmosphere.

3.4 Preparation of catalyst

In the glove box, $Et(Ind)_2ZrCl_2$ 0.0083 g ($1.98x10^{-5}$ moles) was added in 20 mL of toluene solution stirred at room temperature at least 30 min or until giving yellow transparent solution.

3.5 Ethylene polymerization

All obtions were conducted under argon atmosphere using schlenk techniques and/or glove box.

3.5.1 *In situ* ethylene polymerization

The ethylene polymerization reactions were performed in a 100 ml semi-batch stainless steel autoclave reactor equipped with a magnetic stirrer. From the beginning, the desired amount of the nanoclay (5, 10, 20, and 40 wt%) and methylaluminoxane (MAO) 1.1 mL ($[Al]_{MAO}/[Zr]=1135$) were mixed and stirred for 30 min aging at room temperature. Then, $Et(Ind)_2ZrCl_2$ 1.5 mL ($5x10^{-5}$ M) along with toluene (to make total volume of 30 ml) was put into the reactor. The reactor was frozen in liquid nitrogen to stop reaction for 10 min, and then the reactor was evacuated to remove argon. The reactor was heated up to polymerization temperature (70°C). Then, ethylene was fed into the reactor equipped with pressure gauge to start polymerization. After all ethylene was consumed (6 psi from pressure gauge), the reaction was terminated by addition of acidic methanol (0.1% HCl in methanol) and stirred over night. Finally, filtered this suspension to obtain wet polymer, washed it with methanol and dried at room temperature to obtain dried polymer as white power.

3.5.2 Effect of aging time

The ethylene polymerization reactions were performed in a 100 ml semi-batch stainless steel autoclave reactor equipped with a magnetic stirrer. From the beginning,

appropriate amount of the nanoclay from section 3.5.1 and 1.1 mL of methylaluminoxane (MAO) ($[Al]_{MAO}/[Zr]$=1135) were mixed and stirred for 30, 60, 90 and 120 min aging at room temperature. Then, the similar procedure as the *in situ* polymerization was conducted. The stirred times was varied at 60, 90 and 120 min.

3.5.3 *In situ* ethylene/1-hexene copolymerization

The ethylene polymerization reactions were performed in a 100 ml semi-batch stainless steel autoclave reactor equipped with a magnetic stirrer. From the beginning, the desired amount of the nanoclay (5, 10, 20, and 40 wt%) and methylaluminoxane (MAO) 1.1 mL ($[Al]_{MAO}/[Zr]$=1135) were mixed and stirred for 30 min aging at room temperature. Then, $Et(Ind)_2ZrCl_2$ 1.5 mL ($5x10^{-5}$ M) along with toluene (to make total volume of 30 ml) was put into the reactor. The reactor was frozen in liquid nitrogen to stop reaction for 10 min, and 1-hexene (ethylene:1-hexene = 1:0.5) was put into the reactor. Then, the reactor was evacuated to remove argon. The reactor was heated up to polymerization temperature (70°C). Then, ethylene was fed into the reactor equipped with pressure gauge to start polymerization. After all ethylene was consumed (6 psi from pressure gauge), the reaction was terminated by addition of acidic methanol (0.1% HCl in methanol) and stirred over night. Finally, filtered this suspension to obtain wet polymer, washed it with methanol and dried at room temperature to obtain dry polymer as white power.

3.6 Characterization

The instruments used for characterizing PE/clay nanocomposites and nanoclay are detailed as follow**;**

3.6.1 Characterization of nanoclay

3.6.1.1 X-ray diffraction analysis (XRD)

XRD was used to determined crystalline size of nanoclay and crystallinity in the polymer nanocomposites. Sample was put into plastic sample holder, and then excess sample was smooth by glass side. XRD pattern of nanoclay was observed using SIEMENS D-5000 X-ray diffractometer at Center of Excellence on Catalysis

and Catalytic Reaction Engineering, Chulalongkorn University. The observation was proceeded by using CuK_α (λ = 1.54439 Å) radiation and the operating conditions for measurement are listed below;

2θ range of detection	: 10-80 degree
Scan range	: 2.4 degree/min
Temperature	: 25°C (room temperature)

3.6.1.2 Thermo Gravimetric Analysis (TGA)

TGA was used to determine thermal stablility in term of percent weight in sample as a function of temperature. Sample preparation consists of weighing a crucible, loading the sample about 2-3 mg into the crucible, weighing the full crucible, and setting it on a tray. Nanoclay was analyzed by thermo gravimetric, PerkinElmer Thermal Analysis Diamond TG/DTA at Center of Excellence on Catalysis and Catalytic Reaction Engineering, Chulalongkorn University. The analysis was performed under nitrogen atmosphere gas at gas flow rate of 100 mL/min. The sample was heated from 25°C to 600°C at a constant rate of 10°C/min and then cooled naturally.

3.6.1.3 Fourier transform infrared spectroscopy (FTIR)

FTIR was used to identified specific structural characteristics (eg. functional group or molecular structure) of the chemical group from the vibrational properties. The sample was weighed a small amount (2-5 mg) directly on the KBr plates. Then, add one drop of solvent to dissolve the sample. Nanocaly were analyzed by Nicolet 6700 FTIR spectrometer which belong to Mektec Manufacturing Corporation (Thailand) Ltd. at Center of Excellence on Catalysis and Catalytic Reaction Engineering, Chulalongkorn University.

3.6.2 Characterization of PE/clay nanocomposites

3.6.2.1 Scanning electron microscopy (SEM)

SEM was used to observe the morphology of polymer nanocomposites. The sample was conductive to prevent charging by coating with gold particle by ion

sputtering device. Sample was analyzed by JEOL JSM-6400 scanning electron microscopy at Center of Excellence on Catalysis and Catalytic Reaction Engineering, Chulalongkorn University.

3.6.2.2 Differential scanning calorimetry (DSC)

DSC was used to determine the thermal properties especially melting temperature (Tm) in term of heat flows associated as a function of time and temperature. Prepare sample about 3-13 mg prior to use. The heating cycle was run twice. In the first scan, sample was heated from 50 to 150 °C in oder to premelt prior to first used and cooled to room temperature. Then, the sample was reheated as the same conditions in the second scan. The melting temperature was determined by a Perkin-Elmer diamond DSC form MEKTEC, at Center of Excellence on Catalysis and Catalytic Reaction Engineering, Chulalongkorn University. The analyses were performed at the heating rate of 20°C/min.

3.6.2.3 Thermo Gravimetric Analysis (TGA)

TGA was used to determined thermal stablility in term of percent weight in sample as a function of temperature. Sample preparation consists of weighing a crucible, loading the sample about 2 to 3 mg into the crucible, weighing the full crucible, and setting it on a tray. PE/clay nanocomposites were analyzed by thermo gravimetric, PerkinElmer Thermal Analysis Diamond TG/DTA at Center of Excellence on Catalysis and Catalytic Reaction Engineering, Chulalongkorn University. The analysis was performed under nitrogen atmosphere gas at gas flow rate of 100 mL/min. The sample was heated from 50°C to 600°C at a constant rate of 10°C/min and then cooled naturally.

3.6.2.4 Small angle X-ray diffraction analysis (SAXRD)

XRD was used to identify the sample by comparison with reference sample and determined the interlayer spacing of nanoclay in polymer matrix. Sample was put into plastic sample holder, and then excess sample was smooth by glass slide. XRD pattern of PE/clay nanocomposites were observed using Bruker AXS Model D8 Discover X-ray diffractometer with VANTEC-1 Detector (Super Speed Detector)

connected to a personal computer for fully control of the XRD analyzer at Scientific and Technological Research Equipment Centre (STREC), Chulalongkorn University. The observation was proceeded by using Cu radiation and the operating conditions for measurement are listed below;

2θ range of detection	: 1-10 degree
Increment	: 0.02 degree/step
Scan speed	: 0.5 sec/step
Temperature	: 25°C (room temperature)
Voltage	: 40 kV
Current	: 40 mA

3.6.2.5 Nuclear Megnetic Resonance (^{13}C NMR)

^{13}C NMR was used to evaluate percent insertion of comonomer in copolymer. For sample preparation, LLDPE/clay nanocomposite was solution, in which prepared by using 1,2,4-trichlorobenzene as solvent and chloroform-d for internal lock, then heat until ensure it was solution. The ^{13}C NMR spectra were recorded at 110°C using JEOL JNM-A500 operating at 125 MHz.

3.6.2.6 Transmission electron microscopy (TEM)

TEM was used to investigate degree of dispersion of nanoclay in the polymer matrix. Sample was analyzed by JEM-2100 transmission electron microscopy at Scientific and Technological Research Equipment Centre (STREC), Chulalongkorn University.

CHAPTER IV

RESULTS AND DISCUSSION

This chapter provides the informations about the synthesis of PE/clay nanocomposite via *in situ* polymerization with zirconocene catalyst upon various conditons. The major objective of this research is to examine the effect of nanoclay types, nanoclay loading, and mixing time on the catalytic activity and properties of the PE/clay nanocomposites.

4.1 Characterization of nanoclay

4.1.1 Size and composition

Figure 4.1 shows XRD patterns of nanoclay. The sizes of nanoclay were investigated by X-ray diffraction (XRD). From Debye-Scherrer formula [35], it was confirmed that the average crystallite size of TOB_2 and TOB_3 are 3.98 and 7.48 nm, respectively.

The clay's XRD patterns present the peaks in the position (2θ) 20, 26.5, and 36°, corresponding to montmorillonite (MMT) crystalline structure [36]. The position at 10.1° corresponds to illite clay mineral, which is a phyllosilicate or layered alumino-silicate. This indicates that these nanoclay are mixed-layer montmorillonite/illite, which are composed of two discrete species. One is montmorillonite with low interlayer charge. Its interlayers are hydrated by at least two layers of water molecules. The second species is illite. Its interlayers are dry. The positions at 20 and 26.5° correspond to the quartz, which generally found in clay. The position at 21.8° corresponds to plagioclase feldspars mineral [37], which is classified into silicate group. It commonly composts of sodium, potassium, and calcium. The peak at 31° corresponds to pyrite mineral, which is an iron sulfide with the formula FeS_2. These assumed compositions of the clay (montmorillonit, illite, quartz, and feldspars) are confirmed by the nature of clay. It may be due to the fact that layers of montmorillonite are naturally converted to layers of illte by a reaction as follow [38];

Montmorillonite Feldspar

$$K^{+}_{0.33}(Al_{1.50}Fe^{3+}_{0.23}Mg^{2+}_{0.27})(Al_{0.06}Si_{3.94}O_{10}(OH)_2 + 0.47KAlSi_3O_8 =$$

$$K^{+}_{0.80}(Al_{1.50}Fe^{3+}_{0.23}Mg^{2+}_{0.27})(Al_{0.53}Si_{3.47})O_{10}(OH)_2 + 1.88SiO_2$$

Illite Quartz

In the above reaction, the conversion of montmorillonite to illite does not change the composition of the octahedral layers.

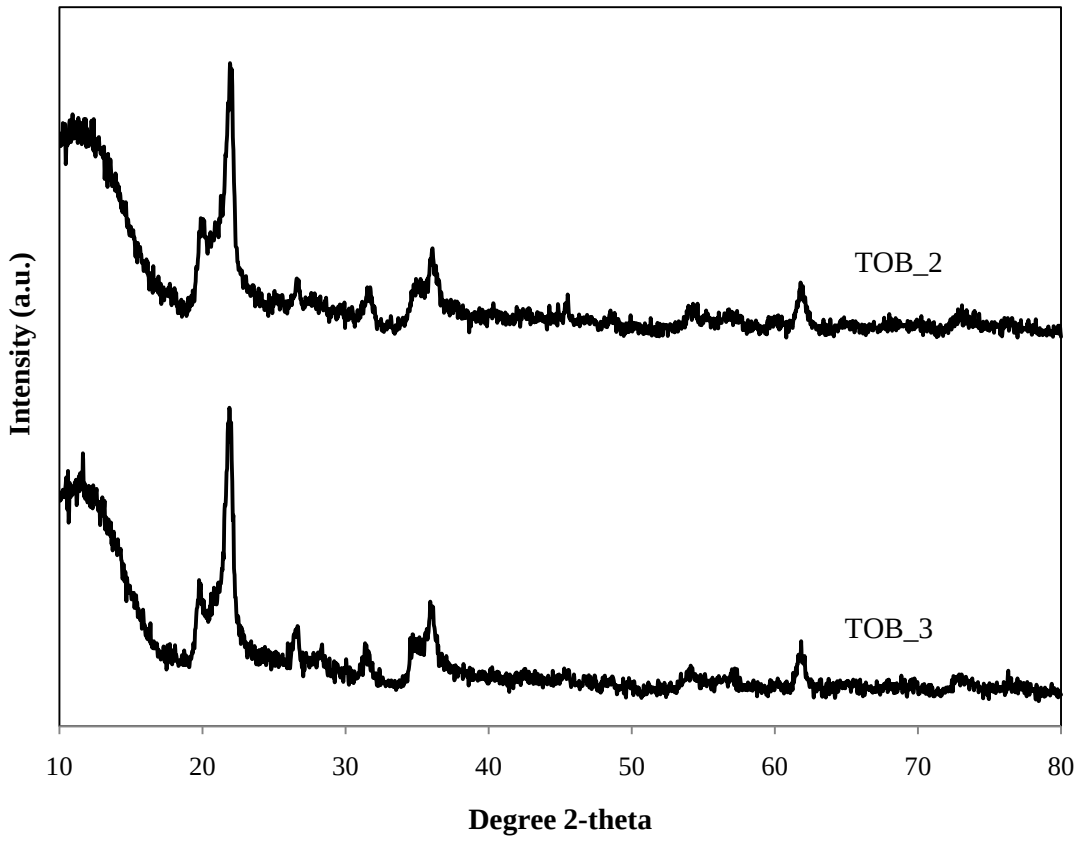

Figure 4.1 XRD patterns of nanoclay

4.1.2 Functional group

The functional groups of two types of nanoclay were compared by FTIR spectra. Their FTIR spectra are shown in Figure 4.2. It was found that the wavenumbers of obtained peaks are not different and the absorbances are also rather equal. FTIR spectra show the main peaks at 1000, 2850, and 2900 cm^{-1} wavenumber which are corresponding to alkene (=C-H bending), CH Stretching vibrations (CH_2) and alkane (C-H stretch), respectively [39]. In addition, the spectra also show the small peaks at 790, 1470, and 3620 cm^{-1} wavenumber, which are corresponding to alkyl halide (C-Cl stretch), alkane (C-H bending), and alcohol group (O-H), respectively. The peak in 3,300 – 3,500 cm^{-1} wavenumber range was considered to amine (N-H stretch) [39], the absorbance peak of TOB_2 is lower than TOB_3. This indicates that amine compound in TOB_2 is less than TOB_3. It may be due to different amounts of alkyl ammonium salt in surface modification of the clay. The addition of alkyl ammonium salt in TOB_2 is less than TOB_3. Moreover, it was possible to different kind of alkyl ammonium salt in surface modification of the clay. It is possible to be primary, secondary, tertiary, or quaternary ammonium salt, which was used in surface modification of the clay. It is a salt of ammonium cation and anion. The general structure formula of secondary ammonium salt is shown in Figure 4.3, which central nitrogen atom is chemically bonded to two alkyl group or organic group (same group or not). It is also bonded to two hydrogen and occur cation. It suggests that these cations can replace sodium ion in the clay platelets to increase the solubility of the associated anion in organic polymer [33]. It is expected well dispersion of clay in the polyethylene matrix. This will be discussed later.

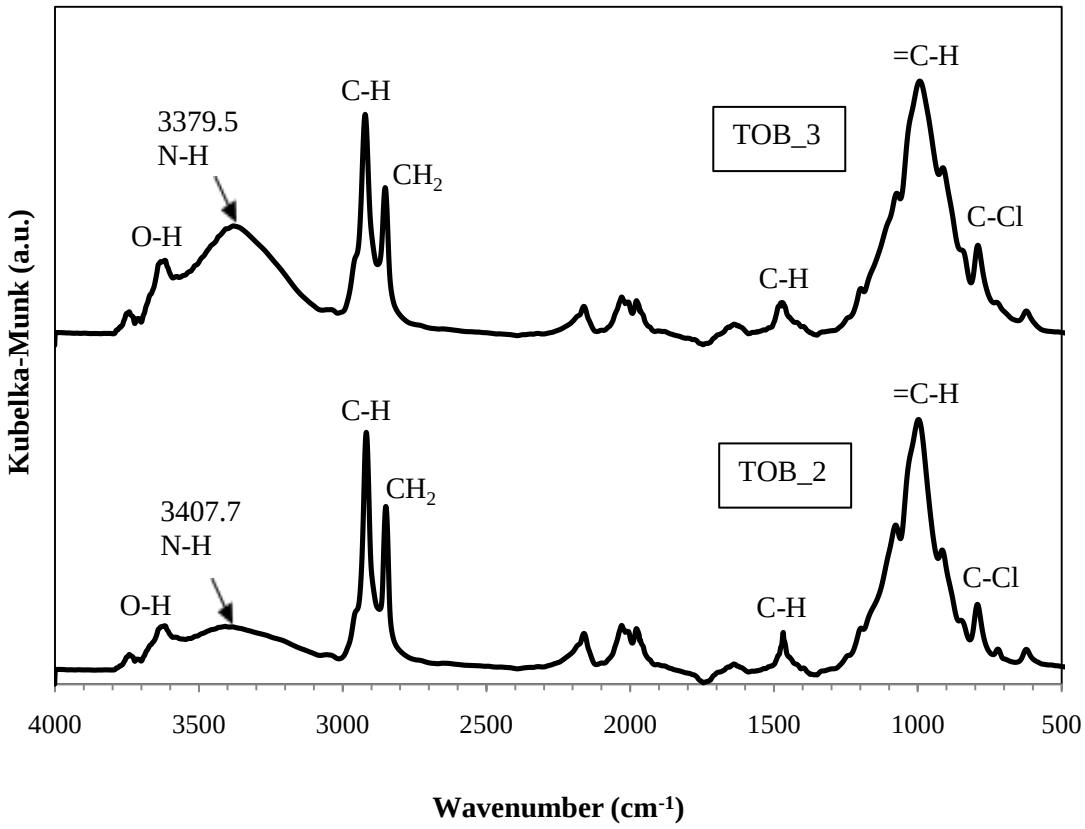

Figure 4.2 FTIR spectra of nanoclay a) TOB_2 b) TOB_3

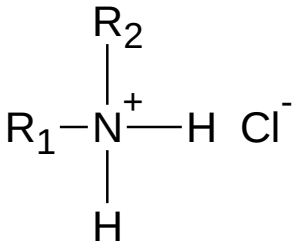

Where R is alkyl or organic group

Figure 4.3 General structure formula of secondary ammonium salt

4.1.3 Thermal stability

Thermal stability of two types of nanoclay was compared by information from TGA measurement. Their TGA curves in nitrogen atmosphere are shown in Figure 4.4, indicating that TOB_2 is more stable than TOB_3 at lower 300°C. The onset temperature of TOB_2 is higher than TOB_3 which are 180 and 90°C, respectively. The thermal stabilities also evaluated in terms of 10% weight-loss temperatures (Td10). Td10 of TOB_2 is higher than TOB_3 which are 273 and 227°C, respectively. This difference in thermal stability was due to difference compositions of these nanoclay. Generally, unmodified clay (such as Na^+-Montmorillonite) has weight loss at about 100°C due to the presence of moisture in the interlayer between clay platelets. However, weight loss at about 100°C in TOB_2 was not observed. This indicates that the surface of the clay platelets had been modified with an organic modifier (alkyl ammonium salt), conveying hydrophobic properties to the hydrophilic clay. From 200°C, the weight loss was observed on TOB_2 due to the decomposition of the alkyl ammonium salt [40]. In TOB_3, the first weight loss was observed below 200°C. It is attributed to the decomposition of remain moisture in this clay. TOB_3 also shows thermal degradation in the same temperature region like TOB_2 at 200°C. This may be due to the decomposition of the alkyl ammonium salt. It can be summarized that the alkyl ammonium salts used in surface modification of TOB_2 and TOB_3 are same types.

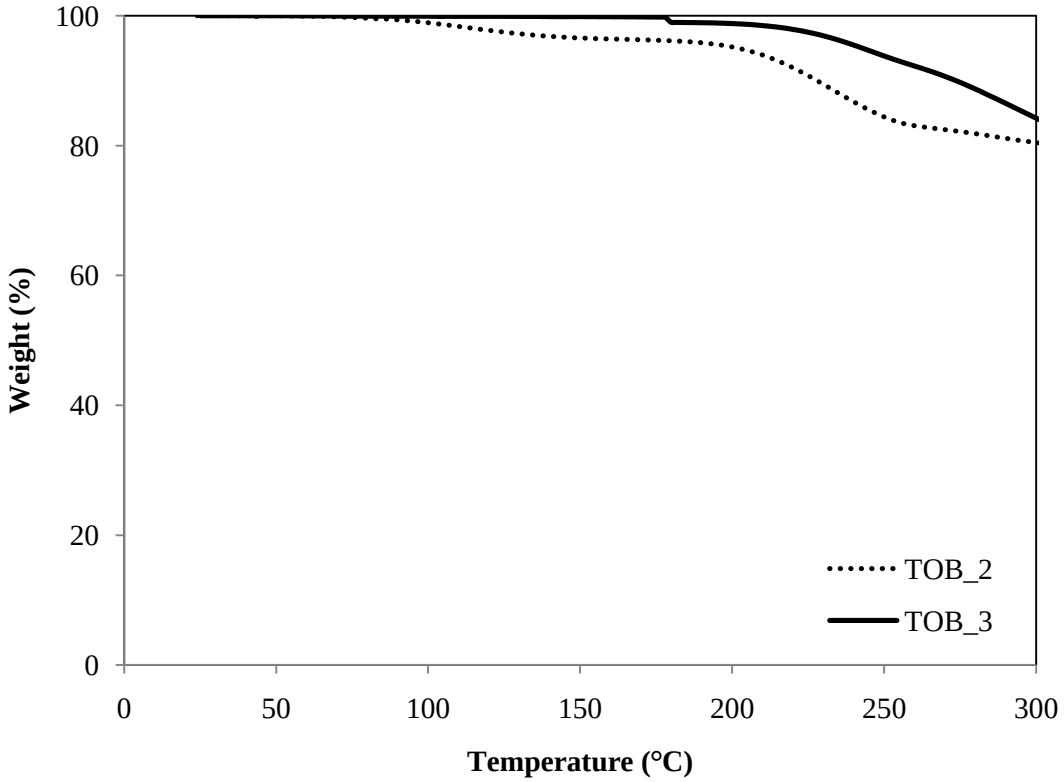

Figure 4.4 Thermal stability of nanoclay

4.2 Ethylene polymerization

Effect of types of nanoclay on the activity of metallocene catalyst as shown in Table 4.1, indicates that polymerization by *in situ* of 10 and 20 wt% of TOB_2 give higher catalytic activity of polyethylene nanocomposite than TOB_3. This is consistent with higher amount of amine group in TOB_3, which may deactivate zirconocene catalyst. Therefore, TOB_2 is more appropriate to use as nanofiller.

Table 4.1 summarizes the catalytic activity results of PE/clay nanocomposites with various amounts of nanoclay. It is seen that catalytic activity of pure polyethylene is the highest, including in copolymerzation system. When 5 % wt of TOB_2 was added to the reaction, the catalytic activity extremely decreased with the same result of copolymerization system. The catalytic activity tended to decrease with the nanoclay content. This result can be attributed to the fixation of the zirconocene on less compatible sites on the clay surface, which cause steric hindrance of clay

particle on zirconocenes, or as a result of deactivation reaction of cationic center of zirconocene with neighboring hydroxyl groups on the clay surface. In addition, this result corresponds to a deactivating effect of the amine group on the zirconocene catalyst [41]. However, increased amount of nanoclay to 40 wt% did not produce polyethylene after polymerization reaction. This is probably due to the fixation of active zirconocene on the excess clay surface. Thus, too much steric hindrance of the clay inhibits the reaction of cationic zirconocene to produce polyethylene chain.

Consider copolymerization system, 1-hexene as comonomer has the effect on catalytic activities of LLDPE/clay nanocomposites. Copolymerization systems give higher catalytic activities than homopolymerization systems as all conditions (Table 4.1 and Figure 4.5). This result corresponds to comonomer effect [42]. In homopolymerization of ethylene, this monomer slowly diffuse through the high crystalline polymer formed. When add a small amount of 1-hexene in copolymerization system, it causes crystallinity reduction of polymer formed. Thus, 1-hexene rapidly diffuses through polymer formed cause higher catalytic activity in copolymerization system. Except for the addition of 20 wt% of clay TOB_2 in the system, the catalytic activity of copolymerization does not differ from homopolymerization system. This result may be due to less 1-hexene insertion in the presence of 20 wt% of TOB_2, where 1-hexene insertion is only 5% as shown in Table 4.3. Thus LLDPE/clay20 nanocomposite exhibits similar catalytic activity to PE/clay20 nanocomposite.

For polymer preparation, methylaluminoxane (MAO) and clay were stirred together for 30, 60, 90, and 120 min. The effect of aging time on catalytic activity was shown in Figure 4.5. It can be seen that increasing the aging time did not improve catalytic activity. On the other hand, catalytic activity slightly decreased with increasing aging time in homopolymerization and copolymerization. This result can be attributed to increasing aging time causes more amount of methyalaluminoxane (MAO) fix on the clay surface. Thus, remain less amount of methylaluminoxane in liquid phase, which methylaluminoxane in liquid phase is more active than MAO on clay surface. Thus, catalytic activities decreased with increasing aging time between clay and methylaluminoxane.

Tale 4.1 Polymerization data with nanoclay/Et(Ind)$_2$ZrCl$_2$

Sample	amount of clay (%wt)		yield[a] (g)	activity[b]
	TOB_2	TOB_3		(kg PE/mol Zr.h)
PE	-	-	1.3643	17,588
PE/clay5	5	-	0.6622	12,851
PE/clay10	10	-	0.7083	8,730
PE/clay20	20	-	0.5894	6,869
PE/clay40	40	-	0.0000	0
PE/clay10	-	10	0.7937	8,007
PE/clay20	-	20	0.2906	5,440
PE/clay40	-	40	0.0000	0.0000
LLDPE	-	-	1.3087	35,534
LLDPE/clay5	5	-	1.1045	20,036
LLDPE/clay10	10	-	1.2241	12,143
LLDPE/clay20	20	-	0.3998	5,578
LLDPE/clay40	40	-	0.0000	0

[a]The polymer yield was limited by the amount of ethylene fed (0.018 mol). The molar ratio of ethylene:comonomer was 2:1.

[b]Activities were measured at polymerization temperature of 70°C, [ethylene]= 0.018 mol, $[Al]_{MAO}/[Zr]_{cat}$ = 1135 in toluene with total volume = 30 mL, $[Zr]_{cat} = 5\times10^{-5}$ Molar and mixing time of MAO and nanoclay was 30 min

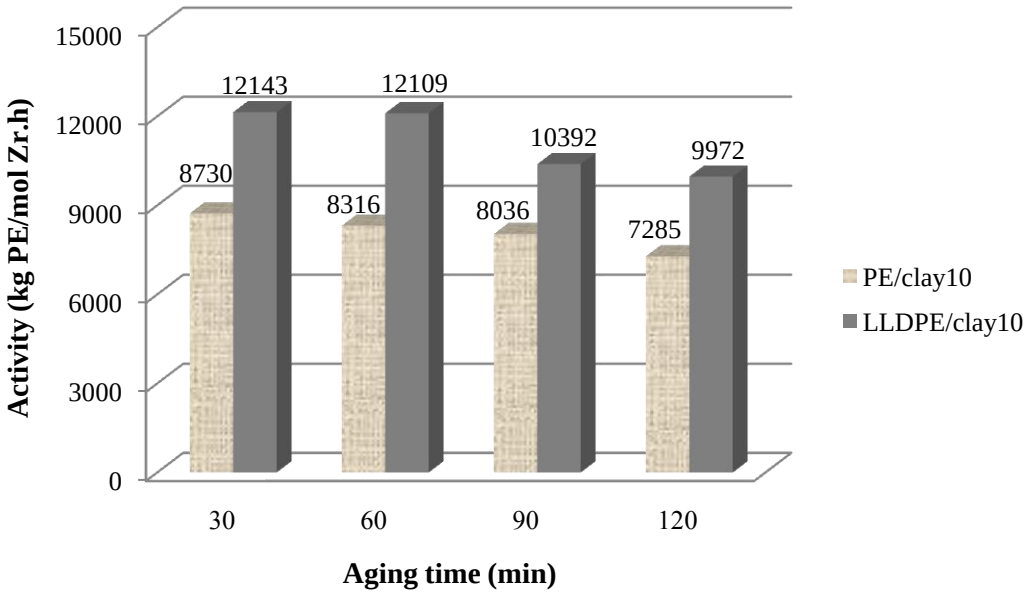

Figure 4.5 Catalytic activities of polyethylene nanocomposites with various aging times

4.3 Characterization of PE/clay nanocomposites

4.3.1 Dispersion of nanoclay

Degree of dispersion of nanoclay in polyethylene metrix was determined by small angle X-ray diffraction analysis (SAXRD). The SAXRD patterns of nanoclay, pure polyethylene, PE/clay nanocomposite, and LLDPE/clay nanocomposite are shown in Figure 4.6. The SAXRD pattern for clay TOB_2 provides diffraction peaks at $2\theta = 2.3$ and 4.7°, whereas the pure PE did not exhibit the diffraction peak at $2\theta = 1 – 10°$ range. The diffraction peaks of all nanocomposites were not observed. The SAXRD patterns of all nanocomposites still show the same peak of pure PE. The peak at about $2\theta = 2.3$ and 4.7° were not observed, which are the peaks of clay. It was suggested that high dispersion of nanoclay throughout polyethylene matrix were obtained [30,43]. This exfoliated degree dispersion of nanoclay may be due to direct mixing process. The methylaluminoxane (MAO) added during the clay treatment step is expected to react with hydroxyl group on clay surface. The zirconocene catalyst added during catalyst supported step was intercalated between the clay platelets, where zirconocene catalyst was reacted with MAO-treated clay and modifier, creating covalent bond that help to avoid catalyst leaching during the polymerization. Thus, it is the cause of well dispersion of nanoclay in the polyethylene matrix [19]. Exfoliation became possible through a strong interaction between the polyethylene chains and the clay surface [44].

Transmission electron microscopy (TEM) images also confirm exfoliated degree dispersion of nanoclay. In Figure 4.7, it can be seen that the clay particles are randomly dispersed throughout polyethylene matrix. Most clay particle agglomerates are broken down to primary particle. Homogeneous dispersion of the nanoclay in the polyethylene metrix is a difficult process. A well dispersion is complete by appropriate surface modification.

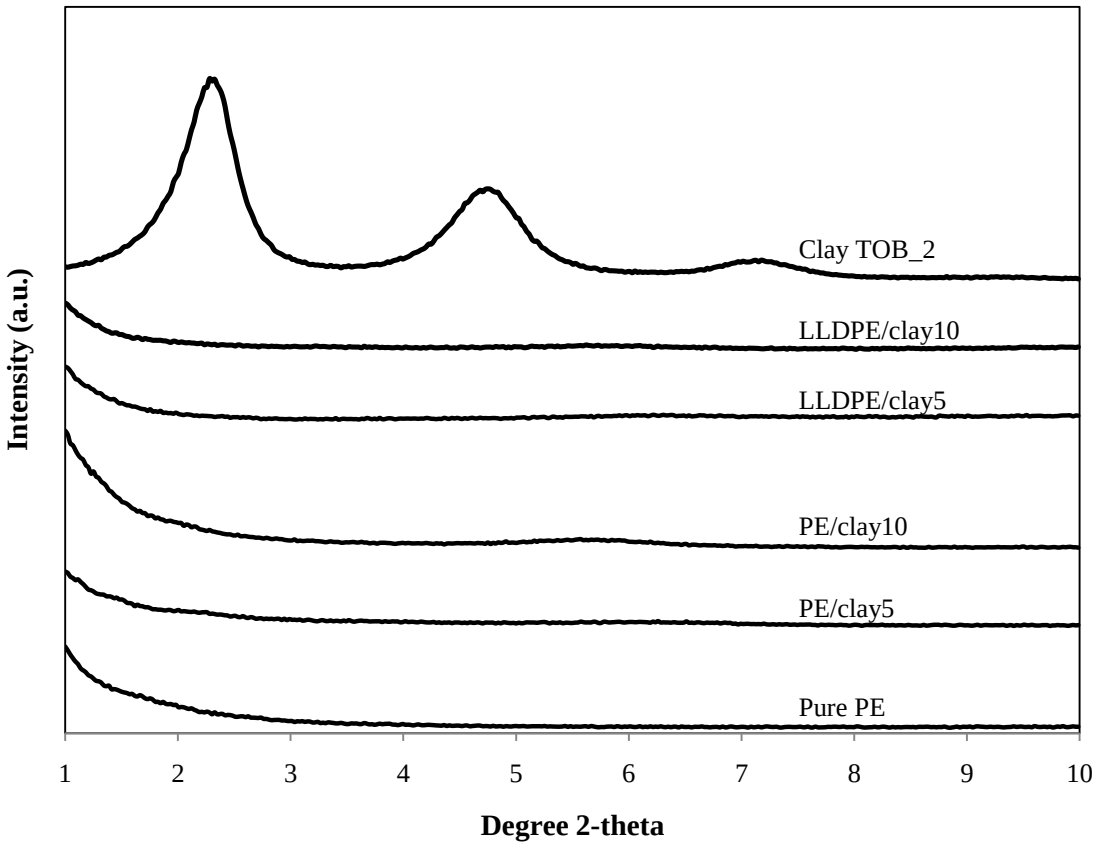

Figure 4.6 SAXRD patterns of nanoclay, pure PE, PE/clay nanocomposites, and LLDPE/clay nanocomposites

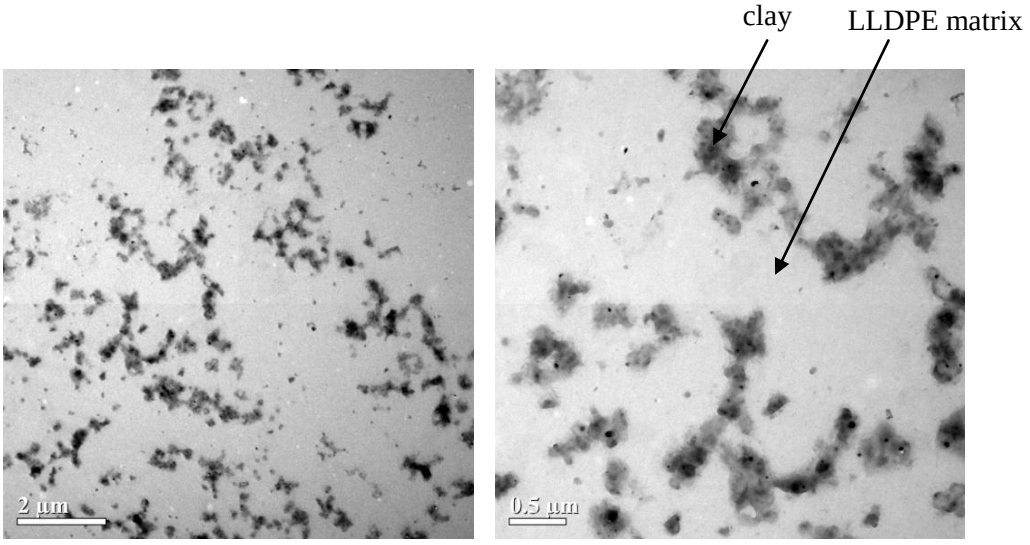

Figure 4.7 TEM image of LLDPE/clay10 nanocomposite

4.3.2 Thermal stability

Figure 4.9 shows TGA and DTG curves of pure PE and PE/clay nanocomposites. It used to describe thermal stability of PE/clay nanocomposites. At the initial stage of degradation at temperature lower than 400°C, PE/clay nanocomposite with the presence of 5 wt% of clay degrades slower than pure PE. This suggests that the presence of anisotropic clay layers hindering heat transfer through the polyethylene nanocomposite [45]. However, degradation of PE/clay nanocomposites at lower 400°C is faster with increasing amount of nanoclay to 10 and 20 wt%. This result may be due to Hofmann elimination reaction [46, 47] as shown in Figure 4.8, that the alkyl ammonium ions in the surface modification can suffer decomposition at about 200°C. Additionally, this reaction product (acidic sites on clay) and clay can catalyze the degradation of the polymer [48]. For PE/clay20 nanocomposites, the first decomposition appears at 70°C. It suggests the decomposition of remained water and solvent (methanol) in the polymer. The second stage (higher than 400°C), thermal stability of PE/clay nanocomposites is improved with increasing clay loading. Other than that, the presence of clay layers can hinder heat transfer through the polyethylene nanocomposite. This may be due to barrier effect of strong interaction between clay and polymer matrix. This interaction exhibits barrier to heat transfer [49]. Thus, PE/clay nanocomposites degrade slower than pure PE. For DTG curve, the maximum decomposition temperatures were observed. The maximum decomposition temperatures of pure PE, PE/clay5, PE/clay10, and PE/clay20 are 463, 481, 452, and 449°C, respectively.

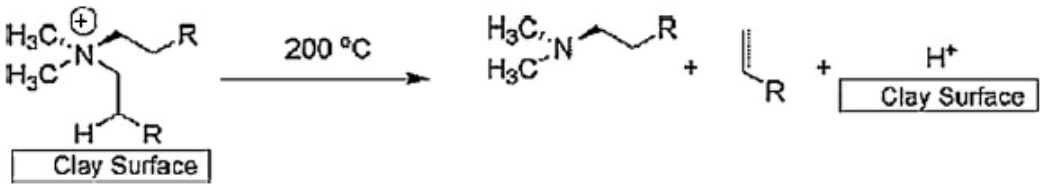

Figure 4.8 Hofmann elimination reaction of alkyl ammonium organic modifier [47]

In summary, clay has two opposite functions on thermal stability of polymer nanocomposites [3]. Thermal stability was improved when a small amount of clay (5 wt%) was added. This may be due to the presence of anisotropic clay layers hindering heat transfer through the polyethylene nanocomposite and the barrier effect of strong interaction between clay and polymer matrix [3,49]. However, increasing clay loading to 10 and 20 wt%, maximum decomposition temperatures were decreased. It indicated that catalyzing effect of clay rapidly rises and becomes dominant. Both two opposite effects on thermal stability occurred with the same result of LLDPE/clay nanocomposites as shown in Figure 4.10. The maximum decomposition temperatures of pure LLDPE, LLDPE/clay5, LLDPE/clay10, and LLDPE/clay 20 are 463, 463, 465, and 442°C, respectively.

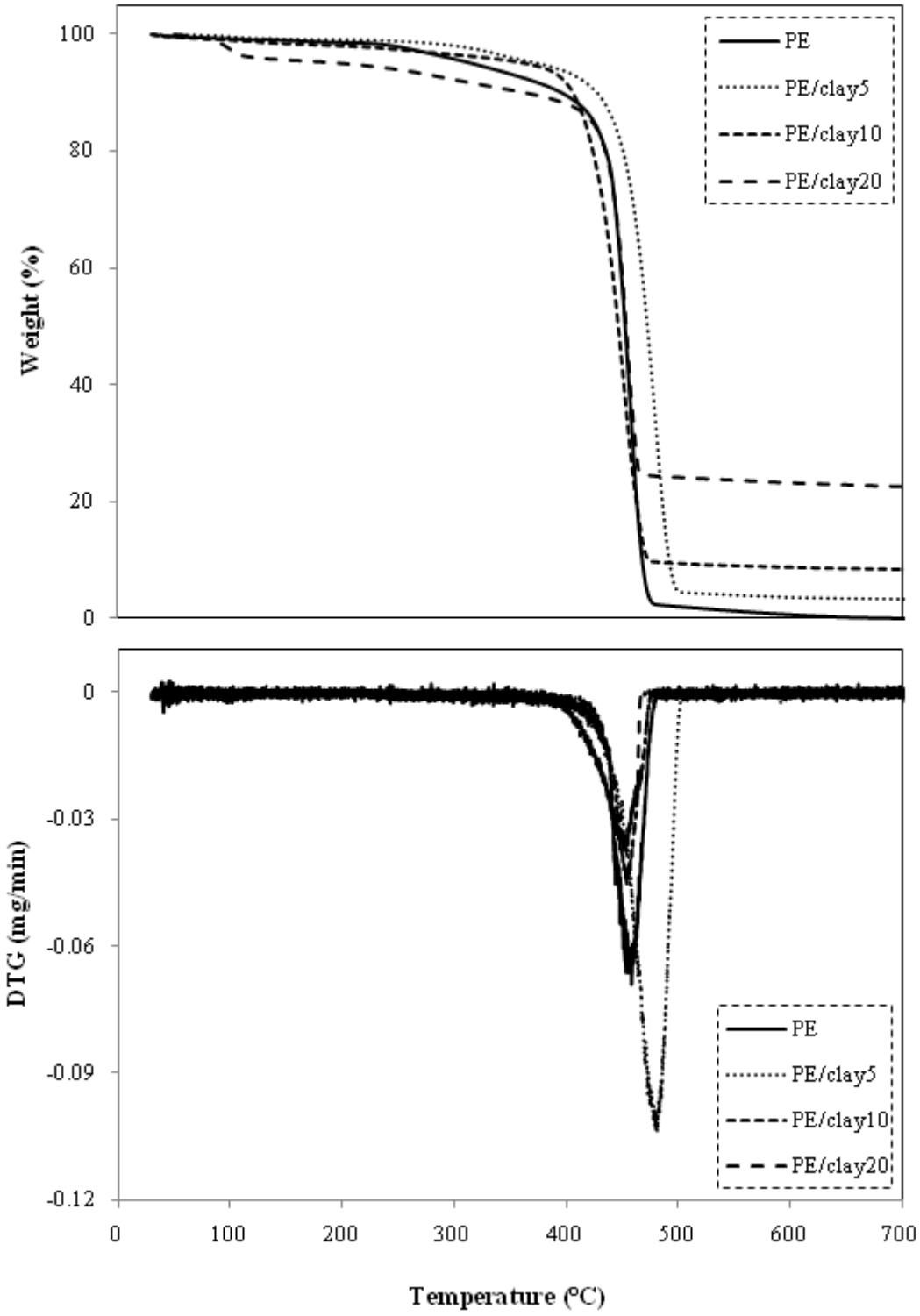

Figure 4.9 TGA and DTG curves of PE and PE/clay nanocompoites

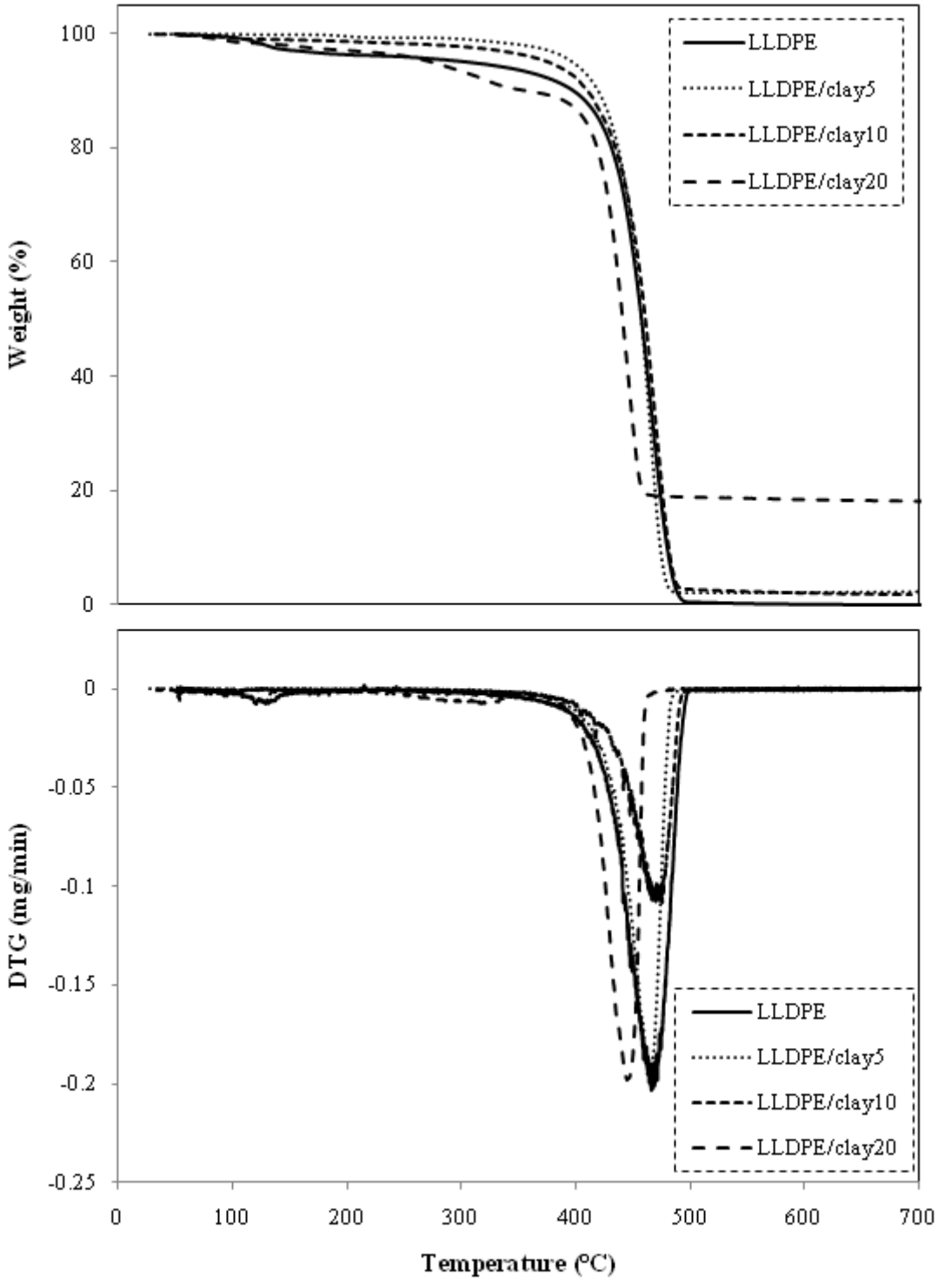

Figure 4.10 TGA and DTG curves of LLDPE and LLDPE/clay nanocompoites

4.3.3 Melting and crystallization behavior

Table 4.2 shows the melting temperature and crystallization behavior of pure PE, pure LLDPE, and the nanocomposites. Considering the effect of clay on homopolymerization, it can be observed that there was no significant change in the melting temperature of PE with the addition of nanoclay. The result was consistent with those obtained from Zapata et al. [41]. These high melting temperatures of the nanocomposites (132 – 134°C) indicates the branchless structure of the composites [50]. However, it is seen that PE/clay nanocomposites with various clay loadings are different in the crystallinity. Cryastallinity of pure PE is 51 %, whereas adding 5 wt% of clay in the composite presents an increase in crystallinity to 57%. This suggests that small amount of clay acting as heterophase crystal nucleation agent in the polymer metrix [51]. However, the crystallinities of PE/clay nanocomposites decreased with increasing the amounts of nanoclay to 10 and 20 wt%. This may be due to large amounts of clay particle locate themselves in the terlamellar spaces, leaving a little room for additional crystallization. Thus, clay particle may hinder the formation of crystalline phase of PE and presents a decrease in crystallinity [52]. Considering the effect of clay on copolymerization system, the crystallinity of pure LLDPE is 3% when 1-hexene is added as comonomer. However, DSC curve of LLDPE with adding 5 wt% of nanoclay does not clearly appear melting temperature. This may be attributes to polyethylene obtained by employing metallocene catalyst is high amorphous. Especially, copolymerization system by adding 1-olefin, the obtained polymer is more amorphous. In this case, the obtained polymer with adding 5 wt% of nanoclay may be too low in melting temperature that is not enough to clearly appear melting temperatures on DSC curve. However, increasing the clay loading to 10 and 20 wt% present a decrease in crystallinity, which are consistent with homopolymerization system.

XRD patterns also confirm the reduction of crystallinity in PE/clay20 and LLDPE/clay20 compared to pure PE. In Figure 4.11, it can be seen that small amorphous peak was observed around 19.5 – 20 degree [53].

Table 4.2 Melting and crystallization behavior

Sample	T_m [a] (°C)	ΔH_{exp} [b] (J/g)	X_c [c] (%)
PE	134	150	51
PE/clay5	134	160	57
PE/clay10	132	140	51
PE/clay20	132	108	44
LLDPE	114	53	3
LLDPE/clay5	N/A	N/A	N/A
LLDPE/clay10	132	78	28
LLDPE/clay20	108	51	23

[a]Melting temperature (T_m) was obtained from DSC measurement.

[b]Heat of fustion (ΔH_{exp}) was obtained from DSC measurement.

[c]Crystallinity (X_c) was calculated from equation in Appendix C.1.

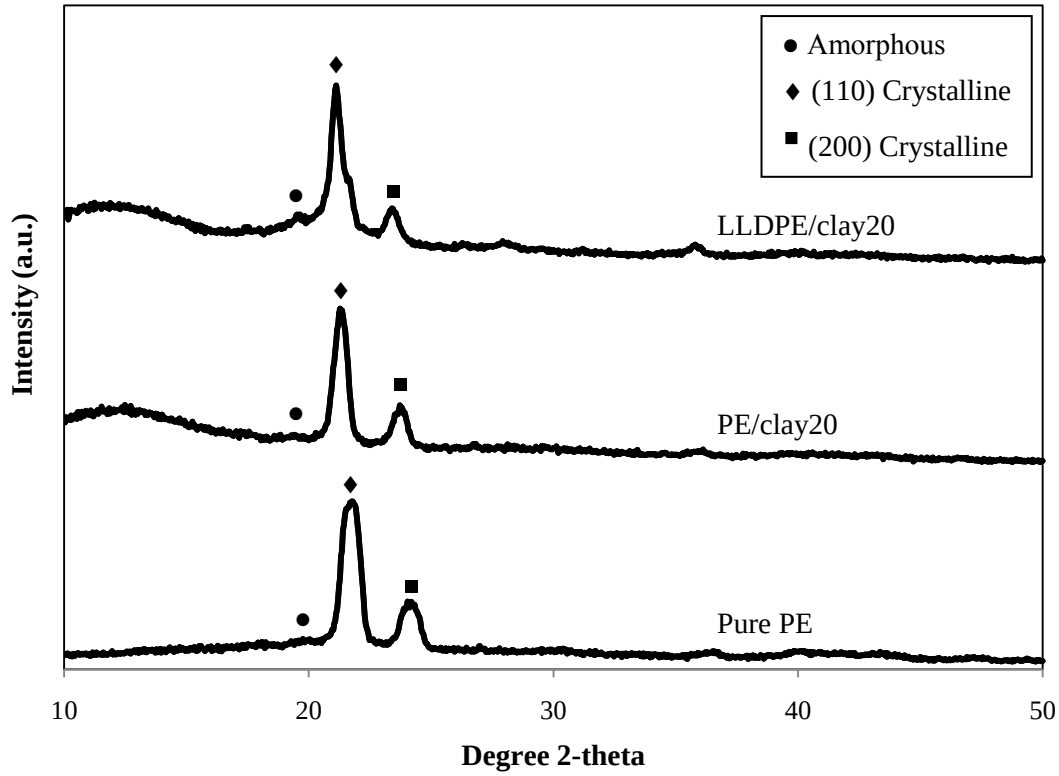

Figure 4.11 XRD patterns of pure PE, PE/clay20, and LLDPE/clay20 nanocomposites

4.3.4 Insertion of comonomer

Insertion of 1-hexene in LLDPE/clay nanocomposites was calculated from ^{13}C NMR spectra, which are listed in Table 4.3. It seems that 1-hexene insertion significantly decreases in the presence of clay particle. 1-Hexene insertion (%) also slightly decreased with increasing clay loading. This may be due to more steric hindrance of clay particle inhibits insertion of 1-hexene. The kind of the obtained copolymer is block copolymer, consisting of multiple sequences of the monomer alternating in series with different monomer blocks, or random copolymer. The blocks or random are covalently bound to each other.

Table 4.3 Triad distribution and insertion of 1-hexene

Sample	Triad distribution[a]						1-Hexene[b]
	[EEE]	[HEE]	[EHE]	[HEH]	[EHH]	[HHH]	insertion (%)
LLDPE	0.453	0.111	0.169	0.114	0.000	0.153	32.21
LLDPE/clay5	0.490	0.140	0.105	0.074	0.191	0.000	29.61
LLDPE/clay10	0.693	0.107	0.095	0.042	0.000	0.063	15.83
LLDPE/clay20	0.875	0.066	0.041	0.007	0.000	0.011	5.19

[a]Triad distribution was calculated from ^{13}C-NMR spectrum equation in appendix C.2.

[b]1-Hexene insertion was calculated from ^{13}C-NMR spectrum in appendix C.2.

4.3.5 Morphology

The morphology of the nanocomposites was obtained using scanning electron microscopy (SEM). The SEM micrographs of the nanocomposites are shown in Figure 4.12. The clay particles were coated by the growing polyethylene chains. It can be suspected that during polyethylene formation, the polyethylene chains chemically bonded to the surface of the exfoliated clay drag each individual layer as the polymer flow to homogeneously distribute the clay platelets in the polyethylene matrix [54]. As observed, all PE/clay nanocomposites upon various clay loadings exhibited the similar morphologies. However, the morphologies of LLDPE/clay nanocomposites as various clay loadings are different from pure LLDPE as shown in Figure 4.13 This is probably due to well dispersion of clay particles in the LLDPE matrix. Conversely, if

the clay particle does not exhibit well dispersion, agglomerated clay at the micro-sized range will be present. Furthermore, the interconnections of the clay particle through polyethylene chain suspect to improve the mechanical strength of the nanocomposites.

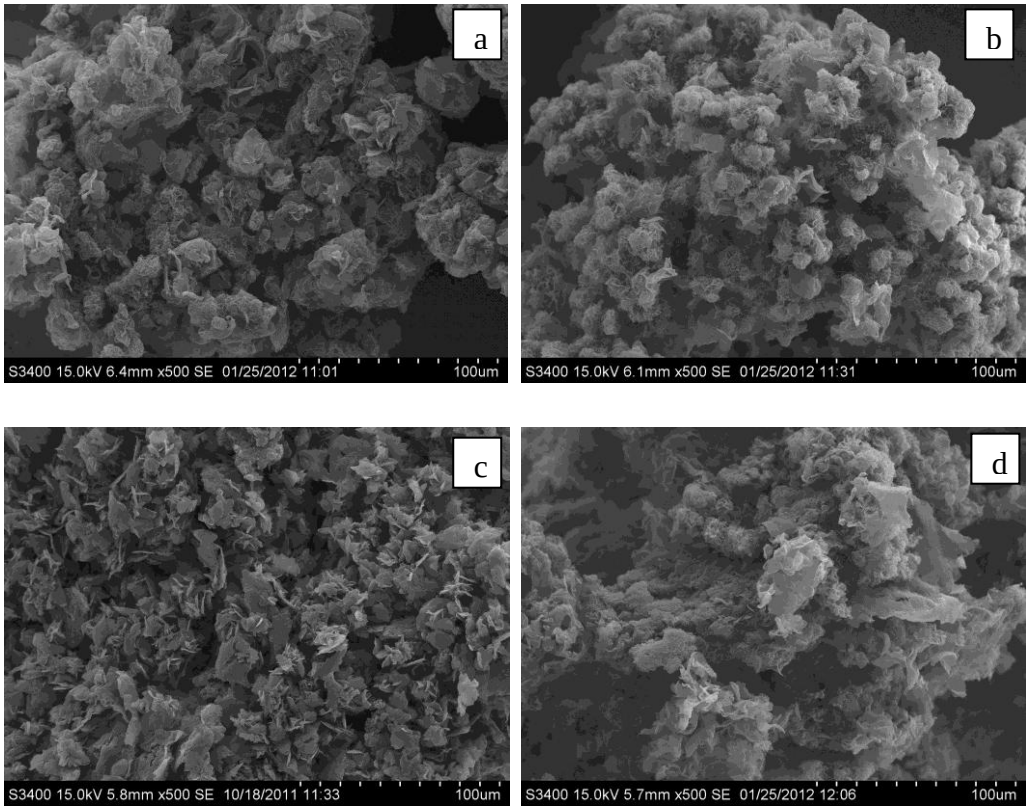

Figure 4.12 SEM images of PE growing on the surface of clay (a) PE (b) PE/clay5 (c) PE/clay10 (d) PE/clay20

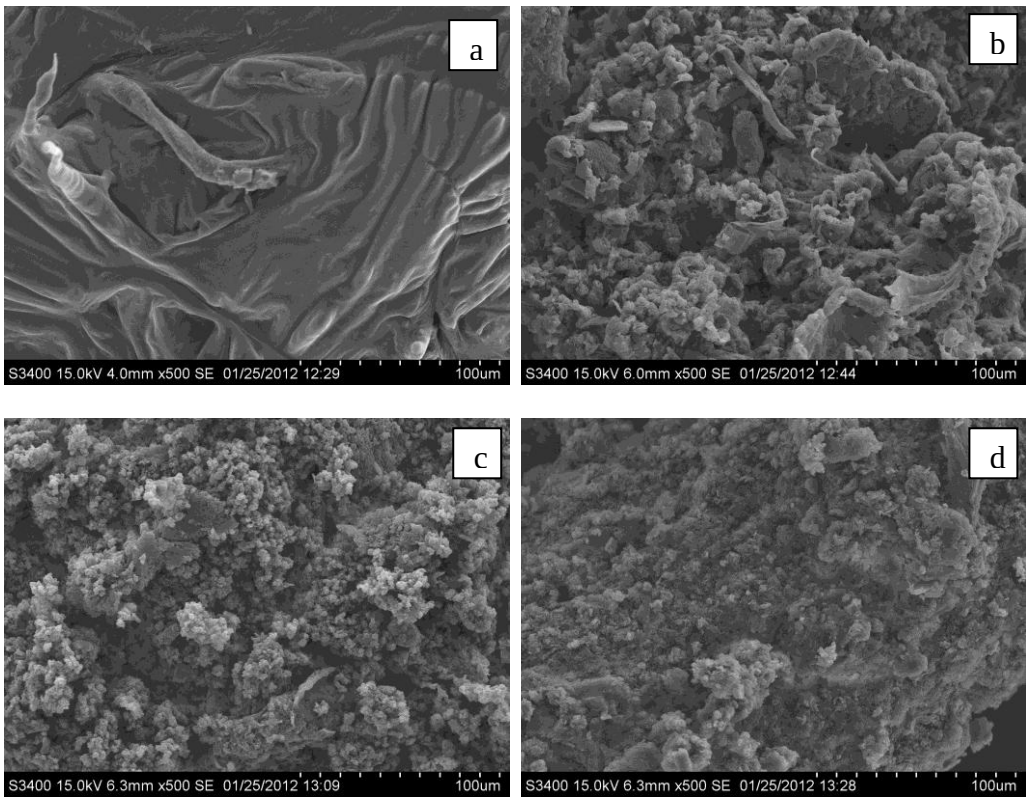

Figure 4.13 SEM images of LLDPE growing on the surface of clay (a) LLDPE (b) LLDPE/clay5 (c) LLDPE/clay10 (d) LLDPE/clay20

CHAPTER V

CONCLUSIONS & RECOMMENDATION

5.1 Conclusions

5.1.1 Effect of nanoclay types

At the beginning, PE/clay nanocomposites and LLDPE/clay nanocomposites can be synthesized via *in situ* polymerization with zirconocene catalyst. It was found that clay particles are well dispersed in the polyethylene matrix. Clay TOB_2 gives higher activity of polyethylene nanocomposite than TOB_3 due to different amine group content in the nanoclay.

5.1.2 Effect of nanoclay loading

The second part of this research examined the effect of clay loading on catalytic activity and polymer properties. It was found that catalytic activities decreased with increasing amounts of nanoclay. This result can be attributed to fixation of the zirconocene on less compatible sites in the clay structure or as a result of deactivation reaction with neighboring hydroxyl groups on the clay surface. The clay has two opposite effects on thermal properties and crystallinity behavior. The addition of 5 % by weight of clay resulted in maximal thermal properties and percentage of the crystallinity (X_c).

5.1.3 Effect of aging time

In the final past of this research, effect of aging time on catalytic activity was investigated. It was found that increasing the aging time resulted in a slight decrease of catalytic activity. This indicates that increasing aging time causes remain less amount of methylaluminoxane (MAO) in liquid phase, which is more active than MAO on clay surface.

5.2 Recommendation

PE/clay nanocomposites should be further determined other main properties for any applications. These are molecular weight and molecular weight distribution (MWD), flame retardant, and mechanical properties.

LLDPE/clay nanocomposites should be further synthesized as other conditions to obtain melting temperature from DSC measurement.

REFERENCES

[1] Sharma, K.G. Easily processable ultra high molecular weight polyethylene with narrow molecular weight distribution. Eindhoven, Doctoral dissertation, Department of Chemical Engineering, Faculty of Engineering, Eindhoven University of Technology, 2005.

[2] Ribeiro, M.R., Deffieux, A., and Portela, M.F. Supported Metallocene complexes for ethylene and propylene polymerizations: preparation and activity. Industrial & Engineering Chemistry Research 36 (1997): 1224-1237.

[3] Zhao, C., Qin, H., Gong, F., Feng, M., Zhang, S., and Yang, M. Mechanical, thermal, and flammability properties of polyethylene/clay nanocomposites. Polymer Degradation and Stability 87 (2005): 183-189.

[4] Lagashetty, A., and Venkataraman. Polymer Nanocomposites. Vol 10, Gulbarga: Resonance, 2005.

[5] Downing-Perrault, A. University of Wisconsin-Stout. Polymer nanocomposites are the future. pp.49-60. Hong Kong: Eco Expo Asia, 2011.

[6] Mittal, V. *In-situ* synthesis of polymer nanocomposites. vol.2. Weinheim: Wiley-VCH, 2011.

[7] Mittal, V. Polymer nanocomposites: Synthesis, microstructure, and properties. Weinheim: Wiley-VCH, 2010.

[8] Kaminsky, W., and Laban, A. Metallocene catalysis. Applied Catalysis A: General 222 (2001): 47-61.

[9] Alfredo Campo, E. The complete part design handbook for injection molding of thermoplastics. Ohio: Hanser, 2006.

[10] Furumiyai, A., Akanai, Y., Ushidai, Y., Masuda, T., and Nakajima, A. Relationship between molecular characteristics and physical properties of linear low density polyethylenes. Pure and Applied Chemistry 57 (1985): 823-832.

[11] Brent Strong, A. Plastics: Materials and processing. Edition 2. New Jersey: Prentice Hall, 2000.

[12] Syed, F.H., and Vernon, W.D. Status of low pressure PE process licensing. New generation polyolefins 7 (June 2002): 18-27.

[13] Kaminsky, W. New polyolefins by metallocene catalysts. Pure and Applied Chemistry 70 (1998): 1229-1233.

[14] Ekrachan Chaichana Linear low-density polyethylene/nano-silica composites synthesized via *in situ* polymerization with metallocene catalyst. Master's Thesis, Department of chemical engineering, Faculty of engineering, Chulalongkorn University, 2005.

[15] Othmer, K. Encyclopedia of chemical technology. Vol. 16, Edition 5. Metallocene catalysts. Hoboken: John Wiley & Sons, 2005.

[16] Van Grieken, R., Carrero, A., Suarez, I., and Paredes, B. Ethylene polymerization over supported MAO/$(nBuCp)_2ZrCl_2$ catalysts: Influence of support properties. European Polymer Journal 43 (2007): 1267 – 1277.

[17] Oh, J., Lee, B.Y. and Park, T.H. Recycling of methylaluminoxane (MAO) cocatalyst in ethylene polymerization with supported Metallocene catalyst. Korean Journal of Chemical Engineering 21 (2004): 110-115.

[18] Luhtanen, T.N.P., Linnolahti, M., and Pakkanen, T.A. Quantum chemical studies on elementary fragments of three-coordinated methylaluminoxanes. Journal of Organometallic Chemistry 648 (2002): 49–54.

[19] Choi, Y., and Soares, J.B.P. Supported single–site catalysts for slurry and gas–phase olefin polymerisation. Chemical engineering 90 (2011): 646-671.

[20] Kristen, M. Supported metallocene catalysts with MAO and boron activators. Topics in Catalysis 7 (1999): 89–95.

[21] Kaminsky, W. Highly active metallocene catalysts for olefin polymerization. Journal of the Chemical Society 9 (1998): 1413-1418.

[22] Piel, C. Polymerization of ethene and ethene-co-α-olefin: Investigations on short- and long-chain branching and structure-property relationships. Doctoral dissertation, Department of Chemistry, University of Hamburg, 2005.

[23] Nakano, H., Takahashi, T., Hideshi Uchino, Tayano, T., and Sugano, T. Polymerization behavior with Metallocene catalyst supported by clay mineral activator. Studies in Surface Science and Catalysis 161 (2006): 19-24.

[24] Simon, L.C., Patel, H., Soares, J.B.P., and de Souza, R.F. Polyethylene made with *in situ* supported Ni-diimine/SMAO: Replication phenomenon and effect of polymerization conditions on polymer microstructure and morphology. Macromolecular Chemistry and Physics 202 (2011): 3237-3247.

[25] Weiss, K. et al. Polymerisation of ethylene or propylene with heterogeneous metallocene catalysts on clay minerals. Journal of Molecular Catalysis A: Chemical 182–183 (2002): 143–149.

[26] Bunjerd Jongsomjit, Sutti Ngamposri, and Piyasan Praserthdam. Application of silica/titania mixed oxide-supported zirconocene catalyst for synthesis of linear low-density polyethylene. Industrial & engineering chemistry research 44 (2005): 9059-9063.

[27] Choudalakis, G., and Gotsis A.D. Permeability of polymer/clay nanocomposites: A review. European Polymer Journal 45 (2009): 967–984.

[28] Marosfo, B.B. et al. Complex activity of clay and CNT particles in flame retarded EVA copolymer. Polymers for Advanced Technologies 17 (April 2006): 255–262.

[29] Kubisova, H., Merinska, D., and Svoboda, P. PP/clay nanocomposite: optimization of mixing conditions with respect to mechanical properties. Polymer Bulletin 65 (2010): 533–541.

[30] Lee, Y.H., Kuboki, T., Park, C.B., Sain, M., and Kontopoulou, M. The effects of clay dispersion on the mechanical, physical, and flame-retarding properties of wood fiber/polyethylene/clay nanocomposites. Journal of Applied Polymer Science 118 (May 2010): 452–461.

[31] Mittal, V. Optimization of polymer nanocomposite properties. Weinheim: Wiley-VCH, 2010.

[32] Salavati-Niasari, M., and Ghanbari D. In Reddy, B. (ed.), Polymeric nanocomposite materials, pp.529-548. Austria: InTech, 2011.

[33] Kiliaris, P., and Papaspyrides C.D. Polymer/layered silicate (clay) nanocomposites: An overview of flame retardancy. Progress in Polymer Science 35 (March 2010): 902–958.

[34] Lambert, A. Review of gel permeation chromatography. British Polymer Journal 3 (January 1971): 13-23.

[35] Theivasanthi T., and Alagar M. X-ray diffraction studies of copper nanopowder. Archives of Physics Research, 2 (June 2010): 112-117.

[36] Oliveira Vilela, S., Soto-Oviedo, M.A., Fonseca Albers, A.P., and Faez, R. Polyaniline and Mineral Clay-based Conductive Composites. Materials Research 10 (March 2007): 297-300.

[37] Menking, K.M., Musler, H.M., Fitts, J.P., Bischoff, J.L., and Anderson, R.S. Core OL-92 from Owens Lake, southeast California. Edition 1. Clay Mineralogical Analyses of the Owens Lake Core. California: U.S. Department of the Interior, 1993.

[38] Garrels, R.M. Montmorillonite/illite stability diagrams. Clay and clay minerals 32 (1984): 161-166.

[39] Silverstein, R.M., Bassler, G.C., and Morrill, T.C. Spectrometric identification of organic compounds. Edition 4. New York: John Wiley and Sons, 1981.

[40] Kim, S.-K., Kwen, H.-D., and Choi, S.–H. Radiation-induced synthesis of vinyl copolymer based nanocomposites filled with reactive organic montmorillonite clay. Radiation Physics and Chemistry 81 (2012): 519–523.

[41] Zapata, P., Quijada, R., Covarrubias, C., Moncada, E. and Retuert, J. Catalytic activity during the preparation of PE/clay nanocomposites by *in situ* polymerization with Metallocene catalysts. Journal of Applied Polymer Science 4 (August 2009): 2368–2377.

[42] Van Grieken, R., Carrero, C., Suarez, I., and Paredes, B. Effect of 1-hexene comonomer on polyethylene particle growth and kinetic profiles. Macromolecular Symposia 259 (2007): 243–252.

[43] Sanchez-Valdes, S., and Ramos-deValle, L.F. Compatibilizers improve exfoliation in polymer-clay nanocomposites. Society of Plastics Engineers 10 (August 2010): 1-3.

[44] Wang, X. et al. Enhanced exfoliation of organoclay in partially end functionalized non-Polar polymer. Macromolecular Materials and Engineering 294 (2009): 190–195.

[45] Lomakin, S.M., Novokshonova, L.A., Brevnov, P.N., and Shchegolikhin, A.N. Thermal properties of polyethylene/montmorillonite nanocomposites prepared by intercalative polymerization. Journal of Material Science (2008) 43: 1340–1353.

[46] Araujo, E.M., Barbosa, R., S. Morais, C.R., B. Soledade, L.E., Souza, A.G., and Vieira, M.Q. Effect of organoclays on the thermal processing of PE/clay nanocomposites. Journal of Thermal Analysis and Calorimetry 90 (2007): 841–848.

[47] Kiliaris, P., and Papaspyrides, C.D. Polymer/layered silicate (clay) nanocomposites: An overview of flame retardancy. Progress in Polymer Science 35 (2010): 902–958.

[48] Leszczynska, A., Njuguna, J., Pielichowskia, K., and Banerjee, J. R. Polymer/montmorillonite nanocomposites with improved thermal properties. Thermochimica Acta 453 (February 2007): 75-96.

[49] Humphreys, S. Polymer/layered silicate nanocomposite. United Kingdom: Rapra technology Limited, 2003.

[50] Murthy, Z. V. P., and Parikh, P.A. *In situ* synthesis of nanoclay filled polyethylene using polymer supported metallocene catalyst system. Quimica Nova 34 (2011): 1157-1162.

[51] Tarinee Nampitch, Ranumas Thipmanee, and Rathanawan Magaraphan. Thermal properties of polylactic acid / epoxidized natural rubber / organoclay nanocomposites. in Proceedings of 48th Kasetsart University Annual Conference: Agro-Industry, pp.34-41, Bangkok: Kasetsart University, 2010.

[52] Ekrachan Chaichana, Bunjerd Jongsomjit, and Piyasan Praserthdam. Effect of nano-SiO_2 particle size on the formation of LLDPE/SiO_2 nanocomposite synthesized via the *in situ* polymerization with metallocene catalyst. Chemical Engineering Science 62 (2007): 899 – 905.

[53] Perez, E., Benavente, R., Quijada, R., Narvaez, A., and Galland, G.B. Structure characterization of copolymers of ethylene and 1-octadecene. Journal of Polymer Science: Part B: Polymer Physics 38 (March 2000): 1440–1448.

[54] Shing, S.Y.A., Simon, L.C., Soares, J.B.P.,and Scholz, G. Polyethylene–clay hybrid nanocomposites: *in situ* polymerization using bifunctional organic modifiers. Polymer 44 (2003): 5317–5321.

[55] Randall, J.C. A review of high resolution liquid ^{13}carbon nuclear magnetic resonance characterizations of ethylene-based polymers. Journal of Macromolecule Science 29 (1989): 201-317.

[56] Galland, G.B., Quijada, P., Mauler, R.S., and Menezes, S.C. Determination of reactivity ratios for ethylene/α-olefin copolymerization catalyst by the $C_2H_4[Ind]_2ZrCl_2$/methylaluminoxane system. Macromolecular Rapid Communications 17 (1996): 607-613.

[57] Silverstein, R.M., Bassler, G.C.; and Morrill, T.C. Spectrometric identification of organic compounds. Edition 4. New York: John Wiley and Sons, 1981.

APPENDICES

APPENDIX A

Differential scanning calorimetry (DSC)

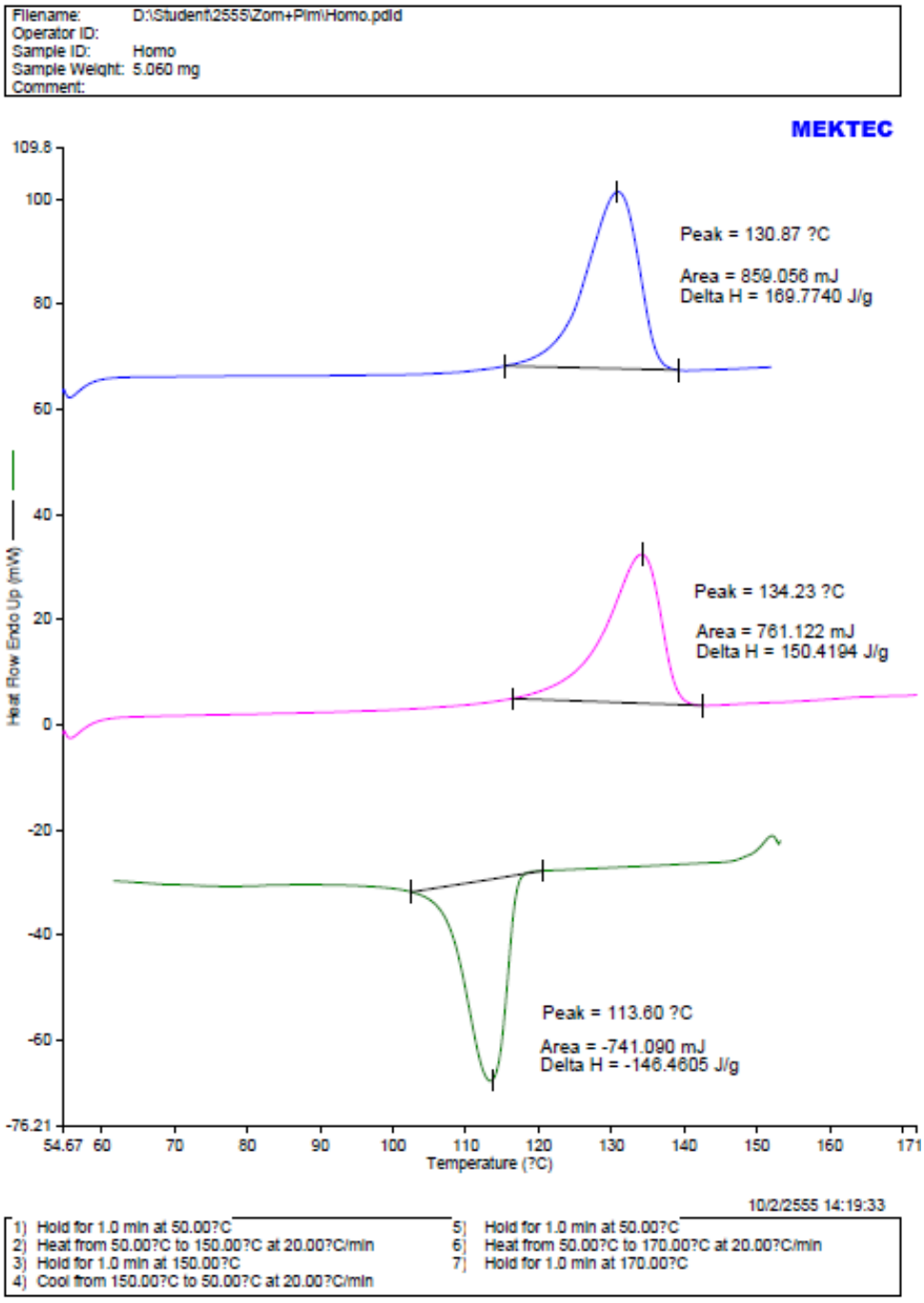

Figure A-1. DSC curve of PE

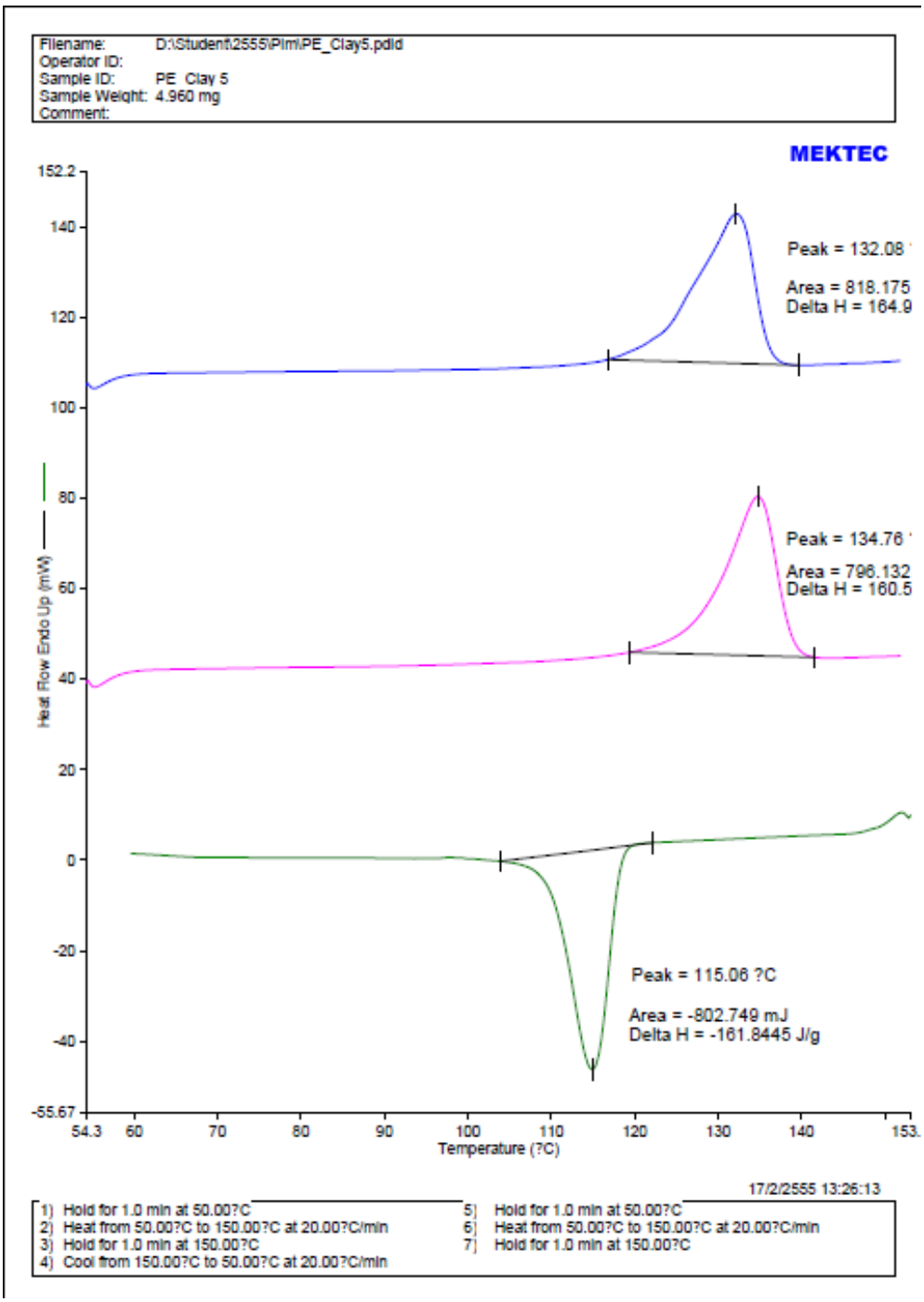

Figure A-2. DSC curve of PE/clay5 nanocomposite

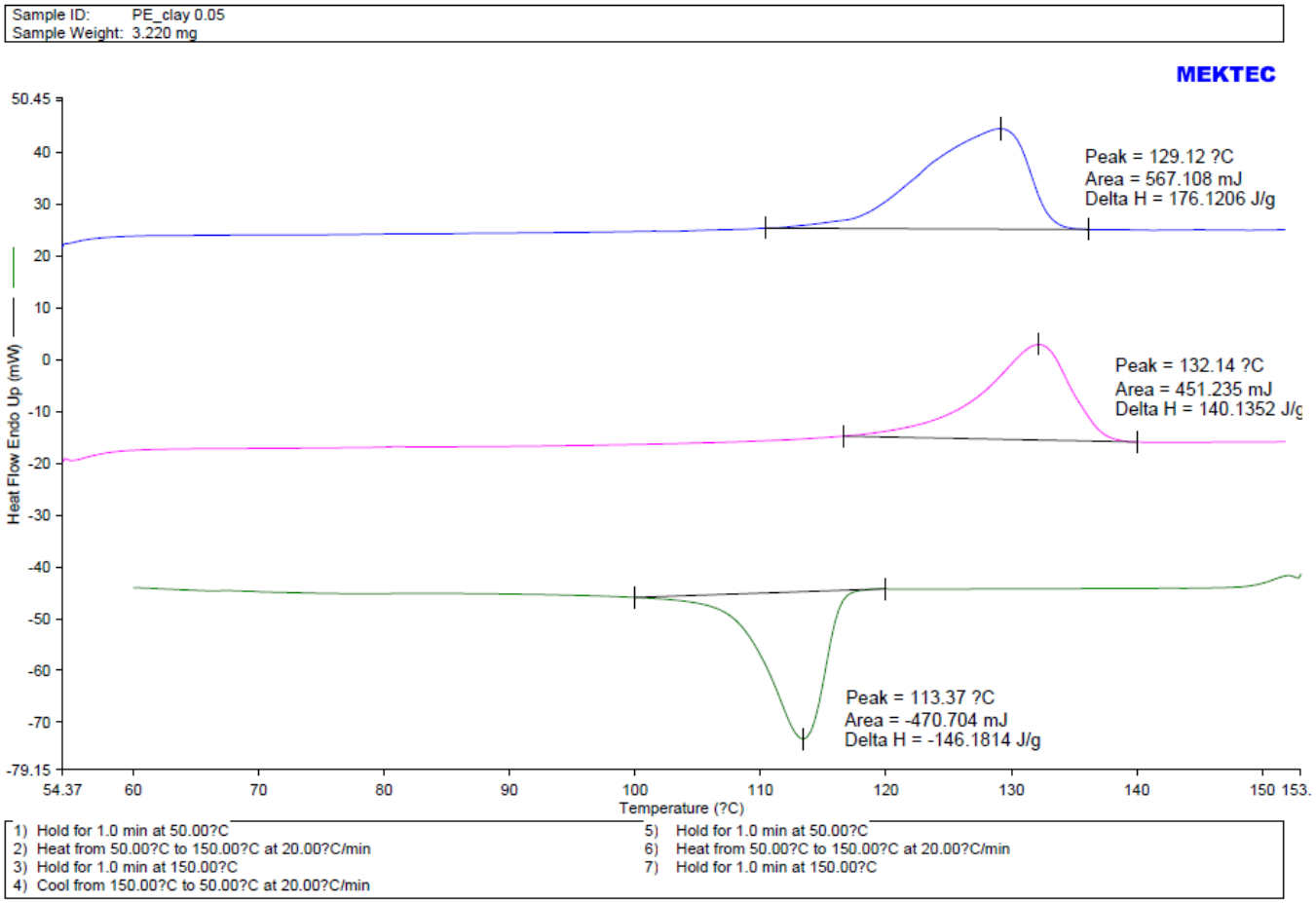

Figure A-3. DSC curve of PE/clay10 nanocomposite

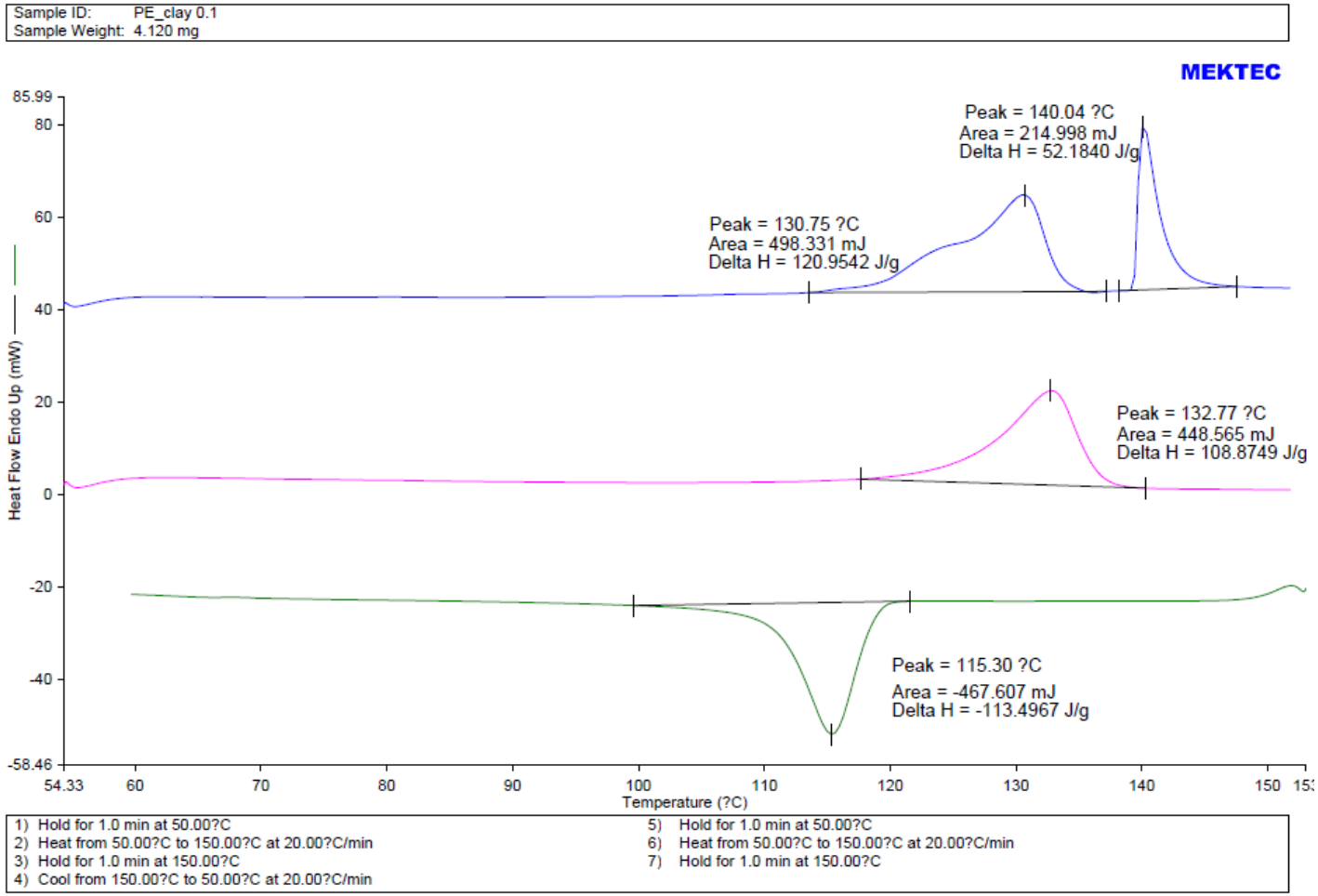

Figure A-4 DSC curve of PE/clay20 nanocomposite

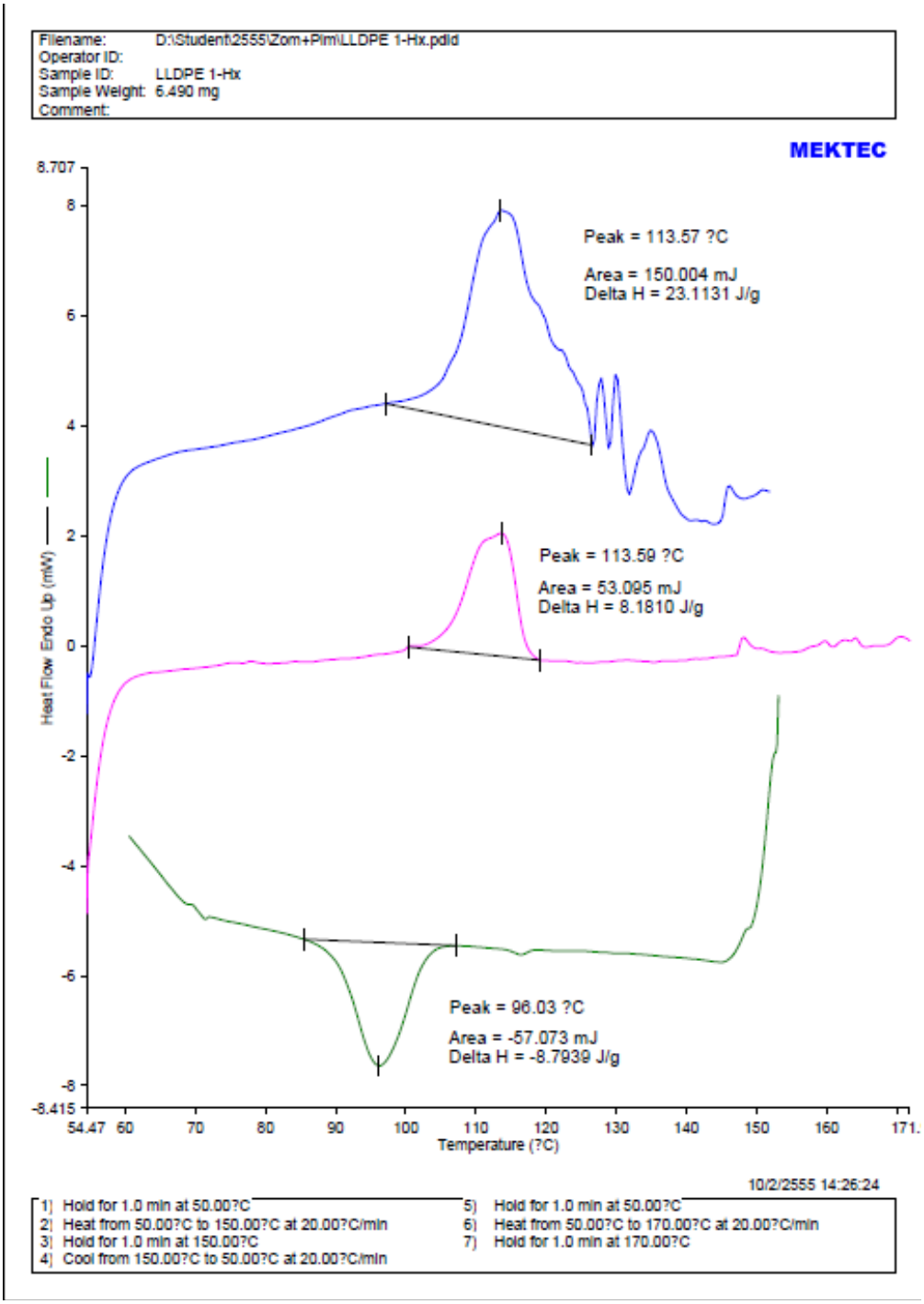

Figure A-5 DSC curve of LLDPE

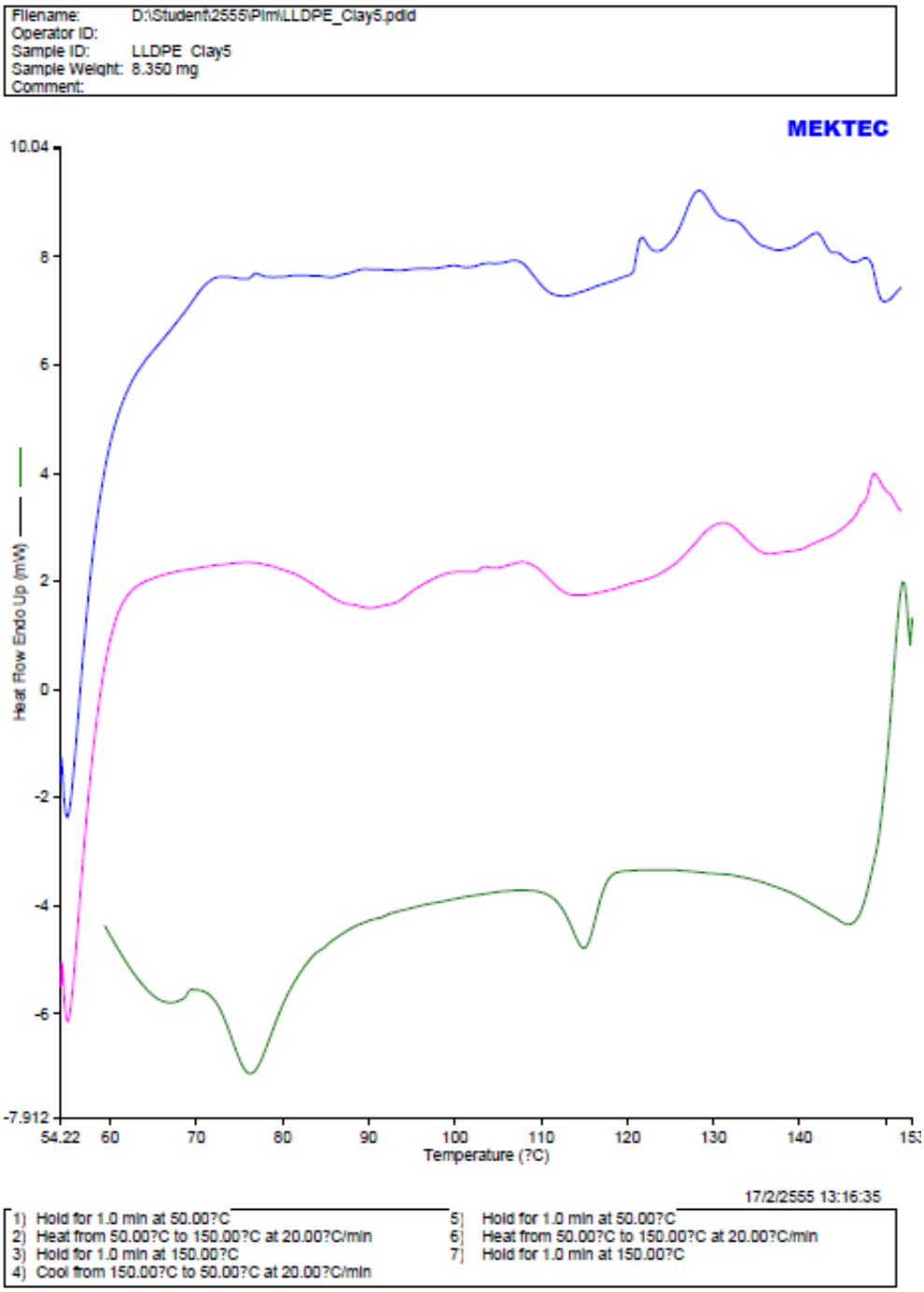

Figure A-6 DSC curve of LLDPE/clay5 nanocomposite

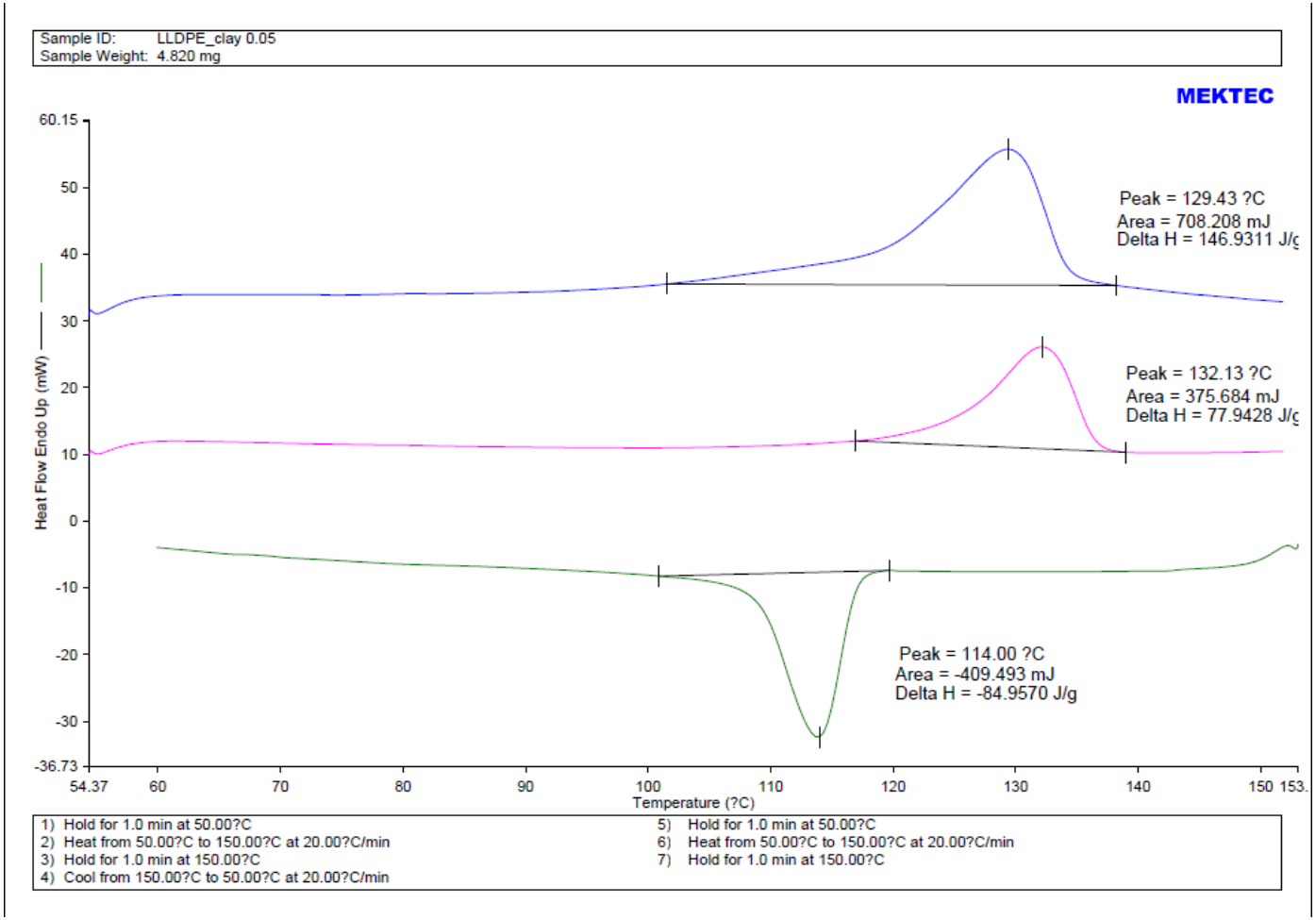

Figure A-7 DSC curve of LLDPE/clay10 nanocomposite

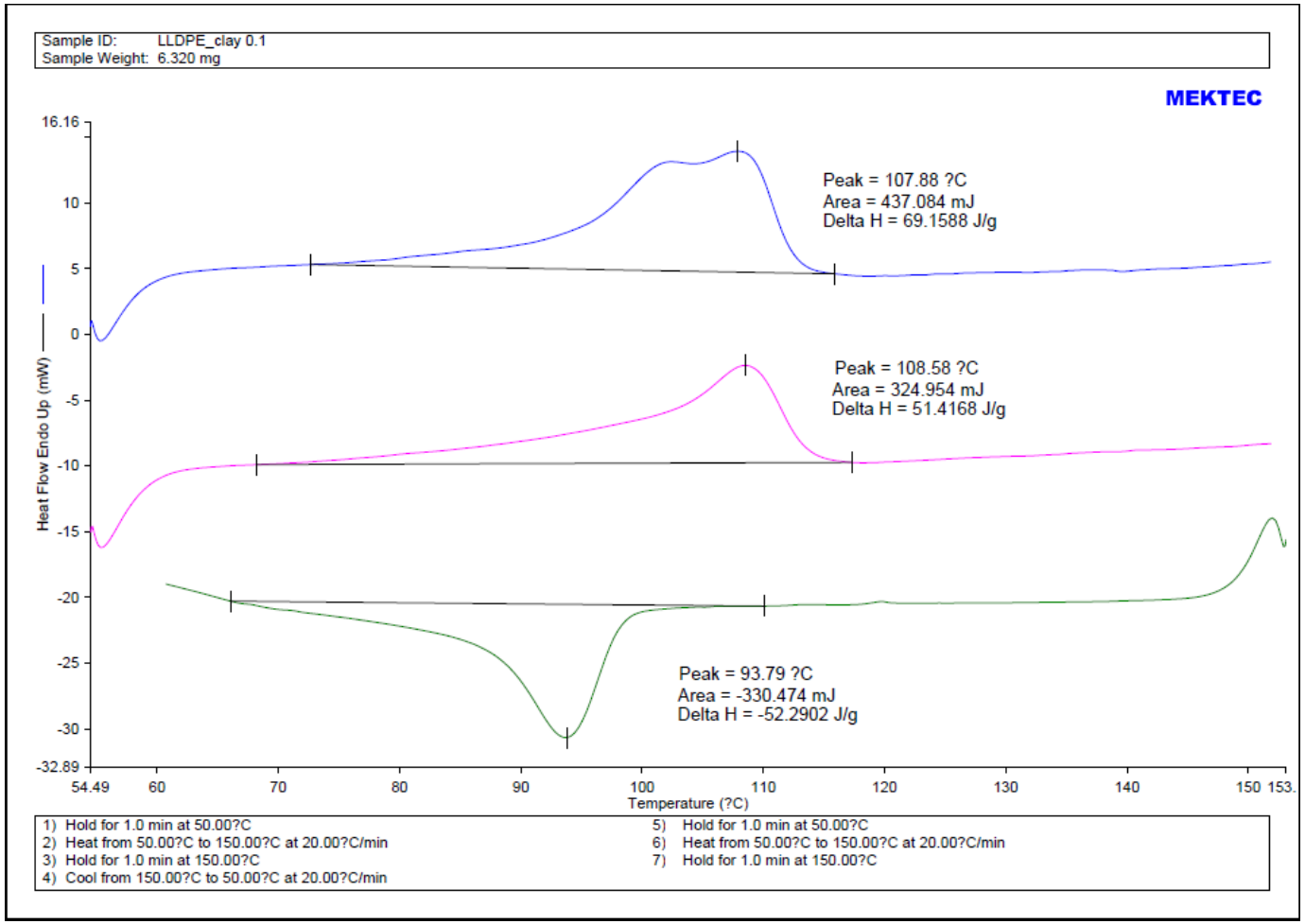

Figure A-8 DSC curve of LLDPE/clay20 nanocomposite

APPENDIX B

^{13}C Nuclear magnetic resonance (^{13}C NMR)

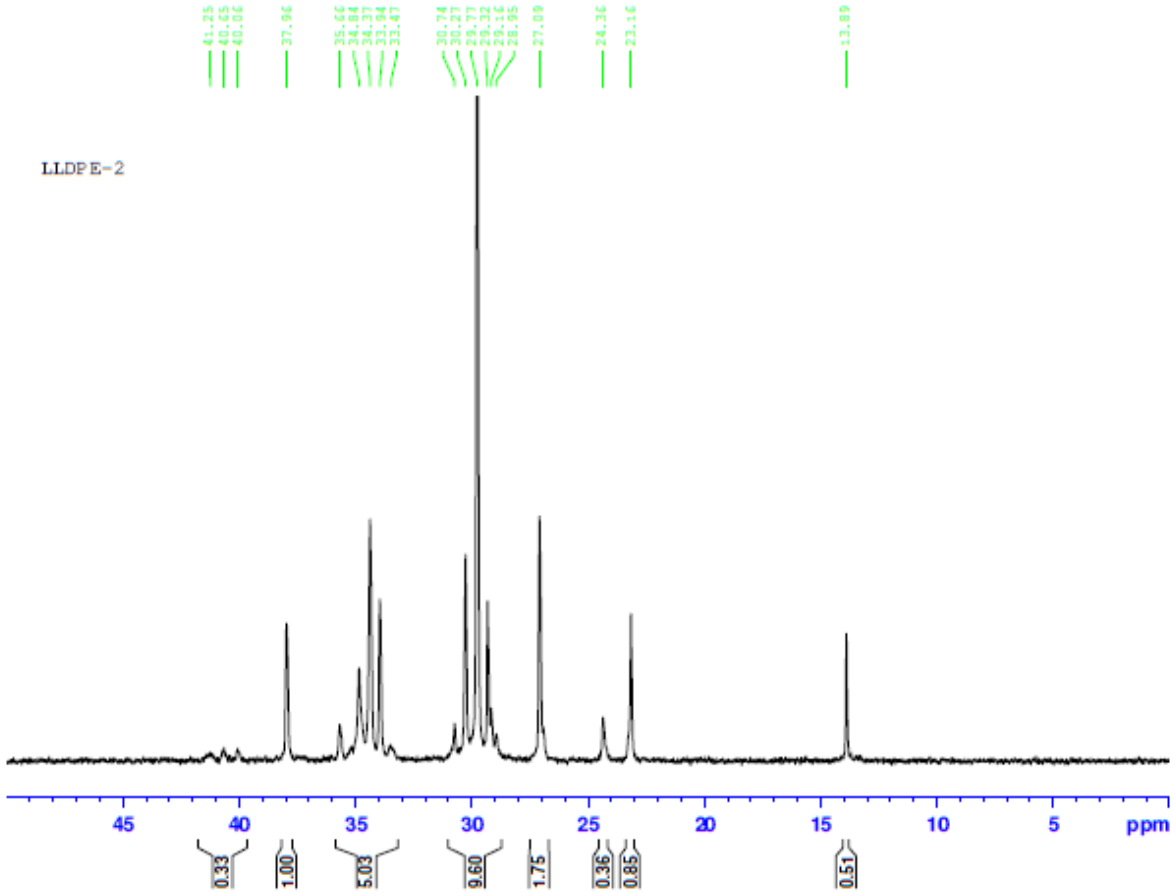

Figure B-1. ^{13}C NMR spectra LLDPE

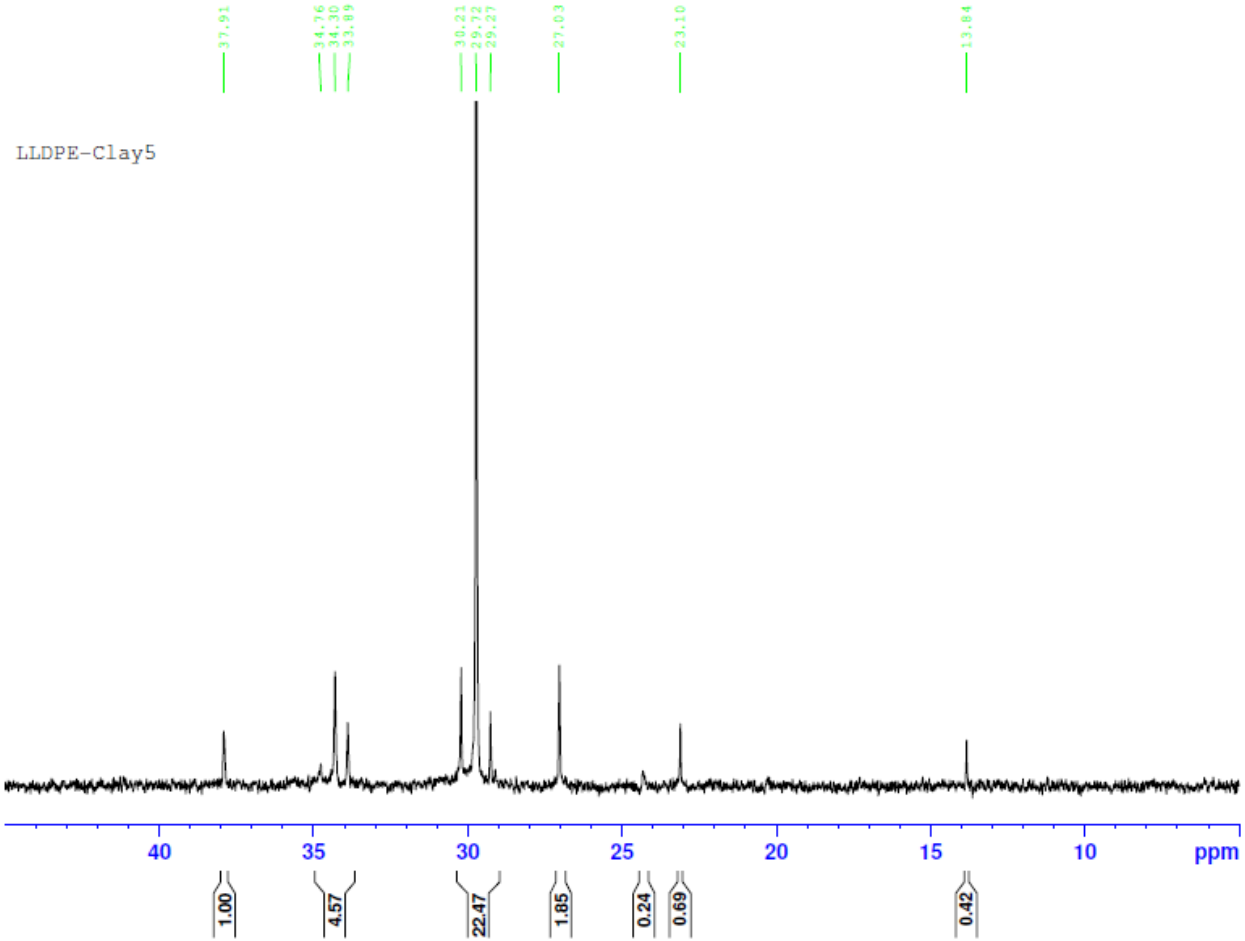

Figure B-2. ^{13}C NMR spectra LLDPE/clay5 nanocomposite

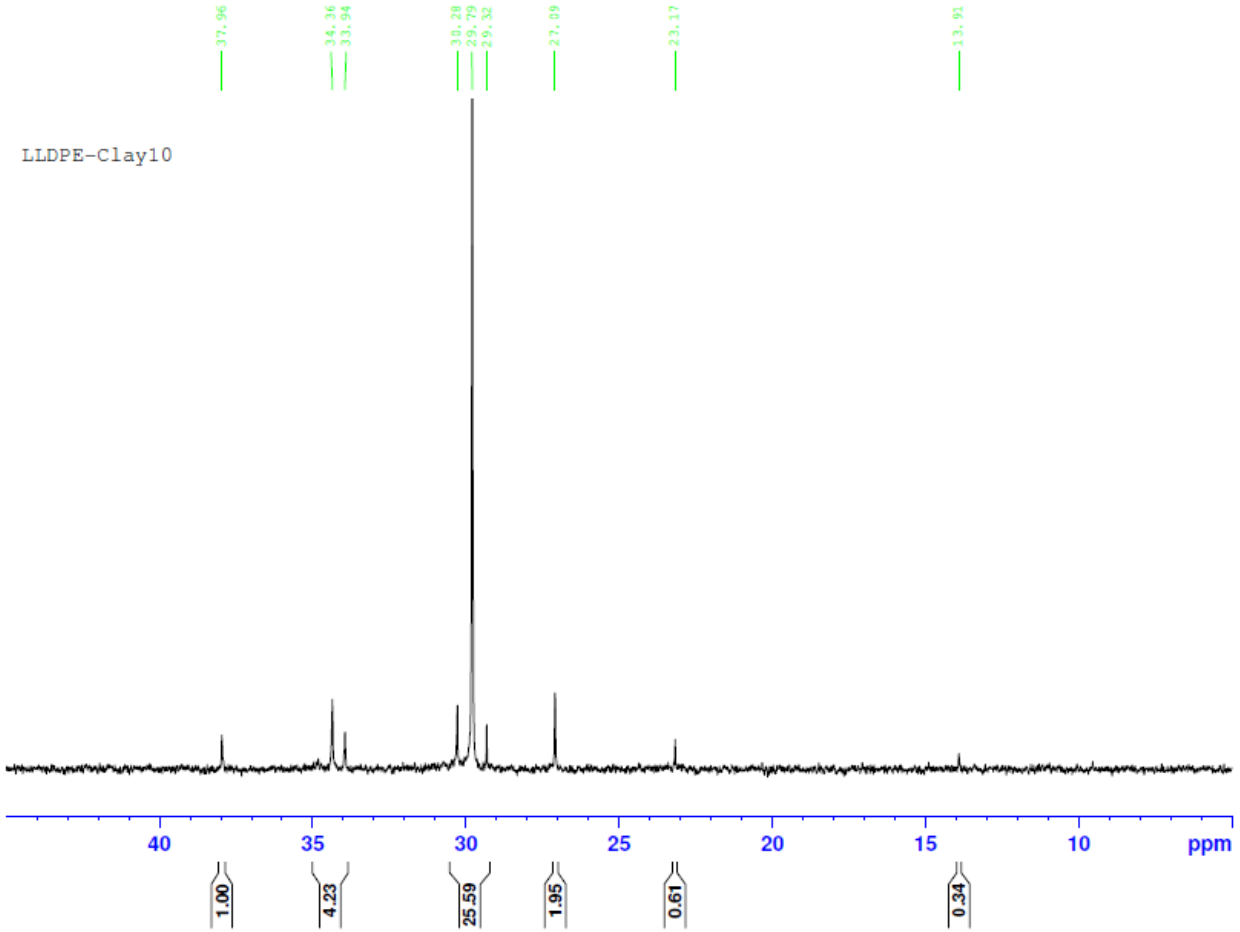

Figure B-3. ^{13}C NMR spectra LLDPE/clay10 nanocomposite

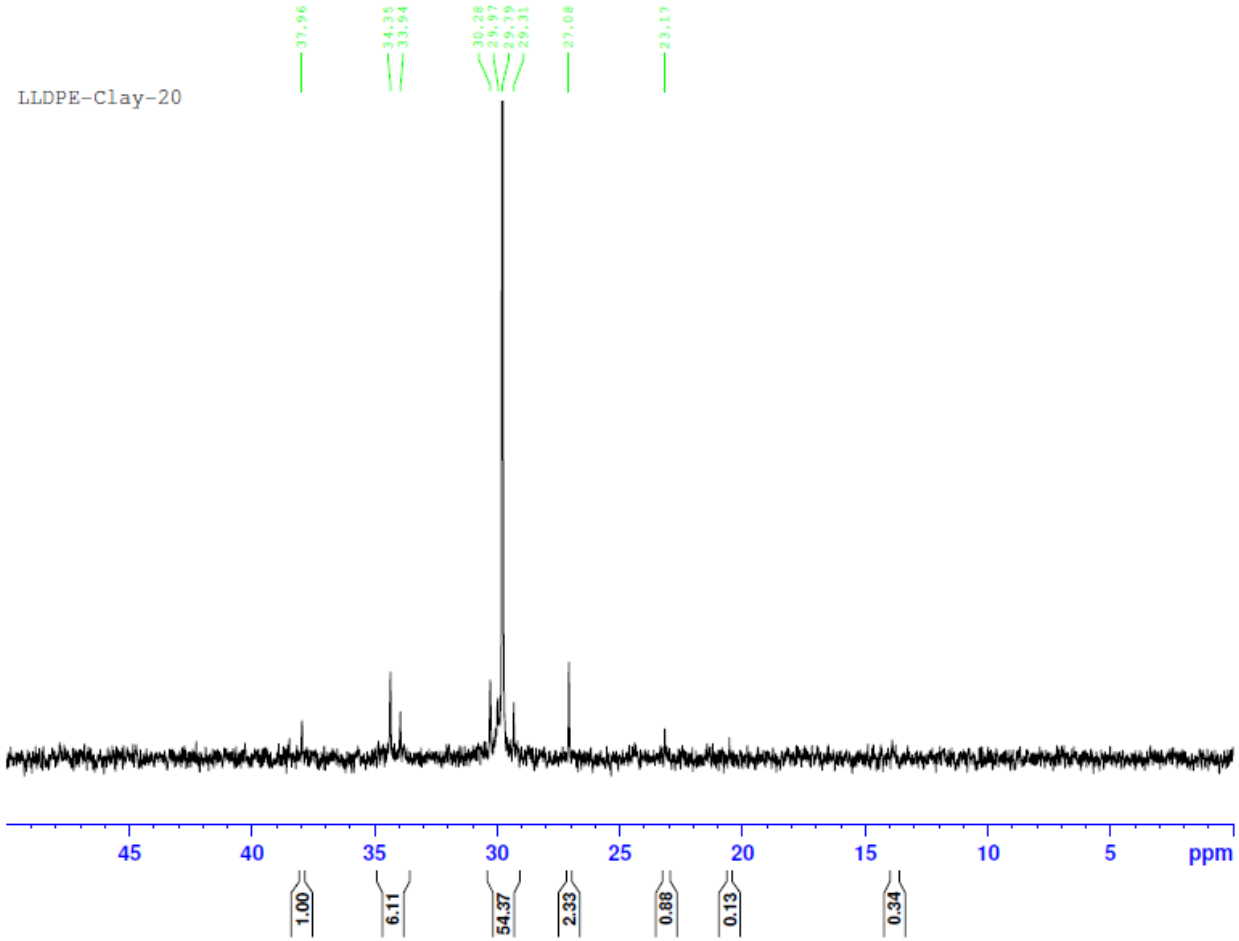

Figure B-4. ^{13}C NMR spectra LLDPE/clay20 nanocomposite

APPENDIX C

Calculation of polymer properties

C.1 Calculation of crystallinity in polymer nanocomposites

The degree of crystallinity (X_c) of polymer nanocomposites were estimated in accordance with the following equation [30]:

$$X_c = \frac{\Delta H_{exp}}{\Delta H^*} \times \frac{1}{W_f}$$

Where ΔH_{exp} is heat of fusion which obtained from DSC.

ΔH^* is heat of fusion of complete crystalline of HDPE (293 J/g).

W_f is weight fraction of HDPE in the polymer nanocomposite.

C.2 Calculation of 1-hexene insertion in LLDPE/clay nanocomposite

Insertion of 1-hexene in LLDPE/clay nanocomposites are calculated from ^{13}C NMR spectrum, according to the relationship [55,56].

The integration areas of ^{13}C-NMR spectrum in the specific ranges are listed below.

T_A = 39.5 - 42 ppm
T_B = 38.1 ppm
T_C = 33 - 36 ppm
T_D = 28.5 - 31 ppm
T_E = 26.5 - 27.5 ppm
T_F = 24 - 25 ppm
T_G = 23.4 ppm
T_H = 14.1 ppm

Triad distribution was determined as the followed;

k[HHH] = $2T_{A+}$Tb-Tg
k[EHH] = 2(Tg-Tb-Ta)
k[EHE] = T_B
k[EEE] = 0.5(Ta+Td+Tf-2Tg)
k[HEH] = T_F
k[HEE] = 2(Tg-Ta-Tf)

Finally, the fractions of ethylene and 1-hexene insertions were determined;

%E = [EEE] + [EEH] + [HEH] ; E is ethylene.
%H = [HHH] + [HHE] + [EHE] ; H is 1-hexene.

APPENDIX D

Characteristic Infrared Spectroscopy (IR) Absorption Frequencies

Table D-1. Characteristic IR absorption frequencies of organic functional group [57]

Functional Group	Type of Vibration	Characteristic Absorptions (cm^{-1})	Intensity
Alcohol			
O-H	(stretch, H-bonded)	3200-3600	strong, broad
O-H	(stretch, free)	3500-3700	strong, sharp
C-O	(stretch)	1050-1150	strong
Alkane			
C-H	stretch	2850-3000	strong
-C-H	bending	1350-1480	variable
Alkene			
=C-H	stretch	3010-3100	medium
=C-H	bending	675-1000	strong
C=C	stretch	1620-1680	variable
Alkyl Halide			
C-F	stretch	1000-1400	strong
C-Cl	stretch	600-800	strong
C-Br	stretch	500-600	strong
C-I	stretch	500	strong
Alkyne			
C-H	stretch	3300	strong,sharp
-C≡C-	stretch	2100-2260	variable, not present in symmetrical alkynes
Amine			
N-H	stretch	3300-3500	medium (primary amines have two bands; secondary have one band, often very weak)
C-N	stretch	1080-1360	medium-weak
N-H	bending	1600	medium
Aromatic			
C-H	stretch	3000-3100	medium
C=C	stretch	1400-1600	medium-weak, multiple bands
Carbonyl			
C=O	stretch	1670-1820	strong
Ether			
C-O	stretch	1000-1300 (1070-1150)	strong
Nitrile			
CN	stretch	2210-2260	medium
Nitro			
N-O	stretch	1515-1560 & 1345-1385	strong, two bands

Table D-2. Characteristic IR absorption frequencies of functional groups containing a carbonyl (C=O)

Functional Group	Type of Vibration	Characteristic Absorptions (cm-1)	Intensity
Carbonyl			
C=O	stretch	1670-1820	strong
Acid			
C=O	stretch	1700-1725	strong
O-H	stretch	2500-3300	strong, very broad
C-O	stretch	1210-1320	strong
Aldehyde			
C=O	stretch	1740-1720	strong
=C-H	stretch	2820-2850 & 2720 -2850	medium, two peaks
Amide			
C=O	stretch	1640-1690	strong
N-H	stretch	3100-3500	unsubstituted have two bands
N-H	bending	1550-1640	
Anhydride			
C=O	stretch	1800-1830 & 1740-1775	two bands
Ester			
C=O	stretch	1735-1750	strong
C-O	stretch	1000-1300	two bands or more
Ketone			
acyclic	stretch	1705-1725	strong
cyclic	stretch	3-membered - 1850 4-membered - 1780 5-membered - 1745 6-membered - 1715 7-membered - 1705	strong
a,b-unsaturated	stretch	1665-1685	strong
aryl ketone	stretch	1680-1700	strong

Table D-3. Characteristic IR band positions

Group	Frequency Range (cm^{-1})
OH stretching vibrations	
Free OH	3610-3645 (sharp)
Intramolecular H bonds	3450-3600 (sharp)
Intermolecular H Bonds	3200-3550 (broad)
Chelate Compounds	2500-3200 (very broad)
NH Stretching vibrations	
Free NH	3300-3500
H bonded NH	3070-3350
CH Stretching vibrations	
=-C-H	3280-3340
=C-H	3000-3100
C-CH_3	2862-2882 , 2652-2972
O-CH_3	2815-2832
N-CH_3 (aromatic)	2810-2820
N-CH_3 (aliphatic)	2780-2805
CH_2	2843-2863 , 2916-2936
CH	2880-2900
SH Stretching Vibrations	
Free SH	2550-2600
C=-N Stretching Vibrations	
Nonconjugated	2240-2260
Conjugated	2215-2240
C=-C Stretching Vibrations	
C=-CH (terminal)	2100-2140
C-C=-C-C	2190-2260
C-C=-C-C=-CH	2040-2200
C=O Stretching Vibrations	
Nonconjugated	1700-1900
Conjugated	1590-1750
Amides	~1650
C=C Sretching Vibrations	
Nonconjugated	1620-1680
Conjugated	1585-1625
CH Bending Vibrations	
CH_2	1405-1465
CH_3	
C-O-C Vibrations in Esters	

Group	Frequency Range (cm^{-1})
Formates	~1175
Acetates	~1240, 1010-1040
Benzoates	~1275
C-OH Stretching Vibrations	
Secondary Cyclic Alcohols	990-1060
CH out-of-plane bending vibrations in substituted ethylenic systems	
$-CH=CH_2$	905-915 , 985-995
-CH=CH-(cis)	650-750
-CH=CH-(trans)	960-970
$C=CH_2$	885-895

VITAE

Miss Pimpatima Panupakorn was born in July 24th, 1987 in Songkhla, Thailand. She finished high school from Mahavajiravudth School, Songkhla and received Bachelor's Degree in Chemical Technology from the Faculty of Science, Chulalongkorn University in 2009. She subsequently completed the requirements for a Master's Degree in Chemical Engineering at the Department of Chemical Engineering, Faculty of Engineering, Chulalongkorn University in 2011.

List of publication

Panupakorn P., and Jongsomjit B "Synthesis of polyethylene/clay nanocomposite with metallocene catalyst". (The proceeding of the Thai Institute of Chemical Engineering and Applied Chemistry Conference 2011 (TIChE 2011), Songkhla)